Functional and Structural Analysis of the Yeast SWI/SNF Complex: a Dissertation

Corey Lewis Smith
University of Massachusetts Medical School

Let us know how access to this document benefits you.

A Dissertation Presented

By

Corey Lewis Smith

Submitted to the Faculty of the

University of Massachusetts Graduate School of Biomedical Science, Worcester

In partial fulfillment of the requirements for the degree of

DOCTOR OF PHILOSOPHY

July 16th, 2004

Biomedical Sciences

COPYRIGHT

Portions of this thesis appeared in:

Smith CL and Peterson CL
ATP-dependent Chromatin Remodeling. *Current Topics in Developmental Biology.*
Current Topics in Developmental Biology. 2005;65. *In Press.* Review

Smith CL and Peterson CL
Coupling tandem affinity purification and quantitative tyrosine iodination to determine
subunit stoichiometry of protein complexes. Methods. 2003 Sep;31(1):104-9.

Smith CL, Horowitz-Scherer R, Flanagan JF, Woodcock CL, and Peterson CL.
Structural analysis of the yeast SWI/SNF chromatin remodeling complex.
Nature Structural Biology. 2003 Feb;10(2):141-5.

Smith CL and Peterson CL
Understanding Chromatin: how it affects the control of gene expression.
Trends in Biochemical Sciences. 2002 June 27(6) Supplemental poster.

FUNCTIONAL AND STRUCTURAL ANALYSIS OF THE YEAST

SWI/SNF COMPLEX

A Dissertation Presented

by

Corey Lewis Smith

Approved as to style and content by:

_____

Anthony Imbalzano. Ph.D., Chair of Committee

_____

Kendall Knight, Ph.D., Member of Committee

_____

David Lambright, Ph.D., Member of Committee

_____

John Gross, Ph.D., Member of Committee

_____

Robert Kingston, Ph.D., Member of Committee

_____

Craig L. Peterson, Ph.D., Dissertation Mentor

_____

Anthony Carruthers, Ph.D.,
Dean of Graduate School of
Biomedical Sciences

Interdisciplinary Graduate Program
Program in Molecular Medicine
July 16th, 2004

ACKNOWLEDGEMENTS

Graduate school has been a rewarding experience for me and a lot of this I attribute to those individuals I have been in contact with. At the top of this list is Craig Peterson. Craig has been the ideal mentor, knowledgeable and approachable while allowing me to pursue avenues of research that have interested me greatly. His door has always been open for scientific discussion as well as for those of less scientific merit. Thanks Craig, for all your efforts and support, it has been a pleasure to work with you.

As a researcher, you are only as good as your colleagues, and in this case I have had the pleasure to work with a fine group of people. Over the last few years lab members have left and others joined, but one thing has stayed constant: this has been a great atmosphere to work in. I would like to thank Joan Flanagan and Emilie Richmond for laying the groundwork for this project. I would also like to thank Mariela Jaskelioff who shared my experience in the lab as a graduate student. I would also like to give special thanks to Marc-André Laniel and Peter Horn for being good friends and reading this manuscript as well as introducing me to a new obsession; golf.

I would also like to express considerable gratitude to Rachel Horowitz-Scherer and Christopher Woodcock of the University of Massachusetts, Amherst with whom we have had a very fruitful collaboration over the years.

My research committee, Tony Imbalzano, Ken Knight, David Lambright, and John Gross, have been invaluable for their expertise during this process and I would like

to thank them for all their help. Special thanks to Robert Kingston of MGH/Harvard, who agreed to sit as my outside member and help evaluate my research.

Last of all I would like to thank my friends and family for being there during this process. I have been lucky to have a group of close friends to share the experience of graduate school with. Thanks Eric, Jen, Leanne, Susan, and Todd for making this such an enjoyable experience. I would also like to thank my parents for their love and support and who can finally stop wondering when I will finish school.

ABSTRACT

Modulating chromatin structure is an important step in maintaining control over the eukaryotic genome. SWI/SNF, one of the complexes belonging to the growing family of ATP-dependent chromatin remodeling enzymes, is involved in controlling the expression of a number of inducible genes whose proper regulation is vital for metabolism and progression through mitosis. The mechanism by which SWI/SNF modulates chromatin structure at the nucleosome level is an important aspect of this regulation. The work in this dissertation focuses on how the *Saccharomyces cerevisiae* SWI/SNF complex uses the energy of ATP-hydrolysis to alter DNA-histone contacts in nucleosomes. This has been approached in a two part fashion. First, the three-dimensional structure and subunit composition of SWI/SNF complex has been determined. From this study we have identified a potential region of the SWI/SNF complex that might a site for nucleosomal interaction. Second, functional analysis of the ATPase domain of Swi2p, the catalytic subunit of SWI/SNF, has revealed that a specific conserved motif is involved in coupling ATP hydrolysis to the mechanism of chromatin remodeling. These results provide a potential model for the function of the SWI/SNF chromatin remodeling complex at the nucleosome level.

TABLE OF CONTENTS

LIST OF TABLES AND EQUATIONS

TABLES

EQUATIONS

LIST OF FIGURES

LIST OF ABBREVIATIONS

Å	Angstrom
aa	amino acid
AFM	atomic force microscopy
AMPPNP	Adenosine 5'-(β,γ-imido)triphosphate
ATP	Adenosine 5'-triphosphate
ATRX	alpha-thlassemia X-linked mental retardation
ATRXt	ATRX truncated splice variant
BAP	Brahma associated proteins
bp	base pair
BRG1	Brahma-related gene 1
BRM	Brahma
BSA	Bovine serum albumin
CBD	calmodulin binding domain
CSA/CSB	Cockayne Syndrome complementation group A or B
C-terminal	carboxyl terminal
dCTP	deoxycytidine 5'-triphosphate
Dm	*Drosophila melanogaster*
DNA	deoxyribonucleic acid
DNase I	Deoxyribonuclease I
DSBs	double strand (DNA) breaks
dsDNA	double stranded DNA
DTT	dithiothreitol
E buffer	extraction buffer
EDTA	Ethylenediaminetetraacetic acid
EGTA	Glycol ether diamine tetraacetic acid
EM	electron microscopy
Endo VII	T4 endonuclease VII
Exo III	Exonuclease III
FSC	Fourier shell correlation
GDa	gigadaltons
HA	influenza A virus haemagglutinin
HAT	histone acetyltransferase
HCV	Hepatitis C Virus
HDAC	histone deacetylase
HMT	histone methyl transferase
HP1	heterochromatin protein 1
HR	homologous recombination
Hs	*Homo sapiens*
hSWI/SNF	human SWI/SNF

IFN-α	interferon-alpha
IgG	immunoglobin G
Kb	kilobase
kDa	kilodalton
kV	kilovolts
MDa	Megadalton
MNase	micrococcal nuclease
N-terminal	amino terminal
NURF	nucleosome-remodeling factor (ISWI family)
OD$_{[\lambda]}$	optical density at wavelength
oligo	oligonucleotide
P	phosphate
PAGE	polyacrylamide gel electrophoresis
PBAP	Polybromo Brahma-associated proteins complex
PDB	Protein Database
PEI-cellulose	polyethyleneimine cellulose
PHD	pleckstrin homology domain
pmols	picomoles
RAD	radiation sensitive
rDNA	ribosomal DNA
RNA	ribonucleic acid
rpm	revolutions per minute
RSC	remodels the structure of chromatin
SANT	Swi3p, Ada2p, N-CoR, and TF$_{III}$B
Sc	*Saccharomyces cerevisiae*
SDS	Sodium dodecyl sulfate
SF1 or 2	helicase super family 1 or 2
SIN	SWI independent
SIR	silent information regulators (yeast gene)
SNF	sucrose non-fermenting (yeast gene)
Sp	*Schizosaccharomyces pombe*
ssDNA	single stranded DNA
STEM	scanning transmission electron microscopy
SWI	mating type SWItching
TAP	tandem affinity purification cassette
TBE	Tris, Boric acid, EDTA
TCA	Trichloroacetic acid
TE	Tris NaEDTA buffer
TEV	Tobacco Etch Virus
TLC	thin layer chromatography
TMV	Tobacco Mosaic Virus
U	Enzyme Units
(v/v)	volume to volume
(w/v)	weight to volume

WT   wild type
YEP   yeast extract, peptone, media
YEPD   YEP supplemented with 2% Dextrose

CHAPTER I

INTRODUCTION

The study of chromatin and how this dynamic structure modulates events in the eukaryotic nucleus has become an increasingly important topic in biomedical research. A large number of enzymes have been discovered that are responsible for modifying and altering chromatin structure either globally or specifically at particular gene promoters or regions of the chromosome. This chapter will provide an introduction to the structure of chromatin and then describe how special classes of enzymes modulate chromatin structure to allow access to DNA.

Chromatin Structure: A Short Primer

The structure and function of chromatin is inherently dynamic. During mitosis individual chromatids become highly compact, align on the metaphase plate, separate into mother and daughter cells, and then decondense after anaphase. In interphase, local chromatin structure at gene promoters must be perturbed to allow the binding of a multitude of factors necessary for proper gene activation. Likewise, detection and repair of DNA damage must take place in the context of a chromatin environment. Furthermore, chromatin structure must also be maintained and propagated during replication.

Chromatin structure is an interesting paradox. How do you maintain a compacted genome that will fit in the eukaryotic nucleus while still maintaining a DNA template that is readily accessible for replication, transcription and DNA damage repair? The answer lies in the fact that chromatin is a dynamic structure with many layers of complexity and regulation. The basic unit of chromatin, the nucleosome core particle, consists of two copies of each of the four core histones, H2A, H2B, H3 and H4 (Thomas and Kornberg, 1975). The histones H3 and H4 fold together to form a tetramer to which two H2A-H2B dimers bind, resulting in the canonical histone octamer (Arents et al., 1991). Around this roughly cylindrical octamer are wrapped 147 base pairs of DNA (Luger et al., 1997). The individual histones have short N-terminal (~15-40 amino acids in length), and in some cases C-terminal domains, which radiate out from the core nucleosome structure (Luger et al., 1997). Amino acid residues in these "tails" have been found to be the targets of numerous post-translational modifications (See Figure 2, and reviewed in Fischle et al., 2003; Hake et al., 2004).

The contacts made between DNA and histones are important for the stability and organization of the nucleosome core particle. Recently it has been demonstrated that the mechanical forces needed to disrupt DNA-histone contacts at the entry/exit sites of DNA around the nucleosome are lower then at the central, dyad axis (Brower-Toland et al., 2002). It has also been shown, *in vitro*, that there is a slow intrinsic, yet spontaneous accessibility of DNA in the absence of nucleosome movement (Anderson et al., 2002). This nucleosome breathing could, *in vivo*, allow protein binding at the edges of nucleosomes. Once bound, these proteins might recruit other chromatin modifying

enzymes, which might then disrupt the stronger histone-DNA interactions located near the nucleosome dyad.

100 - 400nm

Long Range
Fiber-Fiber
Interactions

Linker Histones

Maximally Folded
Chromatin Fiber

30nm

Maximally Folded
Nucleosomal
Array

Short Range
Internucleosomal
Interactions

G1
Chromatid

Moderately Folded
Nucleosomal
Array

Extended
Nucleosomal
Array

10nm

RNA
Polymerase

DNA

Nucleosome
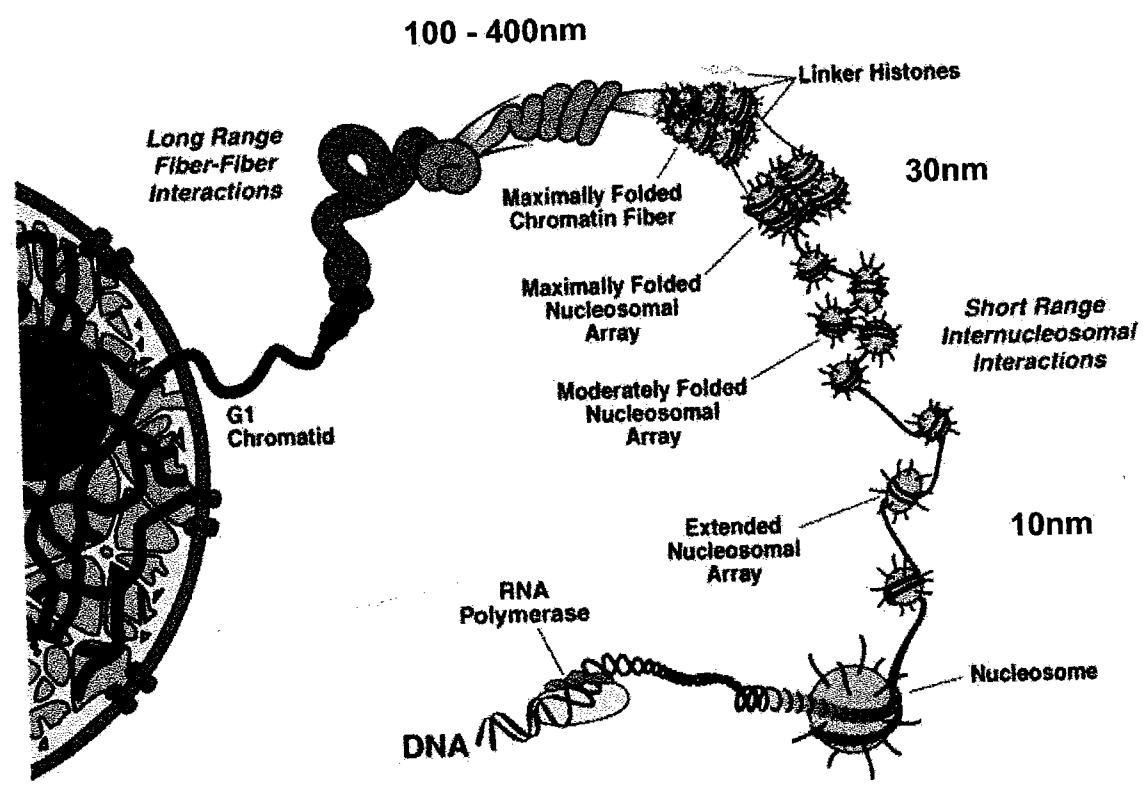
Figure 1. Chromatin fiber condensation. The various levels of compaction of the chromatid fiber are illustrated here. A number of chromatin associated proteins are involved in organizing chromatin folding from the simple "bead on a string" array to the fully condensed G1 chromatid. Adapted from (Hansen, 2002).

At the next layer of complexity, nucleosomes are arranged into long linear arrays with a width of ~10 nm (See Figure 1) (Olins and Olins, 1974; Thoma and Koller, 1977; Thoma et al., 1979). These linear arrays are further compacted by intra- and inter-nucleosomal interactions into compacted chromatin fibers (reviewed in Hansen, 2002).

Such interactions are mediated and stabilized by association of the histone N-terminal domains with neighboring nucleosomes. As such, removal of the histone tails eliminates the folding of model nucleosomal arrays *in vitro* (Carruthers and Hansen, 2000). The incorporation of linker histones into the nucleosomal arrays also stabilizes array folding. These histones are different from the canonical histones in that they are not found within the nucleosome core particle. Linker histones (e.g. H1 and H5), bind at the DNA entry/exit point on the nucleosome with a stoichiometry of one linker histone per nucleosome *in vivo* (Hansen, 2002). The binding of linker histones stabilizes an additional 20 bp of DNA with the nucleosome (167 bp total), forming a particle called a chromatosome (Muyldermans et al., 1981; Noll and Kornberg, 1977; Simpson, 1978). While abundant in vivo, linker histones alone are not sufficient for folding; the histone N-termini are still necessary (Carruthers and Hansen, 2000; Garcia-Ramirez et al., 1992).

As chromatin compaction increases further, long-range interactions, either direct or mediated through other non-histone proteins, increase the level of folding and condensation (Wolffe, 1998). Several groups have used electron microscopy (EM) or atomic force microscopy (AFM) to investigate the structure of nucleosomal arrays. These experiments have used both *in vitro* generated arrays as well as chromatin fibers isolated from chicken erythrocytes (Bednar et al., 1995; Zlatanova and Leuba, 2003). At low ionic strengths the extended linear arrays of nucleosomes appear as beads on a string (Olins and Olins, 1974; Thoma and Koller, 1977; Thoma et al., 1979). At higher ionic strengths these arrays fold into a thick, sausage-like fiber that is commonly known as the 30 nm fiber (Carruthers et al., 1998; Hansen et al., 1989). Electron microscopy and

analytical ultracentrifugation of both folded and unfolded arrays have elucidated some of the characteristics and shapes that chromatin arrays can assume (see Figure 1). In the late 1970s and early 1980s researchers using electron microscopy began to look at higher order chromatin folding. Early EM studies suggested that nucleofilaments (~40mer nucleosomal arrays containing linker histone H1) isolated from rat liver nuclei might be organized into a superhelical structure, or solenoid structure (Finch and Klug, 1976). Other groups found that the addition of linker histones into nucleosomal arrays creates a zigzag repeating pattern in the arrays seen in chromatin fibers purified from chicken erythrocytes (Thoma et al., 1979; Woodcock et al., 1984). This has led to two models for folding into the 30nm fiber. At this level of compaction the chromatin arrays could fold into either a solenoid structure with the nucleosomes forming a helical arrangement or in a zigzag pattern where nucleosomes are positioned such that the entry/exit sides are buried inside of the chromatin fiber (reviewed in Hansen, 2002). These theories are still being investigated to determine exactly how chromatin folds *in vivo*.

Numerous variants exist for some of the histones, which are incorporated into nucleosomes in different regions of chromatin and play specific roles in the organization of chromatin and the establishment of specific domains with different folding characteristics (reviewed in Horn and Peterson, 2002). The basic histone fold remains highly conserved from yeast to humans but the composition of nucleosomes at different regions within chromatin can change. For instance, at centromeres, the histone H3 variant centromere protein A (CENP-A) replaces the major form of H3 (Ahmad and Henikoff, 2001; Lo et al., 2001). While evidence supports that H3 is replaced, all the

other histones H2A, H2B and H4 are still present. Centromeres are known areas of heterochromatic composition with higher than average levels of compaction, and CENP-A might play a key role in the maintenance of this condensation. Disruption of CENP-A gene expression in yeast, flies and worms has illustrated that deposition of this histone variant is important for proper generation of new centromeres (Smith, 2002). Interestingly, it was found that CENP-A is deposited in a replication independent manner which seems to be true of all the histone variants (Ahmad and Henikoff, 2001). Other histone variants are known to exist such as H2AZ, H2AX, macroH2A and H3.3 (Ahmad and Henikoff, 2002; Ladurner, 2003; Redon et al., 2002).

While it seems that many histone variants are involved in the regulation of specialized chromatin structures like telomeres and centromeres, there is a well characterized histone variant, H2AZ, which has been linked to activation and repression of gene activation (Adam et al., 2001; Dhillon and Kamakaka, 2000). This variant is found in numerous regions of both the *Drosophila* and yeast genomes, and in *Drosophila* H2AZ is essential and cannot be substituted for by canonical H2A (Leach et al., 2000; Santisteban et al., 2000). *In vitro*, nucleosomal arrays that contain H2AZ are defective for intra-molecular folding suggesting that chromatin domains containing H2AZ might not be compacted to the same degree as chromatin regions containing only H2A (Fan et al., 2002). In general the incorporation of different histone variants within chromatin fibers is likely to create specialized domains with distinct properties.

a

b

H3 NH2-ARTKQTARKSTGGKAPRKQLATKAARKSAPATGGVKKPHR- N   -KKTESHHKAKGK-COOH

H4 Ac-SGRGKGGKGLGKGGAKRHRKVLRD- N

H2B NH2-PEPSKSAPAPKKGSKKAITKAQKKDGKKRKRSRK- N   -VKYTSSK-COOH

H2A NH2-SGRGKQGGKARAKAK-

▼ Acetyl-   ● (mono,di, or tri)-Methyl-

✳ Ubiquityl-   ◌ Phospho-
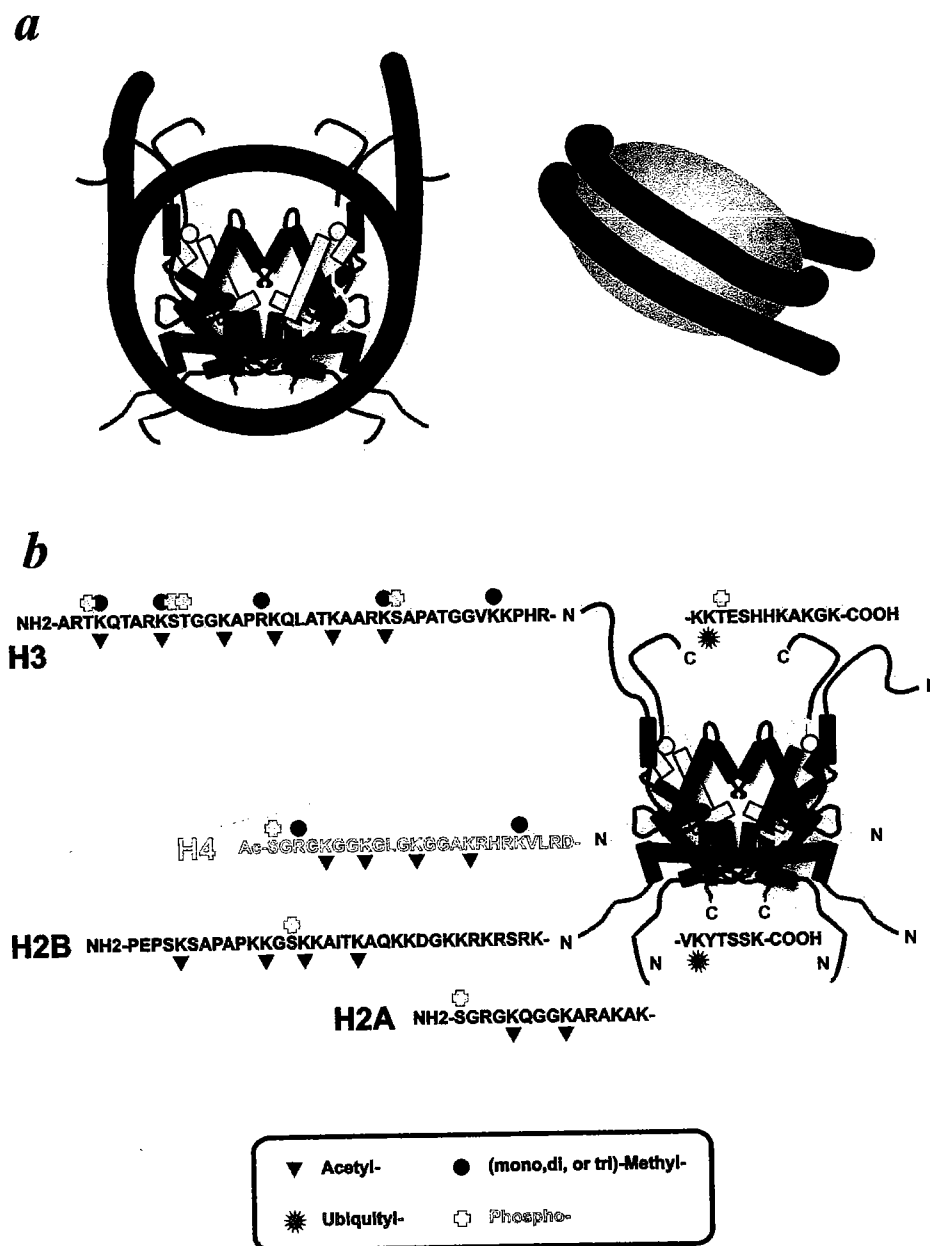
Figure 2. Structural features of the nucleosome core particle. (*a*) Structure of the nucleosome with histones H2A (red,) H2B (light blue), H3 (green), and H4 (yellow) represented based on the 1.9Å crystal structure (Luger et al., 1997). The path of the DNA is represented by the curve around the histone octamer. The various shades represent the wraps of DNA. (*b*) Features of the N and C-terminal tail regions of core histones. The colored shapes represent known modifications of the amino acid residues in the tails. The histone tails can be methylated (blue circles) at lysines and arginines, phosphorylated (yellow croses) at serines, ubiquitylated (orange stars) at lysines and acetylated (green triangles) at lysines.

ATP-Dependent Chromatin Remodeling Enzymes

Among the major contributors to the dynamic nature of chromatin are the chromatin modification and remodeling enzymes. The first class of enzymes, the histone modifying enzymes, directly add or remove post-translational modifications to amino acids in the various histone proteins. As seen in Figure 2, numerous histone modifications have been found to date (reviewed in Khorasanizadeh, 2004). Lysine residues can be the targets of acetylation, methylation (mono, di- or trimethylated), or ubiquitination. Serines and threonines are phosphorylated and arginines can either be mono- or dimethylated. These modifications are likely to alter the structure or function of chromatin fibers. Indeed, different modifications are associated with distinct chromatin-mediated events such as transcriptional activation, silencing, and histone deposition. For example histone hyperacetylation usually correlates with transcriptionally active regions, whereas methylation of H3 at lysine 9 correlates well with transcriptional repression (Hake et al., 2004). Much of the current research into chromatin biology has focused on these histone modifications and their role in the regulation of chromatin mediated events (Fischle et al., 2003; Hake et al., 2004; Jenuwein and Allis, 2001; Khorasanizadeh, 2004).

The second class of chromatin remodeling enzymes contains those enzymes that alter chromatin structure by disrupting or mobilizing nucleosomes in an energy dependent manner (ATP-dependent chromatin remodeling enzymes). For the purpose of this work I will focus on the roles that ATP-dependent chromatin remodeling enzymes

play in altering nucleosomal and chromatin fiber structure. ATP-dependent chromatin remodeling enzymes use the free energy derived from the hydrolysis of hundreds of molecules of ATP per minute to disrupt chromatin structure (Cote et al., 1994; Elfring et al., 1994; Khavari et al., 1993; Kwon et al., 1994; Seelig et al., 1995). These enzymes range from a single catalytic subunit to multi-subunit complexes that can exceed 1 MDa in mass (reviewed in Lusser and Kadonaga, 2003). At the heart of each ATP-dependent chromatin remodeling enzyme is a helicase-like subunit of the SWI2/SNF2 family of SF2 helicases (Eisen et al., 1995). This class of ATPases has been further subdivided into at least three major subfamilies: the SWI2/SNF2, Mi-2/CHD, and ISWI families as well as a potentially new family of Ino80-like complexes. These family assignments are based primarily on sequence homology within the catalytic subunit as well as the peculiarities of their remodeling activities (Boyer et al., 2000a; Eisen et al., 1995; Shen et al., 2000). The helicase containing subunits in these enzymes are large multi-domain proteins that contain additional domains, including bromodomains, pleckstrin homology domains (PHD), chromodomains, SANT domains, and AT hook regions (See Figure 3). These other domains might play a role in stabilizing interactions with histones and/or nucleosomal DNA. For instance, bromodomains interact with acetylated lysines, AT hook regions interact with the minor groove of AT rich regions of DNA, and SANT domains are believed to interact with histone tails (Aravind and Landsman, 1998; Boyer et al., 2004; Goodwin and Nicolas, 2001).

The hallmark of ATP-dependent chromatin remodeling enzymes is the ability to remodel chromatin by altering the DNA-histone contacts within individual nucleosome

Swi2/Snf2p family

Complex	Organism	ATPase	subunits	Size
SWI/SNF	*S. cerevisiae*	Swi2p	11	1.15 MDa
RSC	*S. cerevisiae*	Sth1p	15	~1 MDa
hSWI/SNF-A	*Homo Sapiens*	Brm or Brg1	9	~2 MDa
hSWI/SNF-B	*Homo Sapiens*	Brg1	9	~2 MDa
BRM	*Drosophila melanogaster*	BRM	8	~2 MDa

ISWI family

Complex	Organism	ATPase	subunits	Size
yISW1a	*S. cerevisiae*	ISW1	2	400 kDa
dACF	*Drosophila melanogaster*	ISWI	2	300 kDa
NURF	*Drosophila melanogaster*	ISWI	4	550 kDa
hCHRAC	*Homo Sapiens*	hSNF2h	4	800 kDa
hACF	*Homo Sapiens*	hSNF2h	2	600 kDa

Mi-2 family

Complex	Organism	ATPase	subunits	Size
dMi-2	*Drosophila melanogaster*	dMi-2	7	~1 MDa
xMi-2	*Xenopus laevis*	Mi-2	6	~1MDa
hNURD	*Homo Sapiens*	Mi-2	7	~1.5MDa

Figure 3. Classes of ATP-dependent chromatin remodeling enzymes. This cartoon depicts representative features of each subfamily of chromatin remodeling enzymes. The tables list a number of key chromatin remodeling enzymes with their approximate sizes, ATPase subunit, total subunit compositions and the organism in which they are found. In Swi2/Snf2p grey regions represent low complexity regions, green regions represent predicted coiled-coil and dark blue regions are AT regions.

resulting in either localized disruption of the histone-DNA contacts or mobilization of the nucleosomes on the chromatin fiber. In the rest of this chapter I will focus on the roles of these enzymes *in vivo* as well as how they utilize ATP hydrolysis to remodel chromatin structure. As discussed below, members of each subfamily appear to play unique roles *in vivo*.

ATP-Dependent Chromatin Remodeling Enzymes Are Involved in the Control of Numerous Cellular Processes.

The discovery of the first chromatin remodeling enzyme, the *S. cerevisiae* SWI/SNF complex, was the result of several early genetic studies of two yeast genes, *HO* and *SUC2*. The *SWI1*, *SWI2*, and *SWI3* genes were originally found to act as positive regulators of *HO* transcription, the endonuclease involved in mating type switching, hence the name **SWI**tch genes (Stern et al., 1984). At the same period in time three other genes, *SNF2*, *SNF5*, and *SNF6* (**S**ucrose **N**on**F**ermentors), were found to be positive regulators of *SUC2*, encoding invertase, which is needed for yeast to utilize sucrose as a carbon source (Neigeborn and Carlson, 1984). Subsequent analysis showed that *SWI2* and *SNF2* were in fact the same gene and that all five of these gene products functioned together in a complex as positive regulators of transcription (Laurent et al., 1991; Peterson et al., 1994; Peterson and Herskowitz, 1992). Genetic interactions between *SWI* and *SNF* genes and genes encoding components of chromatin were also observed. A

mutant screen for <u>S</u>WI-<u>In</u>dependent, or *SIN* genes, that could alleviate the effects of *swi⁻*

mutations, identified two chromatin proteins encode by the *SIN1* and *SIN2* genes (Kruger

and Herskowitz, 1991; Peterson et al., 1991). The *SIN1* gene encodes a non-histone

protein with homology to HMG1/2 proteins and the *SIN2* gene was found to encode

histone H3. These genetic studies suggested that this large megadalton complex

regulated transcription by antagonizing chromatin structure. The identification of

SWI/SNF then led to the subsequent identification of numerous, related ATP-dependent

complexes similarly involved in the alteration of chromatin (Vignali et al., 2000).

The SWI2/SNF2 complexes: transcriptional regulators

The yeast SWI/SNF complex comprises eleven subunits (encoded by the SWI1,

SWI2/SNF2, SWI3, SNF5, SNF6, SNF11 SWP82, SWP73, SWP29, ARP7 and ARP9

genes) (Cairns et al., 1998; Cairns et al., 1996a; Cairns et al., 1996b; Peterson et al.,

1994; Peterson et al., 1998). The catalytic subunit of the SWI/SNF complex, Swi2p,

contains a bromodomain and an AT-hook region as well as the helicase-like ATPase

domain. Bromodomains are believed to be involved in interactions with histone tails and

the AT-hook region appears to be involved in binding to AT rich regions of DNA: these

domains might be important for targeting the ATPase subunit to chromatin (Aravind and

Landsman, 1998; Boyer et al., 2004). Swi2 homologs are found in all eukaryotes,

including *Drosophila* (Brahma), and humans (hBRM and BRG1 complexes) (Martens

and Winston, 2003). Sth1p, a very close yeast paralog of Swi2p, is found in the RSC

chromatin remodeling complex (Cairns et al., 1996c; Du et al., 1998; Tsuchiya et al., 1998).

SWI/SNF is important in the activation of a subset of highly inducible genes in yeast, including genes involved in metabolism (*HIS3, SUC2, INO1,* and *PHO8*) and mating-type switching (*HO*) (Winston and Carlson, 1992). Although SWI/SNF activity is only required for ~5% of constitutively expressed yeast genes, an important subset of highly inducible genes require SWI/SNF (Holstege et al., 1998; Krebs et al., 2000; Sudarsanam et al., 2000). Likewise, gene expression at the end of mitosis also appears to require global SWI/SNF activity (Krebs et al., 2000). Interestingly the *Caenorhabditis elegans* homolog of SWI/SNF has been shown to be required in late mitosis for the asymmetric division of T cells (Sawa et al., 2000). A global role for SWI/SNF during mitosis is consistent with the view that SWI/SNF might regulate higher order chromatin structure *in vivo* (Horn et al., 2002; Krebs and Peterson, 2000).

The Brahma complex (BRM), a homolog of SWI/SNF in *Drosophila,* is required for maintenance of homeotic gene expression and E2F-dependent transcription (Kennison and Tamkun, 1988; Staehling-Hampton et al., 1999). In adult flies loss of Brahma causes defects in the peripheral nervous system as well as a more general decrease in cell viability at the larval stages (Elfring et al., 1998). Recently the BRM protein has been found in two separable *Drosophila* complexes, BAP (Brahma-associated proteins) and PBAP (polybromo Brahma-associated proteins), which contain differences in only a few subunits (Mohrmann et al., 2004). Both of these complexes colocalize to regions of hyperacetylated chromatin on polytene chromosomes in a distinct yet overlapping

pattern. The BAP complex also appears to be involved in repression of the wingless target genes *nubbin*, *Distal-less*, and *decapentaplegic*, which are all crucial for proper patterning of numerous structures during fly development (Collins and Treisman, 2000).

In mammals, homologs of SWI/SNF subunits (*BRG1* and *INI1/SNF5*) are essential for early mouse development. A highly conserved subunit of SWI/SNF, *INI1/SNF5*, has been found to be crucial in early steps of fetal development and loss of heterozygosity of *INI1/SNF5* occurs during tumor formation in mice (Guidi et al., 2001; Klochendler-Yeivin et al., 2000; Roberts et al., 2000). Likewise, in human cells, the various SWI/SNF chromatin remodeling enzymes have been found to play major roles in cell differentiation, early development and tumor suppression (Huang et al., 2003; Muller and Leutz, 2001; Neely and Workman, 2002). For instance, induction of muscle and adipocyte cell differentiation requires the hSWI2/SNF2 homologs *BRG1* and *BRM* (de la Serna et al., 2001; Salma et al., 2004). *BRG1* has also been found to activate a subset of IFN-α inducible genes in humans, linking SWI/SNF remodeling to regulation of cytokine mediated gene expression (Huang et al., 2002).

Many links to human disease exist for the human SWI/SNF complexes. Evidence suggests that the ATPase subunits (BRG1 and hBRM) of the hSWI/SNF complexes can act as tumor suppressors in their own right. BRG1 and BRM mutations have been seen in primary lung cancers, and gastric carcinomas (Reisman et al., 2003; Sentani et al., 2001). A number of different mutations have been discovered in the BRG1 gene in numerous other cancers including breast, lung, prostate and pancreatic cancers (Wong et al., 2000). Mutations within *hBRM* as well as *BRG1, BAF155/SWI3, BAF180*, and *BAF250* genes

have also been found to be mutated in cancer cell lines (Decristofaro et al., 2001). *INI1/hSNF5* has also been linked to cancer in humans. Mutations in *INI1/hSNF5* have been found in pediatric malignant rhabdoid tumors (Versteege et al., 1998). The link between chromatin remodeling enzymes and disease is currently experiencing a rapid growth as more direct links are being found with SWI/SNF-like enzymes.

ISWI complexes: Sliding into transcription regulation and chromatin assembly

Another class of energy dependent chromatin remodeling enzymes is the ISWI family. The ISWI family contains multiple complexes found in yeast (ISW1a, ISW1b and ISW2), flies (NURF, CHRAC and ACF) and higher eukaryotes (RSF, ACF, WCRF, and CHRAC (reviewed in Langst and Becker, 2001b). In contrast to the SWI2/SNF2 family members, ISWI ATPases contain SANT and SLIDE domains (Boyer et al., 2004; Grune et al., 2003). These domains share homology to the c-myb DNA binding module and have been proposed to play a role in histone tail (SANT domain) and nucleosomal DNA (SLIDE) interactions (Boyer et al., 2004).

Whereas the SWI/SNF complexes appear dedicated to transcriptional control, the ISWI family members appear to participate in a variety of nuclear processes. In Drosophila, ISWI genes are essential for viability and have been genetically associated with numerous nuclear processes (Corona and Tamkun, 2004). Like SWI/SNF, one ISWI containing complex, NURF, activates transcription via chromatin remodeling at the *Drosophila* hsp70 and *ftz* promoters (Okada and Hirose, 1998; Tsukiyama et al., 1994). ISWI complexes also play roles in repression. For example, Tamkun and colleagues saw

no evidence for colocalization of ISWI and RNA polymerase on *Drosophila* polytene chromosomes suggesting that ISWI does not play a role in transcriptional activation like the SWI2/SNF2 family of chromatin remodeling complexes (Deuring et al., 2000). Instead, ISWI complexes play a repressive role at specific genes in larval developmental stages. Studies in *Drosophila* lacking ISWI have also found that the male fly larvae have a high level of global decondensation in the X chromosome suggesting a global role in the maintenance of chromosome structure (Deuring et al., 2000). The developmental role for ISWI complexes can also be illustrated in mammals as SNF2h, the murine homolog of ISWI, has been found to be essential for early embryonic development. In *Snf2h*^{-/-} mice the embryo never progresses from the pre-implantation stage (Stopka and Skoultchi, 2003). ISWI complexes have also been found to play a global role in chromatin remodeling and reprogramming of chromatin when somatic nuclei are transplanted into unfertilized eggs (Kikyo et al., 2000).

While ISWI is essential in *Drosophila* and mice, there are two redundant copies of ISWI (*ISW1* and *ISW2*) in yeast which are not essential (Tsukiyama et al., 1999). The Isw2p and Itc1p proteins are components of the yeast Isw2 complex, which is required for the transcriptional repression of a set of meiotic genes in conjunction with the Sin3/Rpd3 HDAC complex (Goldmark et al., 2000). Isw1p, on the other hand, is found in two different complexes Isw1a (Isw1p and Ioc3p) and Isw1b (Isw1p, Ioc2p and Ioc4p) (Vary et al., 2003). An interesting role for the two Isw1 complexes in transcriptional elongation and termination by RNA polymerase II (RNAPII) has been found. Both of these complexes have been found to associate with RNAPII during transcription, with the

Isw1a complex associated with RNAPII at the promoter prior to gene activation keeping gene transcription in an off state by ordering nucleosomes over the promoter region. Upon activation, Isw1a becomes dissociated and Isw1b becomes the RNAPII associated Isw1 complex (Morillon et al., 2003). It appears that Isw1b coordinates elongation, termination and mRNA processing. This data suggests that the interplay between these two complexes is necessary for proper transcript processing.

The ISWI complexes do not just play a role in transcription; ISWI containing complexes have also been implicated in chromatin assembly and nucleosome spacing. The ACF complex in both flies and mammals is composed of the two subunits: ISWI and Acf1. *In vitro* ACF is able to assemble, space and mobilize nucleosomes in a cell-free system (Ito et al., 1997). ACF also appears to play a role in replication-coupled histone deposition *in vivo* (Mello and Almouzni, 2001). ACF, as well as a related complex, WSTF, has been found to co-localize with replication foci and is required for replication through heterochromatic regions (Bozhenok et al., 2002; Collins et al., 2002). It is still not clear if these complexes are functionally redundant or if they couple replication and histone deposition in distinct ways. A number of related ISWI complexes (CHRAC, WSTF, and NURF) all contain subunits similar to ACF and are able to catalyze the mobilization of nucleosomes on arrays *in vitro* (Becker and Horz, 2002). The NURF complex also contains NURF-55, a subunit of CAF-1, a histone chaperone conserved in many eukaryotes (Martinez-Balbas et al., 1998). NURF, unlike CHRAC and ACF, does not space nucleosomes but rather is believed to be involved in the randomization of spaced nucleosomal arrays. So it appears that the ISWI family of ATP-dependent

remodeling enzymes is involved in a number of processes including transcriptional activation, replication-coupled histone deposition as well as the creation of regions of silenced chromatin at specific promoter regions.

Mi-2 complexes: General repressors

The Mi-2 (CHD) family of chromatin remodeling enzymes all contain ATPase subunits with one or more chromodomains. The chromodomains in Mi-2 appear to be responsible for binding nucleosomal DNA in a histone tail independent manner (Bouazoune et al., 2002). These enzyme complexes appear to play roles in transcriptional repression since several Mi-2 complexes have been found to contain histone deacetylase (HDAC) subunits (Kehle et al., 1998; Tong et al., 1998; Wade et al., 1998; Wade, 1998). Along with HDACs, methyl-CpG binding proteins have also been found to be part of the Xenopus Mi-2 complex (Wade et al., 1999). The discovery of methylated-DNA binding proteins as part of a chromatin remodeling complex suggests that Mi-2 functions to coordinate histone deacetylation with DNA methylation in order to silence chromatin (Wade et al., 1999).

As with other chromatin remodeling complexes, Mi-2 complexes have been found to play important roles in development. In *Arabidopsis thaliana* the gene PICKLE (PKL) encodes a Mi2 family ATPase necessary for the transition from seed to seedling (Ogas et al., 1999). In *pkl* mutants the silencing of a number of embryonic genes is lost and these genes are then expressed post germination (Ogas et al., 1997; Rider et al., 2004). Mutations in *Drosophila* Mi-2 (dMi-2) are embryonic lethal, and in *C. elegans* LET-

418/Mi-2 is required for the maintenance of somatic cell differentiation, a crucial event in early embryonic development (Khattak et al., 2002; Unhavaithaya et al., 2002). Mi-2 complexes have also been found to play a role in lymphocyte cell differentiation. A class of Zn^{2+}-finger DNA-binding proteins in the *Ikaros* gene family interact directly with the Mi-2 complex NURD (orthologous to dMi-2), and in murine T cells a fraction of Ikaros and Aiolos (another member of the *Ikaros* gene family) were found to be stably associated with the NURD complex (Kim et al., 1999). Upon T cell activation a fraction of Ikaros, Aiolos and NURD all become associated with heterochromatin with similar kinetics (Kim et al., 1999). Ikaros also appears to interact with SWI/SNF in T cells, and this interaction appears to be exclusive of the Ikaros-NURD complex. This link between Ikaros, Mi-2, and SWI2/SNF2 family chromatin remodeling complexes has also been observed in adult erythroid cells (O'Neill et al., 2000). Overall, it was suggested that the interplay between Ikaros-like DNA binding proteins and chromatin remodeling complexes is responsible for the silencing of the γ-globin locus and γ- to β-globin locus switching. Consistent with this proposal, evidence supports a role for Ikaros as a potentiator of chromatin remodeling at heterochromatic sites but not as a traditional activator, especially at pericentric regions of heterochromatin (Koipally et al., 2002).

Other subfamilies: Repair and establishing chromatin domains

Recently, more proteins have been found to have the hallmarks of chromatin remodeling enzymes, including those involved in the repair of DNA damage. Rad54p, a member of the RAD52 epistasis group, plays an essential role in several steps of

homologous recombinational repair of DNA double strand breaks (DSBs) (Peterson and Cote, 2004). Rad54 is a member of the SWI2/SNF2 family of ATPases, and in the last few years it has been discovered that the Rad54 ATPase has all the *in vitro* characteristics of a ATP-dependent chromatin remodeling enzyme (Alexeev et al., 2003; Alexiadis and Kadonaga, 2002; Jaskelioff et al., 2003). It was proposed that Rad54 functions in recombinational repair of DNA DSBs by altering and/or moving nucleosomes that might interfere with joint molecule formation or migration of heteroduplex DNA (Jaskelioff et al., 2003; Peterson and Cote, 2004).

Cockayne syndrome (CS) is another human disorder that involves a SWI2/SNF2 family member. This autosomal recessive disease is associated with mental retardation, cachectic dwarfism, neural degeneration and hypersensitivity to UV light. Two different genetic complementation groups exist for CS; CSA and CSB. CSB cells have defects in their ability to perform transcription-coupled repair. CSB homologs have been found in yeast (RAD26) and humans (ERCC6), both of which have been found to be homologs of the Swi2/Swi2p ATPase (Licht et al., 2003). It has been shown that mutations in the putative helicase motifs in CSB lead to abrogation of the genetic function of CSB in RNA synthesis and survival after UV treatment (Muftuoglu et al., 2002). CSB has also been found to exhibit ATP-dependent chromatin remodeling activity as illustrated by the ability to bind to and alter histone-DNA contacts in mononucleases as assayed by DNase I accessibility (Citterio et al., 2000). The precise role of CSB proteins in damage repair is still under investigation.

Mutations in another SWI2/SNF2-like ATPase gene, *ATRX* (alpha-thlassemia X-linked mental retardation) occur in patients with severe X-linked mental retardation (Gibbons et al., 1995). ATRX has been found to be associated with pericentromeric heterochromatin, PML bodies, and the heterochromatin-associated protein HP1 (McDowell et al., 1999). Recently a truncated isoform of ATRX, ATRXt, has been discovered to associate with pericentric heterochromatin regions, but not with PML bodies, suggesting a role in regulation of chromatin structure at specific chromatin regions (Garrick et al., 2004).

Understanding the Molecular Mechanism of ATP-dependent Chromatin Remodeling.

One of the major avenues of research centers on determining how chromatin becomes remodeled by these ATP-dependent chromatin remodeling enzymes. What exactly is the process by which nucleosomes are disrupted? Do all of these complexes use the same basic mechanism to alter nucleosomes? In this section I outline what is known about these enzymes and their actions on nucleosomes.

The SWI2/SNF2-like ATPase subunit is the master switch.

It is increasingly obvious that these large multi-subunit complexes play a number of diverse roles in the nucleus. Do all of these ATP-dependent chromatin remodeling enzymes share the same basic mechanism or do they each act in subtle yet different

ways? The one thing all these enzymes share is a highly conserved helicase-like ATPase domain similar to yeast SWI2/SNF2.

The ATPase subunit of the various ATP-dependent remodeling enzymes all contain a domain with homology to helicase-like proteins of the SF1 and SF2 superfamiles. This ATPase domain contains all of the seven common helicase motifs of the SF2 superfamily (numbered Motif I, Ia, and II-VI). In helicases these motifs function together to convert ATP hydrolysis to the strand separation activities of the enzyme (Caruthers and McKay, 2002). The SWI2/SNF2-like ATPases contain most of the consensus residues of these motifs. The canonical helicase domain is a bipartite structure with Motifs I-III on one side (subdomain I) and Motifs IV-VI to the other side (subdomain II) of the ATP-binding cleft (Caruthers and McKay, 2002).

The ATPase domain of remodeling enzymes is required for remodeling activity. Single point mutations in the highly conserved ATPase/helicase motifs cause loss of function for these enzymes *in vitro* and *in vivo* (Cote et al., 1994; Khavari et al., 1993; Peterson et al., 1994; Richmond and Peterson, 1996). Similar to traditional helicases, all ATP-dependent chromatin remodeling enzymes have been found to have DNA and/or nucleosome-stimulated ATPase activity, although the preferred cofactor differs between the different classes. The SWI2/SNF2 family of enzymes have similar ATPase activity in the presence of either DNA or nucleosomes, while the ISWI and Mi-2 class of enzymes display a higher ATPase activity with a nucleosomal template (Brehm et al., 2000; Cairns et al., 1994; Cairns et al., 1996c; Corona et al., 1999; Cote et al., 1994; Guschin et al.,

2000a). These differences may result from subtle differences in mechanism or in how each enzyme binds its substrate.

A key difference between canonical helicases and ATP-dependent chromatin remodeling enzymes is the lack of actual DNA duplex strand separation. After the identification of the helicase-related motifs in Swi2/Snf2 protein, the yeast SWI/SNF complex was tested for the ability to act as a DNA helicase, but it failed to induce duplex unwinding with a variety of substrates (Cote et al., 1994). Furthermore, SWI/SNF action does not lead to enhanced sensitivity of nucleosomal DNA to potassium permanganate, indicating a lack of transient duplex unwinding (Cote et al., 1998). Similarly, all other chromatin remodeling enzymes tested have yet to produce any evidence of helicase-like duplex unwinding. It should be noted that the SWI2/SNF2 family of ATPases differs from canonical helicase domains with the addition of a large ~100 amino acid insertion between helicase sub domains I and II (Eisen et al., 1995). This insertion might be responsible for the lack of DNA duplex unwinding and it may play a role in the mechanism of chromatin remodeling.

Since these enzymes don't catalyze strand separation, it had been thought that maybe the SWI2/SNF2-like subunit catalyzes the translocation of the complex along DNA. Indeed a number of these enzymes, including SWI/SNF, RSC, and ISWI can track along DNA as revealed by their ability to remove a short oligonucleotide incorporated into a triple helix (Jaskelioff et al., 2003; Saha et al., 2002; Whitehouse et al., 2003). This assay was first used to look at and measure the rates at which type I restriction enzymes track along DNA (Firman and Szczelkun, 2000). Although this activity might

suggest movement of the enzyme along DNA, it seems more likely that the enzyme will remain anchored to the histone octamer and DNA will be moved relative to the enzyme. In this case ATP hydrolysis might catalyze the twisting or pushing of DNA across the surface of the histone octamer. The movement of the DNA then could yield a remodeled state where the octamer has moved relative to its initial position on the DNA. This model will be addressed in more detail in the following sections.

Chromatin remodeling enzymes are able to introduce helical torsion into DNA and nucleosomal substrates.

Other evidence of helicase-like behavior is seen in ATP-dependent chromatin remodeling enzymes. Havas and colleagues have tested various chromatin remodeling enzymes for the ability to introduce superhelical torsion into DNA and chromatin substrates (Havas et al., 2000). In these studies an assay measures extrusion of a cruciform from a DNA construct containing an inverted $[AT]_{34}$ repeat (McClellan et al., 1990). If an enzyme creates superhelical torsion on DNA the $[AT]_{34}$ repeat forms a cruciform that is cleaved by the junction resolving enzyme, T4 Endonuclease VII (Lilley and Kemper, 1984; Mizuuchi et al., 1982). Results showed that ySWI/SNF, *Xenopus* Mi-2 complex, recombinant ISWI, and recombinant BRG1 were all able to generate superhelical torsion in an ATP-dependent manner (Havas et al., 2000). Both BRG1 and SWI/SNF were able to generate torsion on both DNA or chromatin templates while Mi-2 and ISWI only functioned on nucleosomal templates (Havas et al., 2000). These results showed a similarity to the before mentioned DNA/nucleosome stimulated ATPase

activities of these enzymes; enzymes that are more stimulated by nucleosomes for ATPase activity also showed a need for nucleosomal substrates in the cruciform extrusion assay. The generation of torsion on the DNA duplex could either be a consequence of remodeling or it might be how DNA-histone contacts are disrupted.

The chromatin remodeling enzyme-nucleosome interface

Understanding how chromatin remodeling enzymes interact with the nucleosome has been a major goal in the chromatin field for some time. A few groups are starting to use single molecule methods to look at the structures of these complexes as well as the forces and dynamics involved in chromatin remodeling. Atomic force microscopy (AFM) and electron microscopy (EM) studies have shown that the interaction of SWI/SNF with nucleosomal arrays leads to formation of large DNA loops (Bazett-Jones et al., 1999; Schnitzler et al., 2001). The AFM studies also showed that clustering of nucleosomes occurs on short (dodecameric) nucleosomal arrays, leaving long stretches of unoccupied DNA, thus again confirming the mobilization of nucleosomes, *in vitro*. Furthermore, both studies showed a potential loss of DNA constrained by nucleosomes remodeled by SWI/SNF, most likely at the entry/exit positions.

Recently, the *S. cerevisiae* RSC and SWI/SNF complexes were imaged using 3D electron microscopy reconstructions (Asturias et al., 2002; Smith et al., 2003). Both enzymes show central cavities approximately the same size and dimensions of a single nucleosome. The yeast SWI/SNF structure was also of the same approximate dimensions

as that imaged by both Bazett-Jones and Schnitzler (Bazett-Jones et al., 1999; Schnitzler et al., 2001; Smith et al., 2003).

How do these large megadalton complexes bind to nucleosomes? One of the earliest observations for SWI/SNF interaction with DNA showed a high affinity for four-way junction (4WJ) DNA similar to that displayed by HMG-box domain proteins (Quinn et al., 1996). This 4WJ binding affinity suggests that SWI/SNF and related complexes may bind to the entry and exit segments of the nucleosome. Site-specific DNA photoaffinity labeling has also been used to look at the interactions between both the ySWI/SNF and RSC complexes with nucleosome (Sengupta et al., 1999; Sengupta et al., 2001). These studies show that multiple subunits are in close contact with nucleosomal DNA, and that there does not appear to be a preferential binding site at the nucleosomal edge.

In the ISWI complexes, binding to substrate seems to be mediated by the interface between linker DNA regions and the actual nucleosome core, since ISWI containing complexes only act on substrates that have at least 20 bp of DNA adjacent to the nucleosome (Kagalwala et al., 2004). This binding requires other subunit(s) in the ISWI complex, for instance, Acf1p is necessary for high affinity nucleosome sliding by ISWI in both ACF and CHRAC complexes (Eberharter et al., 2001).

How is ATP hydrolysis coupled to the generation of remodeled chromatin?

Once a remodeling enzyme has bound to a nucleosomal substrate, what does DNA translocation and/or torsion generation do? Two major models have been debated

for the last couple of years. The first model was the "twist diffusion" model discussed by van Holde and Yager in 1985 and readdressed recently (van Holde and Yager, 2003). The twist diffusion model theorizes that migration of DNA around the nucleosome is propagated by the introduction of small twist defects that cause under-winding of the DNA helix which are then diffused around the nucleosome (see Figure 4). If the defect collapses back on itself the result would be no movement. On the other hand if it is propagated forward this model allows for small slipping steps to occur where the DNA strand is continuously pumped across the face of the nucleosome (van Holde and Yager, 2003). This model is consistent with the ability of chromatin remodeling enzymes to generate superhelical torsion (Gavin et al., 2001; Havas et al., 2000).

Recent evidence puts this model into question, however, as ISWI- and SWI2/SNF2- containing complexes can still mobilize nucleosomes on DNA substrates containing nicks, hairpins, or gaps (Aoyagi and Hayes, 2002; Langst and Becker, 2001a; Saha et al., 2002). These experiments argue against a simple twist diffusion model since introduction of single base pair nicks and/or addition of bulky DNA branches could prevent the propagation of twist that initiates outside the nucleosome. Nicks in the DNA might dissipate the accumulation of torsional stress while the branched DNA might interfere with the actual rotation of the DNA relative to the nucleosome.

The second, related model is the reptation or bulge migration model. This model suggests that a wave of DNA is released from the histone octamer and is propagated along the surface of the nucleosome allowing accessibility to DNA binding factors with or without generating movement. The best evidence for the creation of loops during

remodeling comes from experiments conducted using cross-linked nucleosomes (Aoyagi et al., 2002). In these studies the H2B histone was first cross-linked to DNA, and the ability of these mononucleosomes to be remodeled was scored by nuclease accessibility. Interestingly, hSWI/SNF could still enhance DNase I accessibility of nucleosomal DNA even in the absence of nucleosome movement. However, increased accessibility to restriction enzymes was lost. Thus, in the context of the bulge migration model it appears that hSWI/SNF creates loops accessible to some factors (DNase), but other factors require actual movement of the octamer. Alternatively, this data might also be consistent simply with changes in rotational positioning of the DNA helix that would result in changes in the DNase I cleavage pattern of DNA. Surprisingly, remodeling with recombinant ISWI actually seems to be stimulated by nicks in the DNA at the entry/exit sites (Langst and Becker, 2001a). Furthermore another study by the Kingston group has shown differences between the remodeling intermediates for ISWI family members (SNF2h) and SWI2/SNF2 (BRG1 and human SWI/SNF) family members (Fan et al., 2003). From these experiments it has been suggested that BRG1 and hSWI/SNF may allow access to DNA occluded in the nucleosome without drastically mobilizing the nucleosome, while SNF2h seems to preferentially move nucleosomes without creation of stable remodeling intermediates.

Recently van Holde and Yager have argued that the both the reptation model and the results of remodeling on nicked substrates can be explained in the context of the twist defect model (van Holde and Yager, 2003). They argue that DNA writhing and bulging
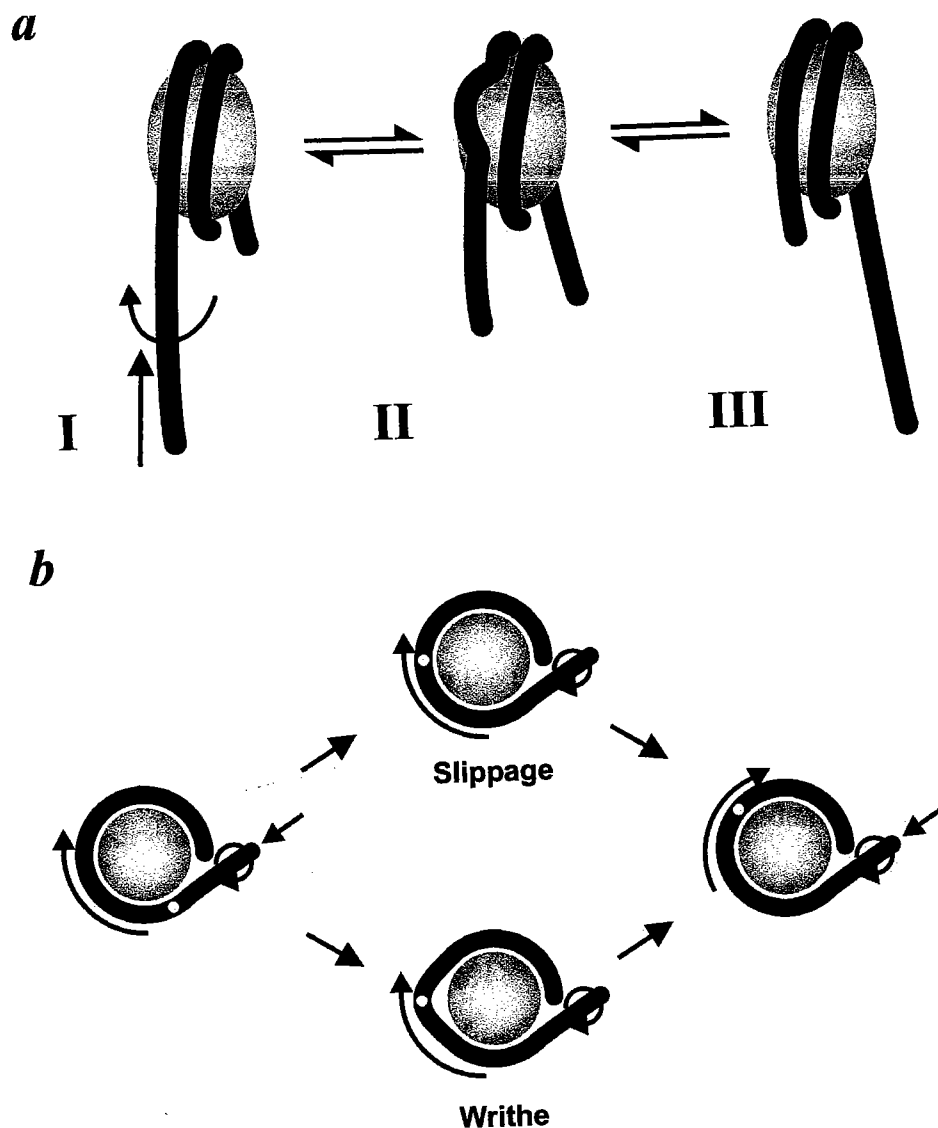
Figure 4. **Torsional model for nucleosome DNA-histone contact disruption.** Generation of helical torsion on nucleosomal DNA either by twisting or pushing the DNA by a chromatin remodeling enzyme results in the generation of a twist defect. This twist defect is propagated along the heteroduplex which could result in either a wave or smaller slippage of DNA moving along the surface of the histone octamer. Relief of the twist defect in the forward direction could result in the movement of the DNA relative to the octamer. (*a*) In a simple slipping model the DNA would appear to only twist along the surface of the nucleosome resulting in conversion of nucleosome **I** to nucleosome **III** with a detectable bulge being detected. A writhing mechanism would result in conversion of nucleosome **I** first to **II** then to **III**. A writhing mechanism also could result in intermediates being trapped at the nucleosome **II** stage. (*b*) Top down view to illustrate differences between slippage and writhing models.

could be the summation of a number of twist defects in a constrained system. That is, an accumulation of twist defects could lead to the generation of a whole writhe of DNA becoming dissociated from the nucleosome if the duplex is not allowed to freely translocate relative to the histone octamer. They also argue that the nicked DNA substrate experiments do not rule out the possibility of the accumulation of twist defects. Base-stacking of the DNA could be maintained in the context of the nucleosome since the histone octamer could stabilize the DNA duplex and any incorporated nicks. Van Holde and Yager argue that nicks might even aid the torsional process thus leading to the increased rate of remodeling seen in the nicked substrate experiments (Langst and Becker, 2001a). Branches and hairpins in the DNA duplex might also be remodeled by a twist diffusion mechanism if accumulation of twist defects leads to a writhe of DNA becoming disassociated from the nucleosome surface, accommodating the bulky DNA formation (van Holde and Yager, 2003). Alternatively, if the step-size of the remodeling reaction is small enough, nicks and bulky DNA formations might not even be a factor. That is, if twist defects were rapidly created and diffused, resulting in slippage of the DNA duplex rather then permanent rotation of the helix, it could be possible that these DNA defects might not affect the ability to translocate DNA.

Nucleosome accessibility and mobilization by chromatin remodeling enzymes

One common feature of all ATP-dependent chromatin remodeling enzymes is the ability to enhance the accessibility of nucleosomal DNA to nucleases and/or transcription factors. In most cases this activity of remodeling enzymes can be explained by the ATP-

dependent movement of nucleosomes in *cis* along a DNA fragment (Fan et al., 2003; Langst and Becker, 2001b; Langst et al., 1999; Logie and Peterson, 1997; Schnitzler et al., 1998; Varga-Weisz et al., 1997; Whitehouse et al., 1999).

Various chromatin remodeling enzymes, from different subfamilies, can mobilize mononucleosomes on short stretches of DNA (146-208bp) either to the end (SWI2/SNF2 family and recombinant ISWI) or to the center (CHRAC and dMi-2) of a DNA template (Brehm et al., 2000; Flaus and Owen-Hughes, 2003; Guschin et al., 2000b; Kassabov et al., 2002; Kassabov et al., 2003; Whitehouse et al., 1999). Some of the ISWI family of remodeling enzyme seem to have a preference for shifting mononucleosomes to a central position on the DNA template while others seem to randomize nucleosome positioning (Fan et al., 2003; Hamiche et al., 2001; Langst and Becker, 2001b). The mechanistic reason for the different directionality of nucleosome movements is still unknown. Flaus and Owen-Hughes used mononucleosome constructs containing additional DNA extensions flanking the nucleosome to investigate the ability of recombinant ISWI and SWI/SNF class chromatin remodeling enzymes (ySWI/SNF and RSC) to mobilize nucleosomes. They showed that mobilization by ISWI correlated with the thermally preferred positioning of nucleosomes on the DNA template. In contrast, the SWI/SNF and RSC complexes were shown to move nucleosomes to the ends of the DNA fragment, away from the thermally preferred position (Flaus and Owen-Hughes, 2003). In fact the SWI2/SNF2 family of complexes could shift the nucleosome off the end of the DNA fragment leaving the dyad axis of the nucleosome only 22 base pairs from one end. The ability of SWI/SNF to mobilize octamers off the ends of DNA fragments may explain

several novel features of SWI/SNF remodeled nucleosomes. First, SWI2/SNF2 complexes have been found to generate dinucleosome structures during remodeling of mononucleosomes (Lorch et al., 1998; Lorch et al., 2001; Phelan et al., 2000; Schnitzler et al., 1998). In addition a few studies have shown that chromatin remodeling enzymes can shift nucleosomes in *trans* from one template to another (Lorch et al., 1999; Phelan et al., 2000). One possibility is that as the nucleosome is pushed off the end of a fragment of DNA it is then able to be captured or "transferred" to either another fragment of DNA or by another remodeled nucleosome. Figure 5 illustrates a number of possible outcomes for remodeling on mononucleosome templates.

Recently, a study of the *Saccharomyces cerevisiae* Isw2 complex has provided evidence that nucleosome mobilization *in vivo*. In this study the researchers used a galactose inducible allele of *ISW2* to study changes in chromatin structure at the promoters of a pair of test genes. The data suggested that the changes were unidirectional and localized to only a few nucleosomes (Fazzio and Tsukiyama, 2003). However, since transcriptional repression was not measured in this study, it is still not clear if nucleosome mobilization directly correlates with the biological function of Isw2.

Disruption of nucleosome structure: Moving dimers around

An important and debated question in the field of chromatin remodeling is whether the histone octamer is disrupted during chromatin remodeling. Ten years ago it was put forth that remodeling by SWI/SNF and other chromatin remodeling enzymes might involve dissociation of the H2A-H2B dimers and/or alteration of the core histone

folds (Cote et al., 1994; Peterson and Tamkun, 1995). Histone-histone cross-linking studies have since shown that it is not absolutely necessary to disrupt nucleosome structure in order to allow restriction enzyme access and nucleosome mobility (Bazett-Jones et al., 1999; Boyer et al., 2000b). However, several recent results suggest that disruption of the H2A-H2B dimer can be catalyzed by some chromatin remodeling enzymes. Bruno and colleagues tested a number of ATP-dependent chromatin remodeling enzymes (ySWI/SNF, RSC, dISWI, ISw1a, and ISw1b) for the ability to exchange H2A-H2B dimers *in vitro*. Using fluorescently labeled histones they measured the ability of various remodeling enzymes to catalyze the exchange of histones from one chromatin substrate to another in an ATP-dependent fashion. SWI/SNF, RSC and ISw1b were able, to some degree, to transfer H2A-H2B dimers from a mononucleosome substrate to H3-H4 tetramers (Bruno et al., 2003). Dimers could also be exchanged from a circular nucleosomal array, but this reaction seems less efficient

Although it is not yet clear whether dimer exchange is relevant to the *in vivo* function of most remodeling enzymes, recent studies indicate that members of the INO80 family do indeed catalyze dimer exchange *in vivo*. Yeast contain two members of the INO80 family, Ino80 and SWR1. Each of these ATPases are subunits of large multi-subunit complexes. Unlike SWI/SNF and ISWI complexes, both Ino80 and SWR1 complexes contain histones as stoichiometric subunits (Mizuguchi et al., 2004). Three groups have recently published findings that the H2AZ variant histone copurifies with SWR1 complex and that this complex is required for the proper recruitment of Htz1 (yeast H2AZ) into chromatin *in vivo* (Kobor et al., 2004; Krogan et al., 2003; Mizuguchi

et al., 2004). Remarkably the SWR1 complex is able to swap H2AZ-H2B dimers for H2A-H2B dimers incorporated into *in vitro* nucleosomal arrays (Mizuguchi et al., 2004). *In vivo* deposition of Htz1 is also SWR1 complex-dependent at specific heterochromatic regions. It has been proposed that these remodeling complexes play a role in establishing boundaries for the spreading of heterochromatin (Owen-Hughes and Bruno, 2004). In this case the incorporation of H2AZ-H2B dimers might prevent the binding of SIR proteins at the boundary of heterochromatin, which are involved in the maintenance of silencing at telomeres. It is not yet clear how dimer-exchange relates to the other outcomes of chromatin remodeling (i.e. generation of torsion, DNA translocation, etc...).
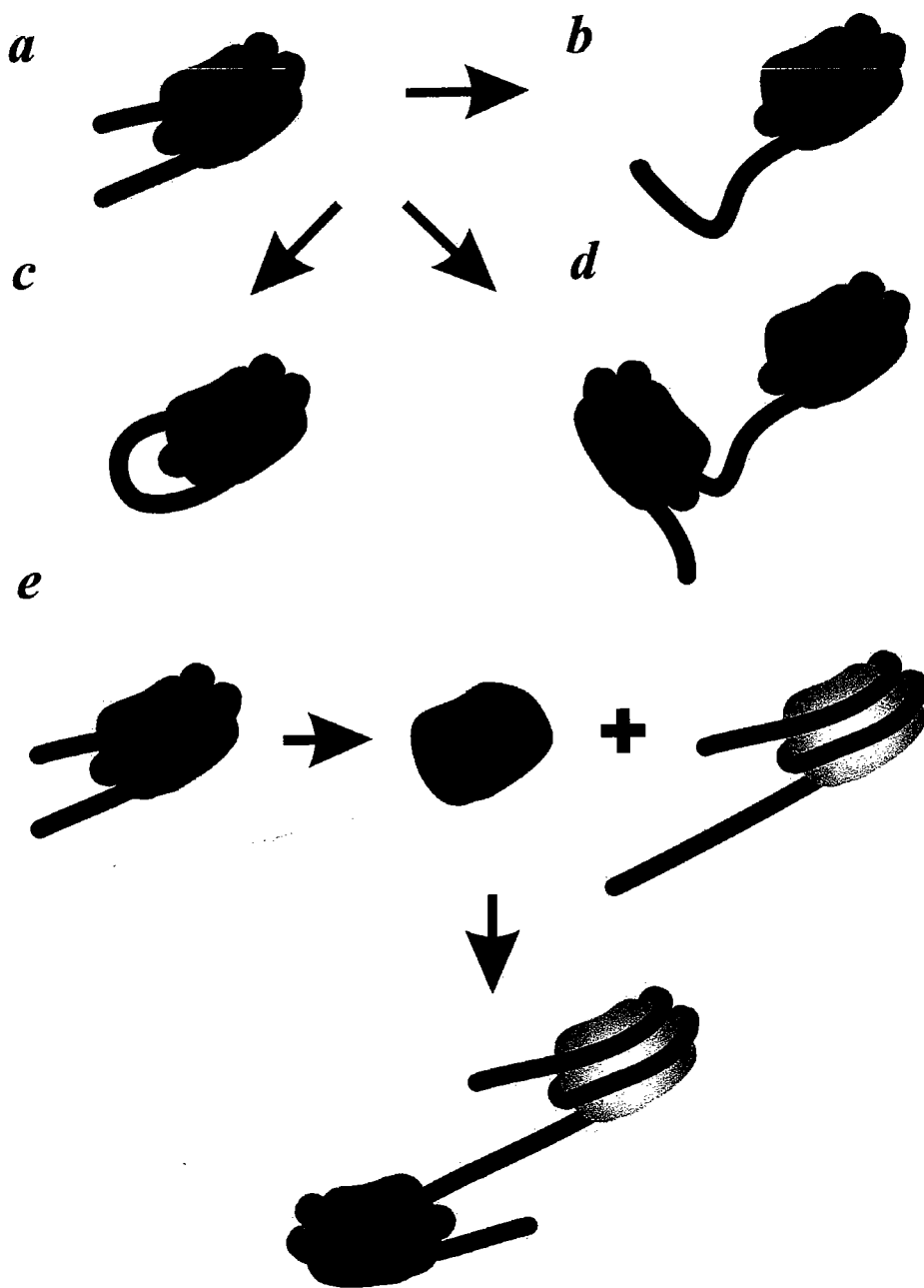
Figure 5. Generation of novel nucleosomal structures during octamer mobilization. This figure illustrates some of the phenotypes of *cis* and *trans* octamer mobilization seen in vitro in various chromatin remodeling assays. Nucleosomes (*a*) can move on stretches on DNA resulting in translocation (*b*), which in turn can result in the exposed end of the DNA fragment making novel contacts with the same nucleosome (*c*) or another remodeled nucleosome creating a dinucleosome (*d*). Nucleosomes can also move via octamer transfer in *trans*. The histone octamer can become disassociated from the first template and then become incorporated into a second nucleosomal array (*e*).

Using structural and mutational analysis to understand the mechanism of ATP-dependent chromatin remodeling.

As described in this chapter, the exact mechanisms of ATP-dependent chromatin remodeling are still not well understood. The research described in the next few chapters investigates how the *S. cerevisiae* SWI/SNF complex functions in chromatin remodeling by looking at structural and functional characteristics of the complex. This was done in two parts: first looking at the physical makeup of the complex and second by investigating the role of the Swi2p ATPase domain in the mechanism of chromatin remodeling.

In Chapter II the subunit stoichiometry and physical structure of the yeast SWI/SNF complex will be described. Determining the structure of these enzymes should yield important information about the physical interactions between the enzyme and its chromatin substrate. In Chapter III a mutational analysis of the Swi2p ATPase domain will be presented. The analysis in this chapter focuses on how ATP hydrolysis is linked to the mechanism of remodeling. Specific mutations were used to look at how the helicase/ATPase domain of SWI2p functions in the mechanism of chromatin remodeling. In Chapter IV the role of a specific ATPase motif is further characterized. Motif V appears to specifically couple ATP hydrolysis to chromatin remodeling. In Chapter V I will present a model that could explain how the SWI/SNF complex specifically interacts with nucleosomes to facilitate remodeling based on the research described in the previous chapters.

CHAPTER II

STRUCTURAL ANALYSIS OF THE YEAST SWI/SNF CHROMATIN REMODELING COMPLEX

Summary

Elucidating the mechanism of ATP-dependent chromatin remodeling is one of the largest challenges in the field of gene regulation. One of the missing pieces in understanding this process is detailed structural information on the enzymes that catalyze the remodeling reaction. Here, in Chapter II, we use a combination of subunit radio-iodination and scanning transmission electron microscopy (STEM) to determine the subunit stoichiometry and native molecular weight of yeast SWI/SNF complex. We also solved a 3-dimensional (3D) reconstruction of yeast SWI/SNF derived from electron micrographs.

This chapter was made possible due to a very fruitful collaboration between the Peterson lab and the Woodcock lab. Joan Flanagan performed the Swi2p immunoprecipitation experiments in Figure 6 and Rachel Horowitz-Scherer (Woodcock Lab) was responsible for the 3D reconstructions of SWI/SNF illustrated in Figures 11-14. The STEM mass analysis was performed at the Brookhaven National Laboratory STEM Facility for mass determination.

The data and the methods presented in this chapter were published in both **Nature Structural Biology**, Volume 10, no. 2 (February 2003) and **Methods**, volume 31, no. 1 (September 2003).

Introduction

Although it is clear that SWI/SNF plays key roles in the regulation of eukaryotic gene expression, the mechanistic basis for how SWI/SNF uses the energy of ATP hydrolysis to alter nucleosome structure still remains a major unsolved mystery. In addition little is known about the physical organization and actual interactions between SWI/SNF and nucleosomes. Bazett-Jones and colleagues used electron microscopy (EM) to look at SWI/SNF coupled to nucleosome arrays. In this study SWI/SNF was shown to bind to arrays and release DNA loops and create multiple nucleosome disruptions on the array (Bazett-Jones et al., 1999). This study further showed that DNA associated with individual remodeled nucleosomes decreases after ATP-dependent remodeling. Another group has used Atomic Force Microscopy (AFM) to image SWI/SNF remodeling on nucleosomal arrays with similar results (Schnitzler et al., 2001). Both of these studies showed that the SWI/SNF complex had a much larger discernable mass than a nucleosome core particle.

Little likewise is known about how the eleven subunits of SWI/SNF (Snf2p, Swi1p, Snf5p, Swi3p, Swp82p, Swp73p, Arp7p, Arp9p, Snf6p, Swp29, and Snf11p) interact to form this chromatin remodeling complex or how these individual subunits contribute to nucleosome recognition and remodeling. In this study we were interested in determining the physical organization of the *S. cerevisiae* SWI/SNF chromatin remodeling complex. To this end we used tyrosine iodination of purified SWI/SNF complex to determine the subunit stoichiometry. In addition we used scanning

transmission electron microscopy (STEM) and EM to obtain a 3D reconstruction of the SWI/SNF complex. The ultimate goal of this ongoing work is to understand how the SWI/SNF remodeling complex interacts with an individual nucleosome and nucleosomal arrays to facilitate remodeling.

Results

Subunit stoichiometry of yeast SWI/SNF.

It was first important to establish the relative stoichiometry of the eleven different SWI/SNF polypeptides. Previous gel filtration analyses have estimated the native molecular weight of both the yeast and human SWI/SNF complexes to be approximately 2 MDa (Cote et al., 1994; Kwon et al., 1994). These previous studies, however, only yielded a rough estimate for the native molecular weight of SWI/SNF since no protein standards larger than 660kDa were used in the analysis. Analysis of purified yeast SWI/SNF by SDS-PAGE suggests that each subunit is present at 1:1 stoichiometry, with the exception of the Swi3p subunit which stains more intensely with both silver and Coomassie blue. However, the summed molecular weights of the individual subunits of the SWI/SNF complex amount to a little over 1 MDa, suggesting the possibility that the SWI/SNF complex contains two copies of each subunit.

As a first step towards determining the stoichiometry of SWI/SNF subunits, we sought to determine the copy number of the Swi2p/Snf2p ATPase subunit. To this end, we used two different epitope-tagged alleles of Swi2p to create three different haploid yeast strains. Two control strains contained either a triple HA-tagged allele (SWI2-3HA) integrated at the URA3 locus, or an eighteen Myc-tagged allele (SWI2-18MYC) integrated at the chromosomal SWI2 locus. The test strain contained both epitope-tagged alleles. Importantly, each epitope-tagged allele was expressed from the normal SWI2

upstream regulatory region, and each epitope-tagged allele was able to complement the phenotypes of a *swi2* deletion allele, indicating that they are fully functional *in vivo*.

Whole cell extracts were prepared from each strain, and SWI/SNF was immunoprecipitated using antibodies specific to either the MYC or HA epitopes (Figure 6). In the case of the control strains, each antibody immunoprecipitated only the expected epitope-tagged Swi2p, confirming the specificity of these sera. In the test strain that contains both tagged alleles, immunoprecipitations with the α-HA serum precipitated only SWI/SNF complexes harboring the HA-tagged Swi2p. Likewise, the α-MYC sera immunoprecipitated the MYC-tagged allele of Swi2p, but not the HA-tagged allele of Swi2p. Thus, these results indicate that yeast SWI/SNF contains only one copy of the Swi2p ATPase subunit.

To determine the stoichiometry of the remaining SWI/SNF subunits, we performed quantitative tyrosine iodination (Kelleher and Gilmore, 1997). In this method, purified SWI/SNF is denatured in SDS, and tyrosines are labeled with ^{125}I in a chloramine T oxidation procedure. ^{125}I-labelled SWI/SNF complex was then electrophoresed on SDS-PAGE, and iodine incorporation was quantified using a PhosphorImager. Since the number of tyrosine residues is known for each SWI/SNF subunit, this method allows determination of the number of copies of each SWI/SNF subunit relative to the known, single subunit of Swi2p. In preliminary experiments, however, we found that ^{125}I-labeling of minor contaminating polypeptides in conventionally prepared SWI/SNF preparations occluded quantification of several SWI/SNF subunits.
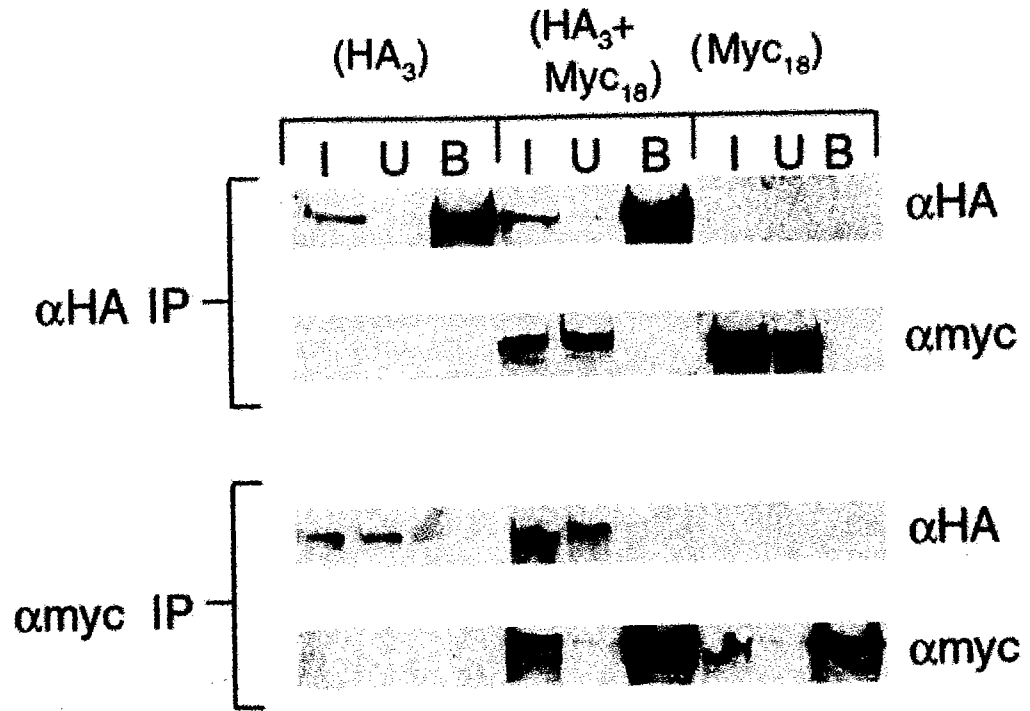
Figure 6. Swi2p is present in only one copy in yeast SWI/SNF. Swi2p was immunoprecipitated from whole cell extracts made from yeast strains CY831 (SWI2-HA₃), CY832 (SWI2-Myc₁₈) and CY889 (SWI2-Myc₁₈/SWI2-HA₃). Lanes are labeled I, U, and B for input (2.5%), unbound (2.5%), or bound (100%), respectively. Immunoprecipitation experiments were performed with either monoclonal anti-HA or anti-Myc immune sera. The presence of Swi2p was detected with either anti-HA or anti-Myc western blot analysis.

Design of yeast strains for high-purity SWI/SNF purification.

In order to improve the purity of SWI/SNF preparations, we used a tandem affinity purification (TAP) scheme (Rigaut et al., 1999; Tasto et al., 2001). The TAP cassette was designed to easily create purification constructs for both *Schizosaccharomyces pombe* and *S. cerevisiae* (Longtine et al., 1998; Tasto et al., 2001). The TAP-tag used in this case contains a Calmodulin Binding Domain (CBD) and four tandem copies of a Protein-A repeat separated by a TEV protease site (Figure 7a). We created a yeast strain harboring a *SWI2* gene with a TAP module inserted at the C-terminus. The *SWI2-TAP* allele is expressed under its endogenous promoter and this allele fully complements the phenotypes of a *swi2* deletion allele (Strain CY944, see Appendix Table A1 for genotype).

Purification of TAP-SWI/SNF and characterization of the complex.

Whole cell extracts were prepared from strain CY994, and SWI/SNF complex was purified by sequential affinity purification on IgG-agarose and calmodulin-agarose resins (Figure 7b). SWI/SNF purified by the TAP protocol was >90% pure by SDS PAGE analysis, and contained the diagnostic 11 polypeptides detectable by silver staining (Figure 7c). The affinity purified SWI/SNF elutes from a Superose 6 gel filtration column with an apparent molecular weight of 2 MDa (fraction 19, Figure 8) and the ATPase and nucleosomal array remodeling activities of this complex were also identical to that of SWI/SNF purified by standard chromatography (Cote et al., 1994).
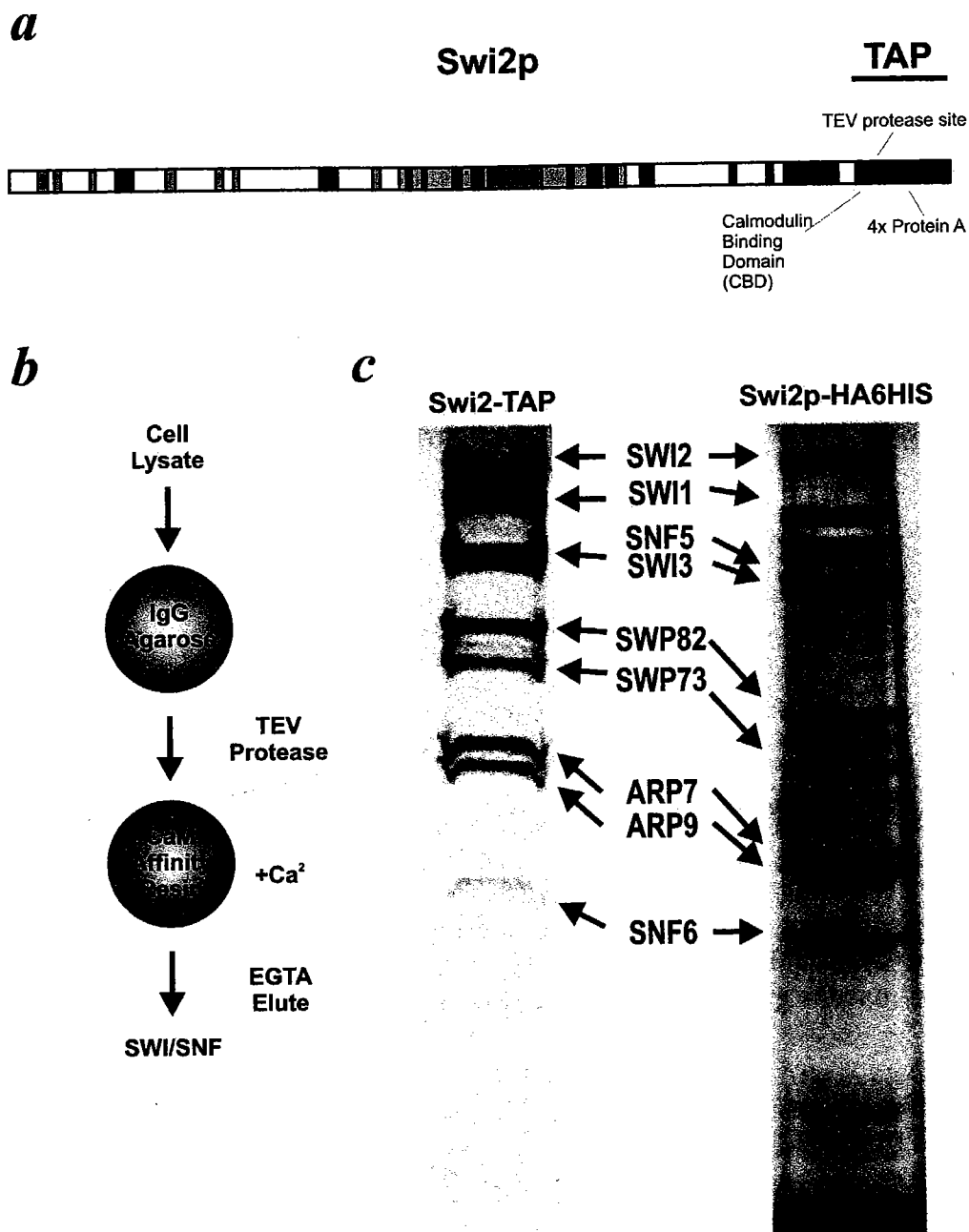
Figure 7. Tagging and purification scheme for ySWI/SNF stoichiometry determination. (*a*) The TAP tag used for SWI/SNF purification consists of a C-terminal cassette with a calmodulin binding domain and four tandem protein A repeats separated by a TEV protease site. (*b*) TAP purification scheme for ySWI/SNF. (*c*) Silver stain of TAP-SWI/SNF compared with HA6HIS-SWI/SNF
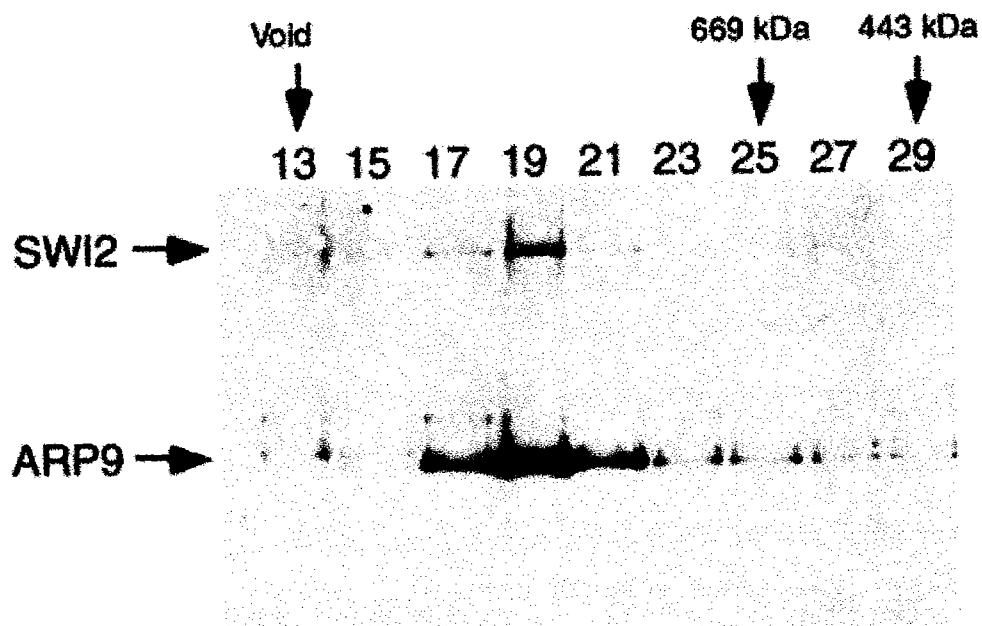
Figure 8. Gel filtration analysis of TAP-tagged SWI/SNF. A 100 µl sample of SWI/SNF purified by the TAP protocol was fractionated on a Superose 6 HR10/20 gel filtration column (Amersham) as described (Cote et al., 1994). The elution positions of protein standards are indicated at the top of the panel. Fractions were assayed for the presence of SWI/SNF using western blot analysis and polyclonal antibodies (Santa Cruz) to the Arp9p subunit, which also cross reacts with Swi2p.

Theory behind direct tyrosine iodination and its use for stoichiometry determination

To determine the stoichiometry of SWI/SNF we decided to use the technique of tyrosine iodination. Radio-labeling proteins with ^{125}I in the presence of the oxidizing compound Chloramine-T is a classic technique that has the advantages of being rapid, efficient and reproducible (Hunter and Greenwood, 1962). The Chloramine-T labeling method results in the majority of the radioisotope being incorporated into tyrosyl residues (see Figure 9). However, minor incorporation into histidyl and sulfhydral residues can occur (Parker, 1990). Altering the amount of time and the concentration of Chloramine-T can prevent non-specific labeling of the target proteins. For a more in depth discussion of radio labeling of proteins see (Parker, 1990).

In the application described here, labeling of tyrosine residues within each protein subunit provides a quantitative measurement of subunit stoichiometry (Kelleher and Gilmore, 1997). This technique assumes that the gene sequence is available for each subunit so that the number of tyrosines is known (and of course a subunit must contain at least one tyrosine in order to be analyzed by this method). In order for the stoichiometry to be accurate, the copy number of at least one subunit must also be known or else this method only yields the relative ratios among subunits. For example in the experiments described here, Swi2p was determined to be present in only one copy per yeast SWI/SNF (see Figure 6).
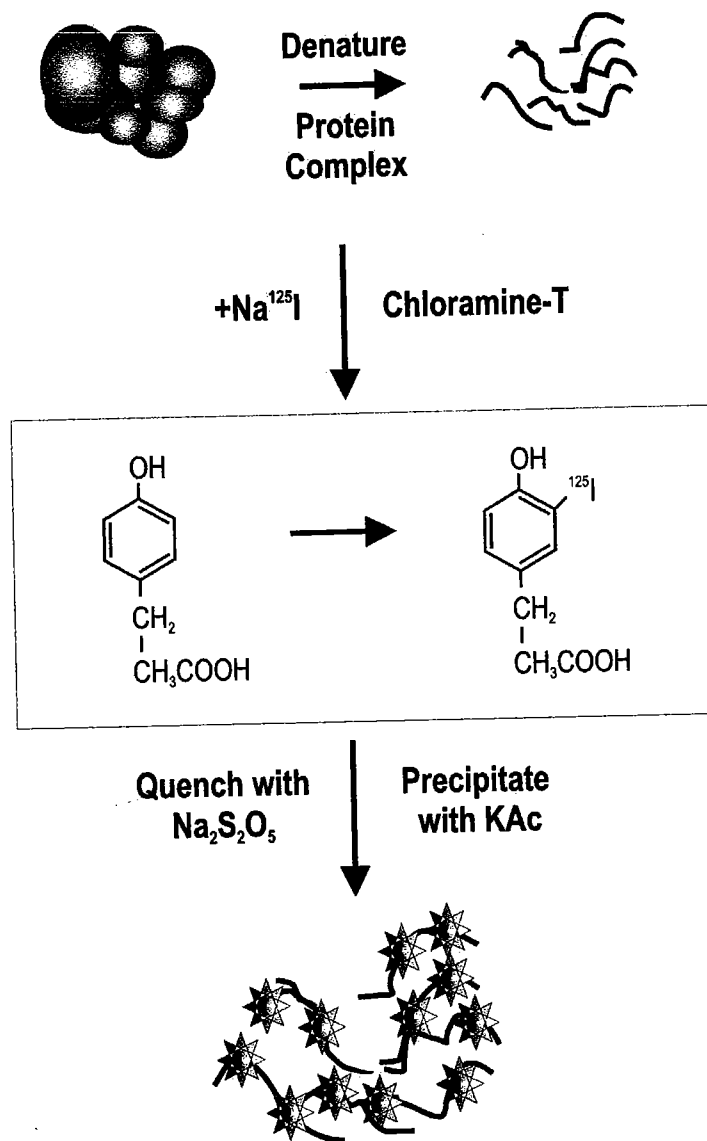
Figure 9. Schematic for Chloramine-T based iodination. The protein complex of interest is denatured by heating in the presence of 0.5% SDS at 50 °C. Incubation with Chloramine-T and ^{125}I is performed at room temperature for one minute and quenched with sodium metabisulfite ($Na_2S_2O_5$). The reaction is then precipitated with potassium acetate (KAc), dissolved in SDS loading buffer and subjected to SDS-PAGE gel electrophoresis. Relative stoichiometries are determined by signal strength quantification and calculations based on the number of tyrosines in each polypeptide.

Subunit stoichiometry determination of SWI/SNF by [125]Iodination

TAP-purified SWI/SNF was denatured in SDS and quantitatively radio-iodinated on tyrosine residues. Labeled SWI/SNF subunits were separated by SDS-PAGE, and iodine incorporation was quantified using a PhosphorImager and analysis performed with Imagequant v1.2 (Figure 10*a*). Signal strength per tyrosine residue was determined and compared to the Swi2p signal to determine relative stoichiometry (Figure 10*b*). The results of the tyrosine iodination indicate that six of the eleven subunits are present in single copy (Swi2p, Swi1p, Snf5p, Swp73p, Arp7p, and Arp9p). The other five are present in multiple copies (2 copies of Swi3p, Swp82p, Snf6p, and Snf11p; 3 copies of Swp29p). Based on this stoichiometry, SWI/SNF is predicted to have a calculated molecular mass of only 1.15 MDa.

a

Silver stain 10-20%   125I-labeled 10-20%   125I-labeled 8%
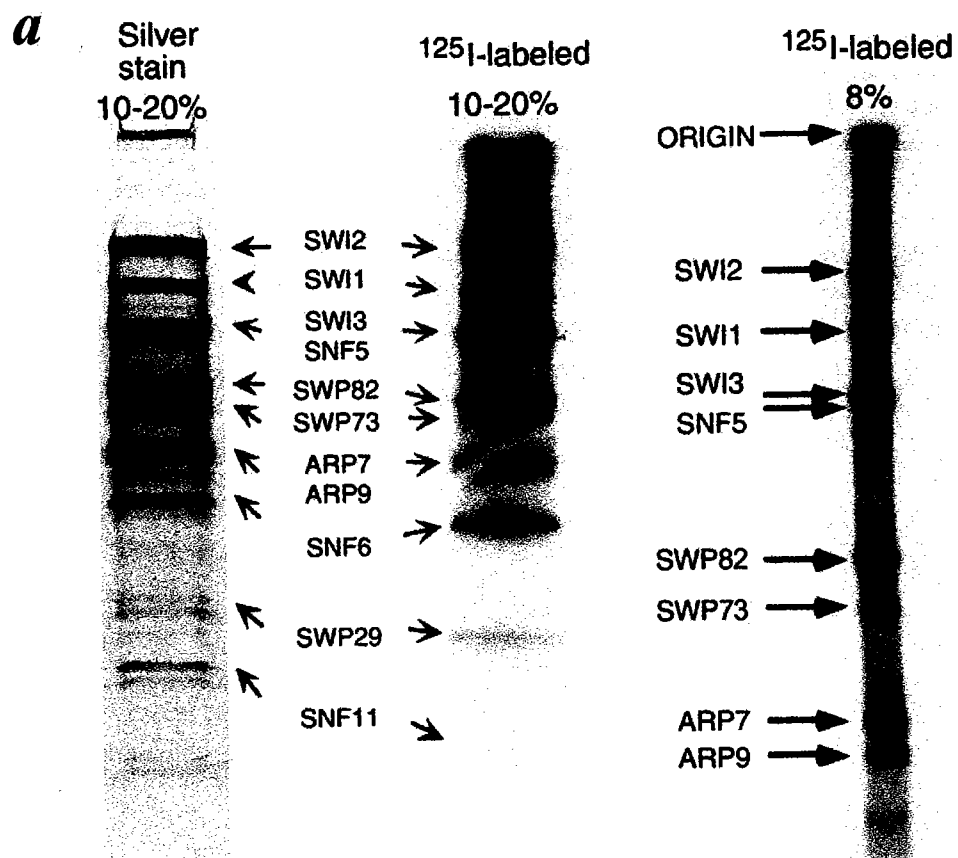
b

Subunit	Relative signal	Relative copy#
Swi2p	41942	1.00
Swi1p	43579	1.03
Swi3p	82711	1.97
Snf5p	49245	1.17
Swp82p	77149	1.84
Swp73p	49573	1.19
Arp7p	37645	0.90
Arp9p	27689	0.66
Snf6p	88938	2.12
Swp29p	130525	3.11
Snf11p	93373	2.22

Figure 10. Stoichiometry of the yeast SWI/SNF complex. Denatured SWI/SNF (5 pmols) was tyrosine-labeled with [^{125}I]NaI in the presence of chloramine T. Labeled complex was electrophoresed on SDS-PAGE gels (10-20%) and (8%) and subjected to analysis by densitometry using a PhosphorImager (Molecular Dynamics, Amersham). Signal intensity was determined per tyrosine in each subunit. Stoichiometry was determined by comparing the tyrosine signal strength of each subunit to that of Swi2p, which was determined to be present in just one copy in the complex. (*a*) ^{125}I-labeled SWI/SNF run on either 10-20% gradient or 8% SDS-PAGE gels compared with silver stain of same preparation. (*b*) PhosphorImager quantification of data shown in (*a*). Relative signal strength reflects the raw PhosphorImager signal normalized to tyrosine number. Copy number shown is relative to Swi2p. Similar results were obtained from several independent labelings and several different gel separations.

STEM Mass Analysis

As an independent method to determine the native molecular weight of ySWI/SNF, we used STEM, in which the linear relationship between electron scattering and sample mass provides accurate determinations up to 10 GDa (Wall et al., 1998). TAP-purified SWI/SNF was crosslinked with 0.1% glutaraldehyde (v/v) for 16 hrs in high salt buffer, freeze-dried on carbon films, and scattering data recorded (see Materials and Methods for details). SWI/SNF complexes, which appeared as roughly circular particles, were selected and the mass determined after correcting for the carbon film background. The histogram in Figure 11, which includes all particles (N=416) from several images, shows a unimodal distribution with a mean of 1.14 MDa (standard error ~20 kDa), in excellent agreement with the stoichiometric data.
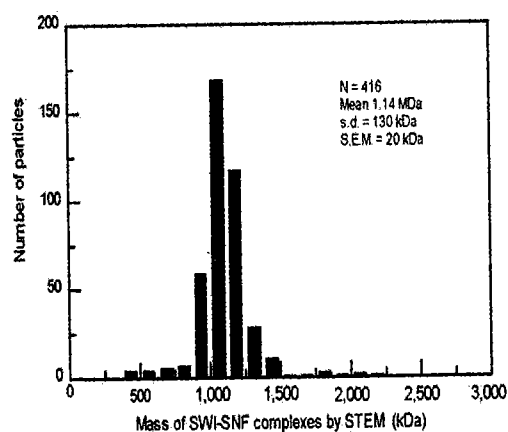
Figure 11. STEM mass analysis. STEM mass analysis of individual SWI/SNF complexes reveals a unimodal distribution with a mean of 1.14 MDa. TAP-purified SWI/SNF was crosslinked, applied to carbon films freeze dried and imaged by STEM. Scattering from individual particles were recorded, and converted to absolute mass. (s.d. = standard deviation, and SEM = standard error of the mean.

3D structure of SWI-SNF in negative stain

Although STEM provides accurate mass values, the images are generally less informative about structure, probably because of interactions with the carbon substrate and collapse during freeze-drying (Wall et al., 1998). To determine the 3D structure of the complex, we imaged TAP-purified SWI/SNF in neutral sodium phosphotungstate. The raw images indicated an oblate shape ~25 nm by ~12 nm, with several prominent lobes (Figure 12a). This is quite similar to the multi-lobed appearance of human SWI/SNF imaged by atomic force microscopy (Schnitzler et al., 2001). Single particle reconstruction (Ludtke et al., 1999) with three separate input data sets of ~5,000 to 10,000 images, resulted in 3D reconstructions with excellent agreement between class averages and their corresponding angular projections from the final reconstruction (Figure 12b, c, d). The three independent reconstructions were calculated with data from different isolations of SWI/SNF, each separately prepared for EM. The starting models were generated by reference-free classification, thereby avoiding the types of bias that can result from selection of external starting models. Very similar 3D shapes and volumes were derived from all three data sets; pair-wise comparisons indicating congruent structures to resolution ranging from 3.5 nm to 0.5 nm (see Materials and Methods section). A view of one reconstructed volume is shown in Figure 12e. The data have been low-pass filtered to a resolution of 3.0nm, and the surface is rendered to enclose a volume corresponding to a 1.14 MDa protein. For comparison, a representation of the nucleosome core particle (Luger et al., 1997) at the same magnification and resolution is shown (Figure 12f). Analysis of the 3D reconstructions revealed distinct

mass centers which may provide clues to the locations of the SWI/SNF polypeptides. Figure 13*d* shows their positions within the complex, and Figure 13*c* is an identical 'front' view in which surface lobes originating from individual centers are labeled. Centers 1-6 form a ring of lobes that create the rim of a large conical depression or pocket ~15 nm in diameter, and ~5 nm in depth. Other lobes appear to originate from centers 7 and 9-12 and are more clearly seen from other views of the complex (Figure 13*a, b, e, and f*). Mass center 8, which is located beneath the depression is unique in having no associated surface lobe. A preliminary analysis of SWI-SNF complexed with 200 bp of DNA did not reveal a unique DNA binding site (not shown), suggesting that a single SWI-SNF particle can bind DNA on multiple sites (Bazett-Jones et al., 1999). However, the distribution of additional mass in the same region as the ring of lobes labeled 1-6 in the DNA-containing reconstructions did suggest that the depression may be a possible DNA binding area.
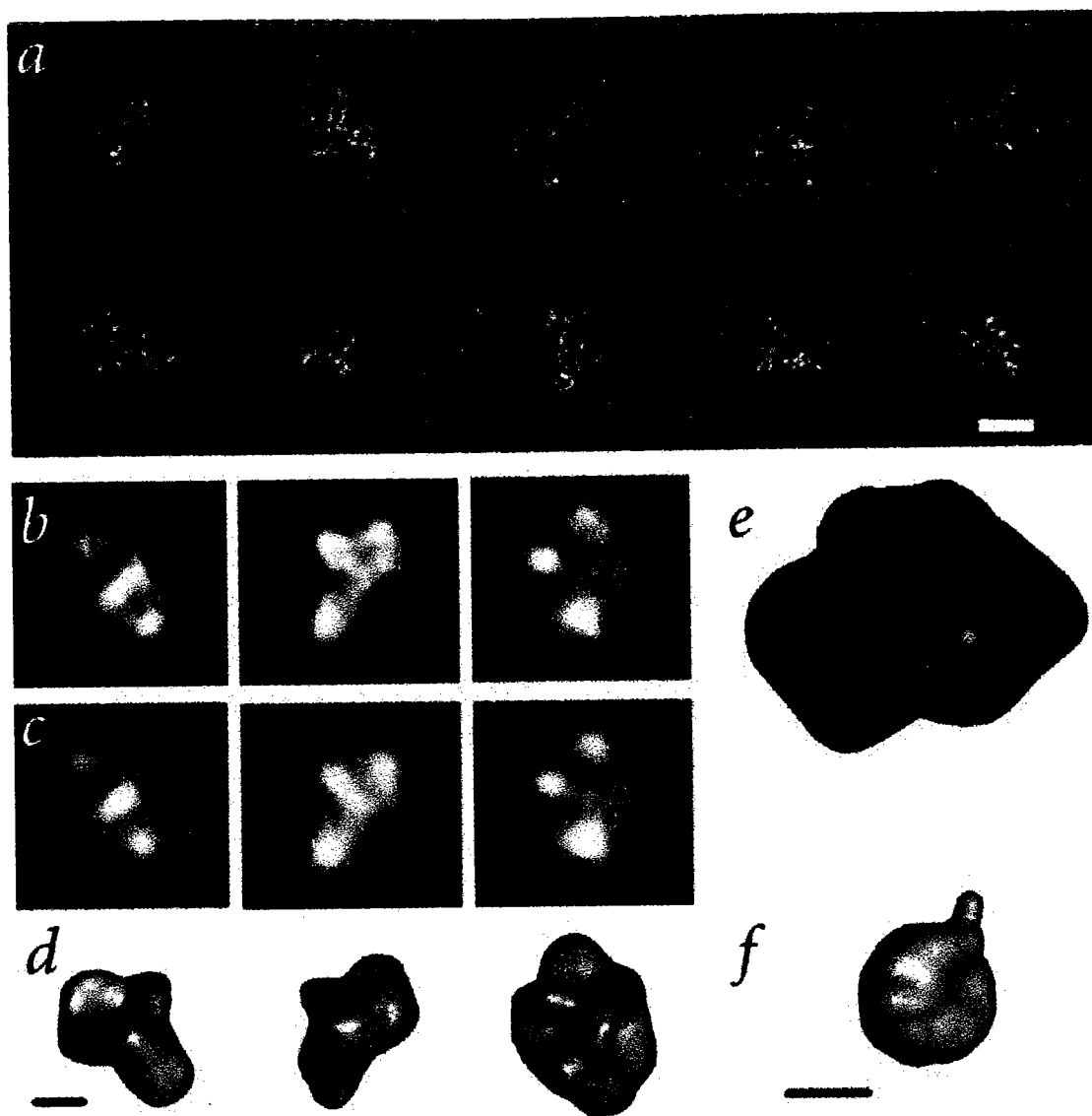
Figure 12. Three dimensional structure of the yeast SWI/SNF complex. (*a*) Raw images. (*b*) Examples of class averages identified by EMAN (Ludtke et al., 1999). (*c*) Projections of the final 3D structure at the same angles as the class averages show an excellent match between the two. (*d*) Rendered surface of 3D structure with the cone-shaped depression at top, filtered to 3.0 nm resolution. (*e*) Projection of SWI/SNF to compare to the rendered surface of the nucleosome core particle (*f*) (Luger et al., 1997), the SWI/SNF substrate, filtered to the same resolution. The scale bars in (*d*) and (*f*) represent 10 nm.
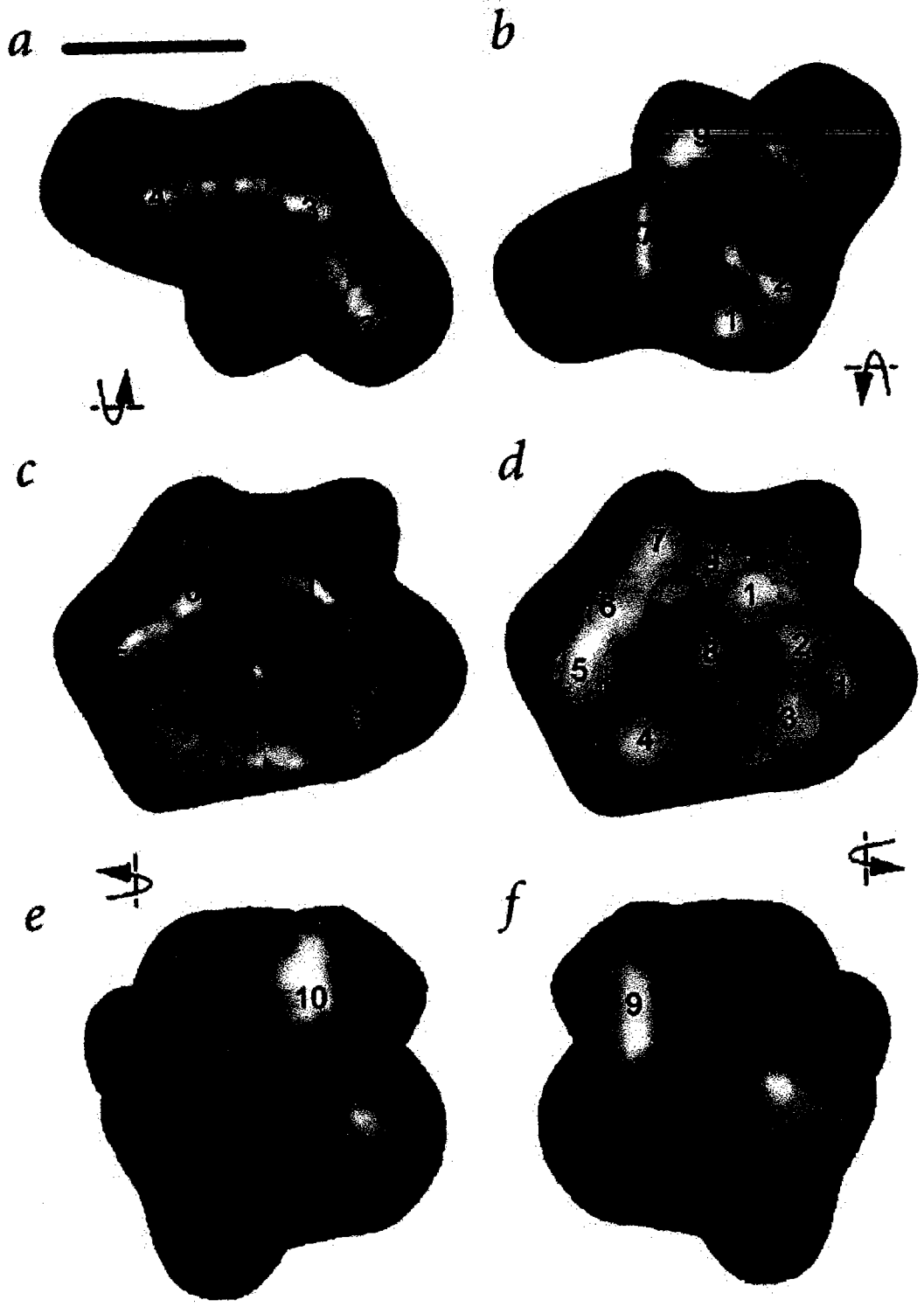
Figure 13. Principal features of the SWI/SNF 3D reconstruction. The views of the SWI/SNF complexe shown in (*a*) and (*b*) are 90° rotations about the horizontal plane of (*c*) and (*d*), the 'front' views, with the surface lobes origination from the individual centers labeled. In (*d*), the semi-transparent areas show the 12 centers of mass (numbered arbitrarily). Note that there is no corresponding lobe in (*c*) for mass center 8. In the other views, the surface lobes arising from each mass center are labeled. (*e*) and (*f*) are 90° rotations about the vertical plane of (*c*) and (*d*). The rim of the cone-shaped depression is formed from masses 1-6, with 8 near the base of the depression. The scale bar represents 10 nm.

Discussion

This work provides the first comprehensive characterization of the mass, polypeptide stoichiometry, and 3D structure of a low abundance, large multi-subunit chromatin remodeling complex, opening the way to identifying the active site of the SWI/SNF ATPase, the locations of the different polypeptides within the 3D volume, and the nucleosome interaction site(s).

The Swi2p immunoprecipitations and tyrosine iodination presented here show the first characterization of the subunit stoichiometry of a large chromatin remodeling enzyme. Half of the subunits in the complex exist in only a single copy including the catalytic subunit Swi2p, Swi1p, Swp73p, the Actin related subunits (Arp7p and Arp9p) and Snf5p. The other five subunits (Swi3p, Swp82p, Snf6p, Swp29p, and Snf11p) appear to be represented in multiple copies.

What does the stoichiometry results reveal about SWI/SNF function? There is only limited information available regarding the function of most of the subunits in ySWI/SNF, with the exception of Swi2p. We expect that a few of the subunits play specific roles in remodeling outside of the actual disruption of DNA-histone interactions. Other work has shown that the Arp7p and Arp9p subunits of both ySWI/SNF and RSC complex form a heterodimer in both of the complexes and that while this heterodimer is not necessary for the mechanism of chromatin remodeling it might play a possible role in contacting DNA-bending proteins (Szerlong et al., 2003). The stoichiometry of the

Arp7p and Arp9p confirms stoichiometry of the heterodimer and suggests that only one heterodimer is present in ySWI/SNF.

Two of the subunits of SWI/SNF (Snf5p and Swi1p) have been shown to interact with transcription activators in *S. cerevisiae* (Neely et al., 2002; Prochasson et al., 2003). It was also shown that while deletion of either of these subunits shows minor *in vivo* phenotype, deletion of both together results in a strong SWI/SNF phenotype (Prochasson et al., 2003). *SNF5*, as mentioned in Chapter I, has also been linked to cancer and plays an important part in early development in mammals (Roberts and Orkin, 2004). In our study Snf5p and Swi1p are each present in one copy suggesting that SWI/SNF has an asymmetric interaction with the nucleosomal substrate when targeted by transcriptional activators.

Swi3p is believed to play a role as a protein scaffold for the rest of the complex. In previous unpublished work by Joan Flanagan it was shown that Swi3p appears to bind numerous SWI/SNF subunits and that disruption of Swi3p affects SWI/SNF integrity (unpublished results). The stoichiometry data for Swi3p shows it to be present in two copies in SWI/SNF. Swi3p also contains SANT domains which suggest a possible role for SWI3 in stabilizing SWI/SNF-nucleosome interactions. This point will be expanded on further below.

Determining how ATP-dependent chromatin remodeling complexes interact with nucleosome(s) is an important part of understanding how chromatin remodeling occurs. Recently another group has solved a negative-stain based 3D EM-reconstruction of RSC complex, a SWI/SNF related ATP-dependent chromatin remodeling complex. This

complex, like SWI/SNF, appears to have a cavity of the right dimensions to accommodate a nucleosome core particle (Asturias et al., 2002). The RSC complex EM-reconstruction appears much flatter then the SWI/SNF structure. The actual shape of the structure is more akin to a C-clamp with a potential nucleosome binding site in the middle. The RSC complex appears to have a similar surface to the projections of our SWI/SNF reconstruction displayed in Figure 13 *c* and *d*. One of the major differences between these two complexes is that the RSC complex is smaller relative to a nucleosome than is the SWI/SNF complex. This is interesting due to the fact that the two complexes are of similar molecular mass (1.2 MDa for RSC and 1.14 MDa for SWI/SNF). This discrepancy might be explained by the fact that the SWI/SNF reconstruction is modeled to have a volume of 1.14 MDa calculated from the STEM results. The RSC 3D-EM reconstruction, on the other hand, didn't use a STEM-determined mass in order to correct for the structure volume. As we showed in this study, gel filtration has caveats for the determination of accurate masses for large flattened complexes.

Since our initial 3D-EM characterization of ySWI/SNF we have continued to refine our structure. Using cryo-EM reconstructions we have refined the reconstruction to a point where we can discern a more defined cavity in the complex (Figure 14). This cavity has the correct dimensions to accommodate a nucleosome core particle and mathematical modeling performed by Rachel Horowitz-Scherer suggests that there is only a 30° of freedom of rotation for the nucleosome in this pocket (see upper right panel in Figure 14). The histone H3 tail from the nucleosome core particle protrudes from the cavity. It is also interesting to note that there are projections to each side of the major

cavity that might correspond to specific subunits of SWI/SNF which could stabilize the nucleosome to allow remodeling to occur. These projections could make attractive candidates for the location of the Swi3p subunit as the SANT domains would be positioned to interact with the histone terminal tails. I will readdress this model and its implications in the Perspectives chapter, Chapter V.

Ongoing studies with the Woodcock lab are also underway to map specific subunits within the complex. We are currently trying to map the Swi2p subunit using a gold bead coupled to calmodulin. The Swi2p subunit contains a small calmodulin binding cassette (from the TAP tagging cassette) which will bind a gold bead-calmodulin conjugate, allowing us to localize Swi2p within the complex. Ultimately, we would like to visualize SWI/SNF bound to nucleosomal substrates. These studies are also currently underway. It will be interesting to see how SWI/SNF interacts with the nucleosome. Interactions between the SWI/SNF complex and the nucleosome core particle might give evidence for how histone tail domains interact with the enzyme complex and might indicate the possible location of subunits that interact with histone components (i.e. Swi3p).

Figure 14. Cryo-EM structure of the TAP tagged yeast SWI/SNF complex. A preliminary ~25 Å reconstruction of cryogenically prepared SWI/SNF. A more prominent cleft exists in this structure than in the negatively stained reconstruction (see Figures 12 and 13). The nucleosome core particle (Luger et al., 1997) is rendered to the same resolution as the SWI/SNF reconstruction. The nucleosome core particle can only rotate 30° within this cleft as illustrated in the upper right panel. There are also two lobes which appear to either side of the large cleft which could interact with the flat sides of the nucleosome. The location of the histone H3 N-terminus, dyad and DNA entry/exit sites on the nucleosome are labeled.

Materials and Methods

Tagged SWI2 strains and immunoprecipitations. Whole cell extracts were made from isogenic W303 yeast strains containing either an HA-tagged SWI2 at the *URA3* locus (CY831), an 18-Myc tagged SWI2 at the endogenous locus (CY832) or by combining both the HA and 18-Myc tagged SWI2 epitopes (CY889). Immunoprecipitations were conducted as previously reported (Cote et al., 1994) and binding was analyzed by SDS-PAGE and Western analysis with anti-HA (HA.11; Babco) or anti-Myc (9E10; Santa Cruz) antisera. Western plots were visualized using ECL reagents (Lumiglo; KPL).

SWI/SNF purification. SWI2 was C-terminally tagged in frame at the endogenous locus with a CBD-protein A TAP tag as previously described (Tasto et al., 2001). The primers used for tagging are as follows: SWI2F2a [CACAGATGAAGCGGACTCGAGCA TGACAGAAGCGAGTGTACG] and SWI2R1a [CGTATAAACGAATAAGTACTTA TATTGCTTTAGGAAGGTAGA]. Cultures were grown in YEP with 2% (w/v) glucose until OD_{600} of 2.0. Cells were harvested and lysed by mechanical bead lysis in E buffer (20mM Hepes pH 7.4, 350mM NaCl, 10% glycerol (v/v), and 0.1% (v/v) Tween and protease inhibitors). Lysates were clarified at 40,000 rpm at 4 °C for 60 minutes (Ti45 Beckman rotor). Cleared lysates were incubated with IgG-Agarose (Sigma) eluted by TEV protease (Invitrogen) cleavage and incubated with Calmodulin Resin (Stratagene) in E buffer plus 2 mM $CaCl_2$. Purified complex was eluted from Calmodulin Resin in E

buffer plus 10 mM EGTA. Samples were then concentrated and dialyzed against E buffer with 50 μM $ZnCl_2$. Purity was verified by silver-staining.

Stoichiometry determination of SWI/SNF. Purified TAP-SWI/SNF was denatured by the addition of SDS and labeled with $Na^{125}I$ in the presence of chloramine T for 2 minutes (Kelleher and Gilmore, 1997). Labeling was quenched by the addition of $Na_2S_2O_5$. Labeled material was precipitated with potassium acetate on ice for 30 minutes and diluted in protein sample buffer (See Figure 9). Labeled SWI/SNF was loaded on SDS-PAGE gels and ran at constant voltage. After electrophoresis, gels were fixed, and washed against 10% acetic acid (v/v) and 40% methanol (v/v) multiple times over 20 hours. Gels were dried, then imaged and densitometry performed using a PhosphorImager (Molecular Dynamics).

Gel filtration of SWI/SNF. One hundred microliters of TAP-SWI/SNF was fractionated over a Superose 6 HR10/20 gel filtration column (Amersham) as previously described (Cote et al., 1994). E buffer was run over the column at a rate 0.1 ml/min and 0.5 ml fractions were collected. Fractions were precipitated with TCA and dissolved in 2x sample buffer. Western blot analysis was used to identify fractions containing SWI/SNF subunits.

Scanning Transmission Electron Microscopy (STEM). For accurate STEM mass measurements, samples must be freed of salts and other buffer components. This was

achieved by crosslinking TAP purified SWI/SNF at ~100 nM in buffer E by direct addition of 0.1% (v/v) glutaraldehyde for 4h followed by dialysis against 50 mM NaCl, 10 mM HEPES pH 7.4, 0.2 mM EDTA, or by dialyzing overnight against E buffer containing 0.1% (v/v) glutaraldehyde without glycerol, zinc or Tween, then against the lower salt 50 mM NaCl buffer. Both methods resulted in stable SWI/SNF complexes with no significant difference in mean mass. Freeze dried specimens were prepared by the wet film method (Wall and Hainfeld, 1986; Wall et al., 1998) and imaged at the Brookhaven National Laboratory STEM Facility. Two µl of 100 µg/ml tobacco mosaic virus (TMV), an internal mass standard, were absorbed for 1 minute onto freshly prepared carbon films supported by a holey film on a titanium grid. After washing the grid four times, 3 µl of fixed SWI/SNF solution was applied by injection into the droplet on the grid. The grid was allowed to adsorb for 1 minute, then rinsed 4 times with sample buffer, followed by 100 mM ammonium acetate (~5 times) and 20 mM ammonium acetate (~5 times) to remove non-volatile salts. After the final wash, the grid was blotted between two pieces of filter paper, leaving a retained layer less than 1 µm thick, and immediately plunged into liquid nitrogen slush. The frozen samples were transferred to an ion-pumped chamber and freeze dried overnight by gradually warming to -80°C. They were then transferred under vacuum to the STEM. Specimens were imaged in the STEM at 40 kV with a probe focused to 0.25 nm. Focusing was at a high magnification near the area of interest and the data acquired on the first scan. The average dose of electrons for the single scan to record the data was less than 1000 e^-/nm^2, assuring that the mass loss from radiation damage was no more than 2% at the -150°C

specimen temperature (Wall et al., 1998). Digital images were recorded from large and small angle detectors for unstained specimens. In images used for mass measurements, the pixels were separated by 1 nm giving a scan width of 0.512 μm. The masses of selected particles were determined using the program PCMass23 (Hainfeld et al., 1982) (written by J. Wall for PCs). This program sums the number of scattered electrons over a defined area bounding the particle, subtracts a background obtained from areas not containing particles, and multiplies the result by a standard STEM calibration constant (115 Da/electron with 1nm pixels) to determine the mass. Further data analysis and histogram generation employed PSI Plot (Polysoftware International, Pearl River, NY).

Electron Microscopy and 3D image reconstruction. Crosslinked SWI/SNF was adsorbed to glow-discharge carbon films, negatively stained with 1.5% sodium phosphotungstate (w/v) pH 7.2 containing 0.015% glucose (w/v) (Woodcock et al., 1991), and observed with a Tecnai 12 electron microscope (FEI Inc) at 80 kV. Digital images were recorded at 800 nm defocus with a cooled 2048x2048 CCD camera (TVIPS GMBH, Munich, Germany) and a pixel size of 6.32Å. Data sets for reconstruction contained 5,000 to 10,000 images free of astigmatism and drift. Examination of the data sets showed that there was no preferential orientation of SWI/SNF on the carbon film.

Single particle reconstruction was carried out with the EMAN program (Ludtke et al., 1999) (ncmi.bcm.tmc.edu/~steve/EMAN). First, an initial model was generated by reference –free classification. This starting model was then utilized to begin an iterative refinement of the classification. Convergence was judged by the absence of change in

the Fourier Shell Correlation (FSC) of subsequent iterations (Ludtke et al., 1999). The resolution of each reconstruction was estimated using the FSC of two semi-independent reconstructions derived by dividing the data in the final class averages in half (Ludtke et al., 1999). FSC was also used to evaluate the similarity of the three different reconstructions, using the 0.5 value as the limit of congruence. Volumes were constrained to a mass of 1.14 MDa, assuming a protein density of 1.35 g/ml (0.81 Da/Å^3), and Gaussian low-pass filtered to the 0.5 FSC threshold. Data processing and visualization with AVS (AVS Inc, Waltham, MA) and VIS5D (vis5d.sourceforge.net) was performed on a multiprocessor Silicon Graphics Octane (SGI Inc., Mountain View, CA).

CHAPTER III

CHARACTERIZING HOW ATP HYDROLYSIS LEADS TO

CHROMATIN REMODELING BY SWI/SNF

Summary

In this chapter I will show the kinetic characterization of a number of SWI/SNF ATPase defective complexes using a variety of ATPase and chromatin remodeling assays. I propose that motif V of the ATPase domain of SWI/SNF might be involved mechanism of ATP-dependent chromatin remodeling. Little is known about the role of specific motifs in Domain II of the SF2 ATPase domains especially for proteins like Swi2p that share homology to helicases but do not display the typical unwinding activities of these enzymes. In this study I use a number of mutations, with known *in vivo* phenotypes, to elucidate the role of specific motifs in the Swi2p ATPase domain. Interestingly, the data shown here suggest an ability of motif V amino acid substitutions to uncouple ATPase activity from the generation of superhelical torsion. Further characterization of this motif and its role in chromatin remodeling will be presented in Chapter IV.

This work was aided by initial characterizations of *swi2* mutants performed *in vivo* by Emily Richmond, a former student in the Peterson lab. Endonuclease VII used in the cruciform extrusion experiments was provided as a gift by Tom Owen-Hughes of the

University of Dundee in Dundee, Scotland. Eric Merithew rendered the PcrA structure in Figure 25b using PyMOL based on the PDB coordinates.

Introduction

A major goal of the chromatin remodeling field is to understand the mechanism of coupling ATP hydrolysis to nucleosome disruption. In this chapter I will present a study of specific mutations in the ATPase domain of yeast SWI2/SNF2 and how these mutations affect the process of chromatin remodeling. The data shown here also suggests that specific mutations within a highly conserved motif of the SWI2/SNF2 family of ATPase domains uncouple ATPase activity from the process of chromatin remodeling.

The hallmark of the Swi2p family of chromatin remodeling enzymes is that they all contain a highly conserved ATPase domain related to the SF2 family of DNA and RNA helicases (Eisen et al., 1995). These ATPases can act as a single subunit (hBrg1 for example) or in concert with a variable number of other subunits to remodel chromatin. The yeast SWI/SNF complex is one of the better understood of the large (>1 MDa) multi-subunit remodeling complexes. It contains 11 subunits, and genetic studies have shown that it is required for expression of a subset of inducible genes in *S. cerevisiae* as well as gene expression in mitosis (Fry and Peterson, 2001). Numerous studies have been conducted to understand the mechanisms by which SWI/SNF and its homologs remodel chromatin. As was described in Chapter I, ySWI/SNF and homologs have been found to affect chromatin in numerous ways. These enzymes are able to mobilize nucleosomes, promote accessibility to restriction enzyme sites occluded by nucleosomes, transfer histone octamers from one chromatin array to another array, and create superhelical torsion on DNA, either alone or in the context of chromatin (Peterson, 2002a). While,

the exact mechanism(s) that underlie theses activities are not well understood, it is believed that these activities are all linked in the process of chromatin remodeling.

The 1708 amino acid yeast SWI2 protein contains a highly conserved ATPase domain fold similar to known helicases in SF1 and SF2 families (Figure 15), as well as two AT hook motifs and a C-terminal bromo domain (Figure 16). The ATPase domain of Swi2p contains a large insertion between the conserved N-terminal subdomain I (motifs I-III) and C-terminal subdomain II (motifs IV-VI) of the SF2 family helicase domain (Figure 16). This insertion is specific to the SWI2/SNF2 family of ATPases and is highly conserved. I will refer to this as the Swi2p subdomain in the remainder of this text.

More biochemical information exists for the N-terminal subdomain motifs (ATP binding and hydrolysis, motifs I-III) of helicases and ATPases than does for the C-terminal subdomain motifs (possible role in energy transduction, motifs IV-VI). This is due in part to the highly conserved nature of the N-terminal subdomain for it is found in other ATPases that are not helicases such as the recombination protein RecA (Caruthers and McKay, 2002). Both subdomains I and II contain a repetitive alpha-beta fold that is tightly conserved in all helicases with solved structures to date. Crystal structures of SF2 helicases like PcrA, NS3 and eIF4a (for schematics of these enzymes see Figure 15) have revealed some possible insight on the function of individual motifs (Caruthers and McKay, 2002).

How is ATP used by chromatin remodeling enzymes to generate nucleosome disruption and mobility? Mutational analyses of helicases and other ATPases show that

certain residues, mostly in subdomain I, are critical for ATP hydrolysis. A highly conserved lysine (K798, in Swi2p) in the P-loop (motif I) is critical for ATP γ-phosphate binding. Disruption of this lysine always results in a catalytically dead enzyme. Furthermore, structural information from a number of SF1 and SF2 helicases has shown a strong conservation of the roles for most of the motifs in subdomain I (motifs I, Ia, and II, where motif III is an exception) which all play roles in the ATP hydrolysis cycle (Caruthers and McKay, 2002). The structural information for the motifs in subdomain II (motifs IV-VI) shows less conservation and it has been proposed that these motifs might play specific roles for each individual subfamily of enzymes.

In this chapter I will show the results of biochemical characterizations of various amino acid substitutions within the Swi2p ATPase domain as well as how these mutations affect aspects of chromatin remodeling. I also show evidence that motif V within the ATPase domain plays a critical role in the generation of DNA superhelical torsion, which will be the focus of Chapter IV.

RecA

Schematic

Walker "A": GxxxGKT
Walker "B": D144
Q194
E96

III: Sensor I
IV
I: Walker "A"
II: Walker "B"
Ia
(OXXR)
(TXGX)

VI   V
Domain 2   Domain 1

N—

PcrA/Rep   UvrB

C   N

eIF4A   HCV

C   N

T7gp4/RepA   RuvB

C   N

C   N
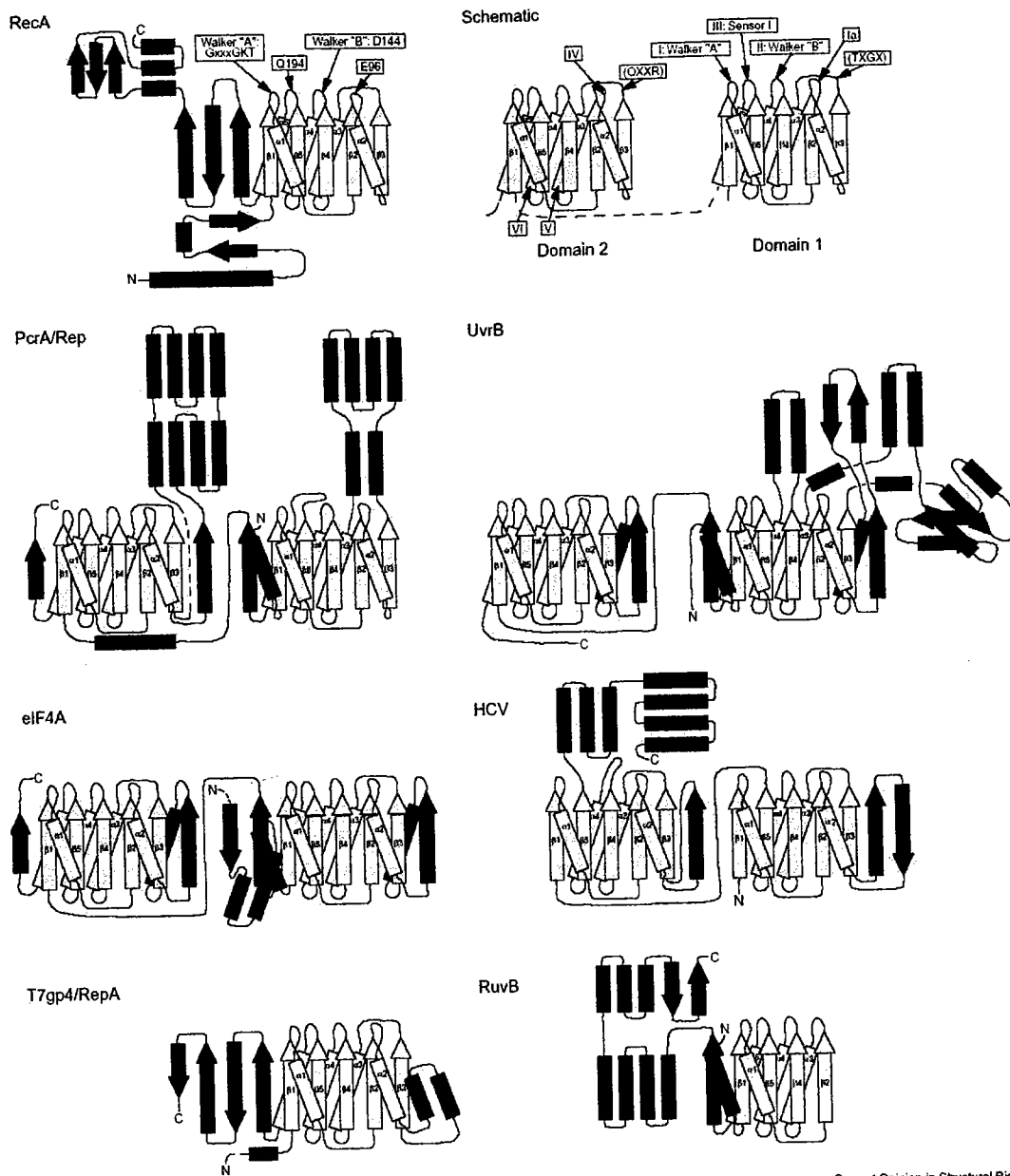
Figure 15. Schematic of helicases with known crystal structures. This figure illustrates the similarity between helicases in the SF1 and SF2 superfamilies. The top right panel contains a generalized schematic of a helicase with the conserved motifs labeled. Alpha helices and beta sheets are numbered from the N-terminus to C-terminus. The canonical alpha-beta fold is illustrated in yellow. Enzyme specific insertions within subdomains I and II are colored red. Blue and green secondary structures represent alpha helices and beta sheets that fold into enzyme specific sub-domains (Caruthers and McKay, 2002)
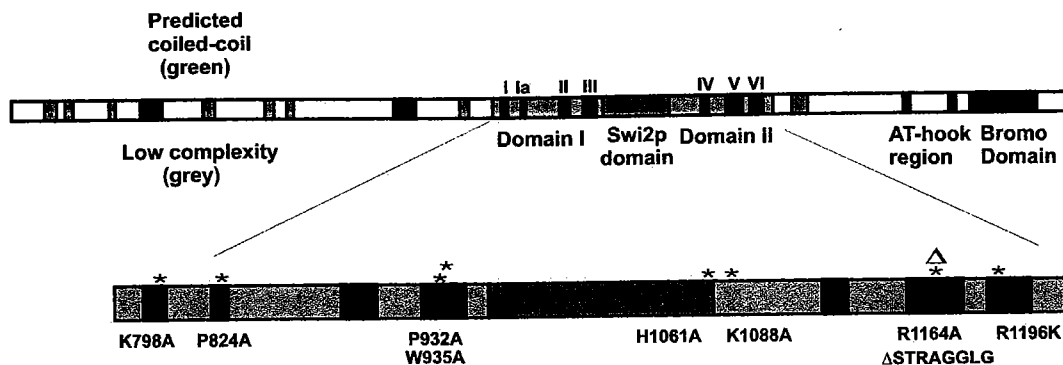
Figure 16. Schematic of the Swi2p protein from *S. cerevisiae*. This cartoon depicts the key features of yeast Swi2p. The ATPase domain (orange with the conserved ATPase/helicase domains in black) of Swi2p is enlarged to illustrate the location of the amino acid alterations used to study the function of this ATPase in this chapter. Roman numerals correspond to the ATPase motifs and Domains I and II represent the conserved alpha-beta repeat domains illustrated in Figure 15. The Swi2p-specific region of the ATPase domain is depicted in dark orange to distinguish it from subdomains I and II. Along with the ATPase domain Swi2p also contains two AT-hook regions (dark blue) and a Bromo domain (red) in the C-terminus of the protein. The N-terminus of the protein contains numerous regions of low complexity (grey) and two predicted coiled-coil domains (green).

Results

Swi2p amino acid alteration containing SWI/SNF complex constructs and purification.

Swi2p is the founding member of a subfamily of enzymes within the SF2 helicase-like family based on the high homology shared within the ATPase domain (See Chapter I: Introduction and Figure 17). Previously, a mutational analysis of the ATPase domain had been performed to investigate the *in vivo* phenotypes of a number of these highly conserved residues (Richmond and Peterson, 1996). Point mutation were made that altered highly conserved residues in specific positions in a number of these ATPase domains as well as other residues in the SWI2/SNF2-specific sub-domain, and the affect on expression of a number of SWI/SNF-dependent genes was investigated. A summary of the *in vivo* phenotypes of these mutants from this study can be found in Table 1. In this study I used a number of these point mutations to investigate the role of specific ATPase motifs in the mechanism of chromatin remodeling *in vitro* (See Figures 16, 17 and Table 1).

The TAP tagging cassette (see Chapter II) was used for the purification of the individual complexes. Because several mutant strains were genetically impaired, the scheme used to purify these complexes was slightly different than the procedure used to purify the wild-type SWI/SNF complexes described previously (Smith et al., 2003; Smith and Peterson, 2003). Previously constructed ATPase mutant-HA6HIS strains were used to generate the *swi2*-TAP constructs (Richmond and Peterson, 1996). These mutant

MATα strains were crossed with a *MATa* strain containing a wild type copy of SWI2 to create diploids (see Yeast Strain list, Table A1 in appendix for genotype of yeast strains). A TAP tag construct was inserted to replace the HA6HIS tag on the mutant allele of SWI2 in these diploids (Figure 18). The WT copy of SWI2 in these diploid strains allowed easier purification from mutant strains by rescuing the slow growth phenotype of these mutants. Complexes were purified using the same TAP strategy as previously reported (Smith et al., 2003; Smith and Peterson, 2003). Previously, SWI/SNF complexes (SWI2-HA6HIS) harboring amino acid alterations were tested for complex integrity by subjecting whole cell lysates to gel filtration chromatography and analyzing subunit composition by western blot analysis (Richmond and Peterson, 1996). Complex integrity of the TAP-tagged complexes was confirmed by both western blot analysis and silver staining (Figure 19). The results confirmed that the purified complexes were intact, including the ΔSTRAGGLG motif V deleted Swi2p variant.

Motif I / Motif Ia

```
                    wwwwwww        wwwwwwwwwwwwwwwww                    wwwwww
SWI2 Sc        780  slfnnhlngIIADEMGLGKTIQtislltylyemknirgpylVIVPLSTlsnwssefakwap
SPCC830.01c    882  slynnnlnglIADEMGLGKTIQtiafityliekknqggpflIIVPLSTltnwimefekwap
BRG1 Hs        767  slynnnlnglIADEMGLGKTIQtialitylmehkringpflIIVPLSTlsnwayefdkwap
BRM Dm         786  slynnnlnglIADEMGLGKTIQtislvtylmdrkkvmgpyLIIVPLSTlpnwvlefekwap
Mi-2b Mm       732  fswaggtdtIIADEMGLGKTVQtavflyslykeghskgpfLVSAPLSTiinwerefemwap
ISW1 Sc        209  slhknkiagILADEMGLGKTLQtisflgylryiekipgpflVIAPKSTinnwlreinrwtp
INO80 Sc       719  nlydqgingILADEMGLGKTVQsisvlahlaenhniwgpflVVTPASTlhnwvneiskflp
```

Motif II / Motif III

```
                    wwwwwww                              wwwwwwwwwwwwwwww
SWI2 Sc        881  allSKVKWVHMIDEGHRMKNaqsklsltlnthyhadyrLILTGTPLQNNLPELWALLNFvlpkifnsvksfdewfntpf
SPCC830.01c    983  pllSRIKWVHMIDEGHRIKNtqskltstlstyyhsqyrLILTGTPLQNNLPELWALLNFvlpkifnsiksfdewfntpf
BRG1 Hs        868  hilAKIRWKYMIVDEGHRMKNhhckltqvlnthyvaprrLLLTGTPLQNKIPELWALLNFllptifkscstfeqwfnapf
BRM Dm         887  avlAKIQWKYMIIDEGHRMKNhhckltqvlnthyiapyrLLLTGTPLQNKIPELWALLNFllpsifkscstfeqwfnapf
Mi-2b Mm       853  ailGSIDWACLIVDEAHRLKNnqskffrvlngyslqhk-LLLTGTPLQNNLEELFHLLNFltperfhnlegfleefadia
ISW1 Sc        310  splKKINWEYIIIDEAHRIKNeesmlsqvlreftsrn-rLLITGTPLQNNLHELWALLNFllpdifsdaqdfddwfsses
INO80 Sc       828  nylQKMKWQYMILDEAQAIKSsqssrwnllsfhcrn-rLLLTGTPIQNSMQELWALLHFimpslfdshdefnewfskdi
```

Motif IV / Motif V

```
                        wwwwwww                 wwwwwwwwwwwwwwwwww
SWI2 Sc        1103 ghrvLIFFQMTQimdimedflryinikylrldghtksdersellrlfnAPDSEYLCFII   R LNLQTADTVIIFDtdwnphqdlqaqd
SPCC830.01c    1203 ghktLMFFQMTQimtimedylrsknwkylrldgstksddrcsllaqfnDPKSDVYIFMI   R LNLQTADTVIIFDtdwnphqdlqaqd
BRG1 Hs        1096 nhkvLLFCQMTSlmtimedyfayrgfkylrldgttkaedrgmlktfnEPGSEYFIFLI   R LNLQSADTVIIFDsdwnphqdlqaqd
BRM Dm         1114 nhrvLLFCQMTQcmtliedylgwrqfgylrldgttkaedrgelrkfnAKGSDVEVFLI   R LNLQTADTVVIFDsdwnphqdlqaqd
Mi-2b Mm       1059 ghrvLIFSQMTKmldllediflehegykyeridggitgmrqeaidrfnAPGAQQFCFLI  R INLATADTVIIYDsdwnphndiqafs
ISW1 Sc        528  gsrvLIFSQMSRlldledycyfrnyeycridgstahedriqaiddynAPDSKKFVFLI   R INLTSADVVVLYDsdwnpqadlqamd
INO80 Sc       1315 ghrvLIYFQMTKmmdlmeeyltyrqynhirldgsskledrrd-lvhdwQTNPEIFVFLI  R INLTAADTVIFYDsdwnptidsqamd
```

Motif VI

```
                    wwwwww        wwwwwwwwwwwwwwwwwwww
SWI2 Sc        1186 nphqdlQAQDRAHRIGQKNEVRILRLIITnsveevileraykkld
SPCC830.01c    1286 nphqdlQAQDRAHRIGQTKEVRILRLITEksieenilsraqykld
BRG1 Hs        1179 nphqdlQAQDRAHRIGQQNEVRVLRLCTVnsveekilaaakykln
BRM Dm         1197 nphqdlQAQDRAHRIGQRNEVRVLRLMTVnsveerilaaarykln
Mi-2b Mm       1142 nphndiQAFSRAHRIGQNKKVMIYRFVTRasveeritqvakkmm
ISW1 Sc        601  npqadlQAMDRAHRIGQKKQVKVFRLVTDnsveekileratqklr
INO80 Sc       1397 nptidsQAMDRAHRLGQTRQVTVYRLLVRgtieermrdrakqkeq
```

Figure 17. Sequence alignment of chromatin remodeling ATPases. The strong conservation of the ATPase domains of a number of catalytic subunits from different chromatin remodeling complexes are shown here. The black bars represent the regions containing the SF2 helicase motifs. The predicted secondary structure is represented above the sequence. Residues outlined in green (or red in case of ΔSTRAGGLG) are the residues that are mutated and used in this study. [**Sc**] *Saccharomyces cerevisiae,* [**Hs**] *Homo sapiens,* [**Dm**] *Drosophila melanogaster,* [**Mm**] Mus Musculus. SPCC830.01c is the Swi2p homolog from *Schizosaccharomyces pombe.*
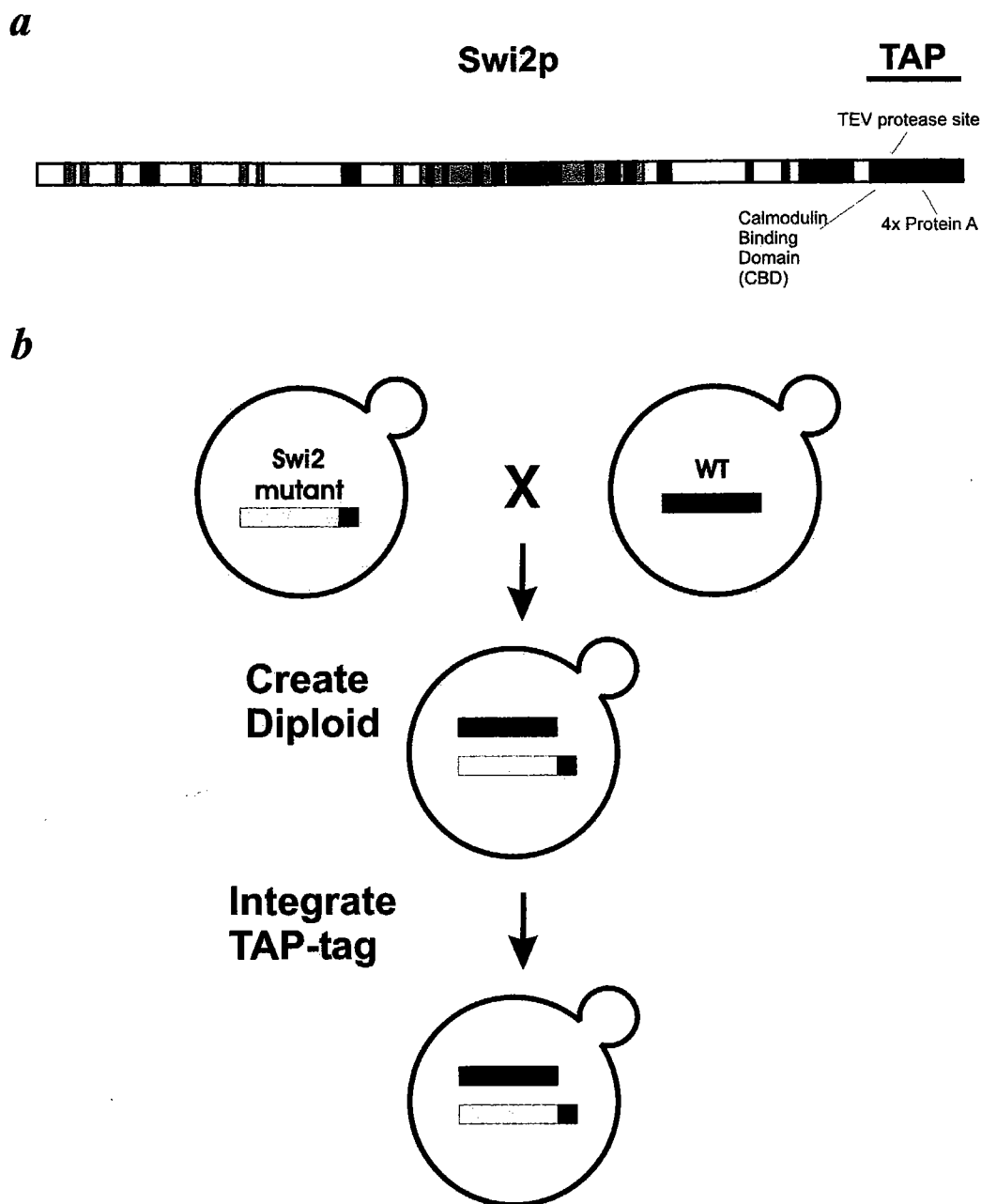
Figure 18. Strategy for the purification of ATPase-defective SWI/SNF complexes. Diploid strains were created to aid expression and purification of the SWI/SNF complexes containing amino acid substitutions in the Swi2p ATPase domain. Homologous recombination was used to specifically TAP-tag the mutant *swi2* allele in the diploids (see Materials and Methods). This strategy was used to purify all of the amino acid substitution containing complexes.
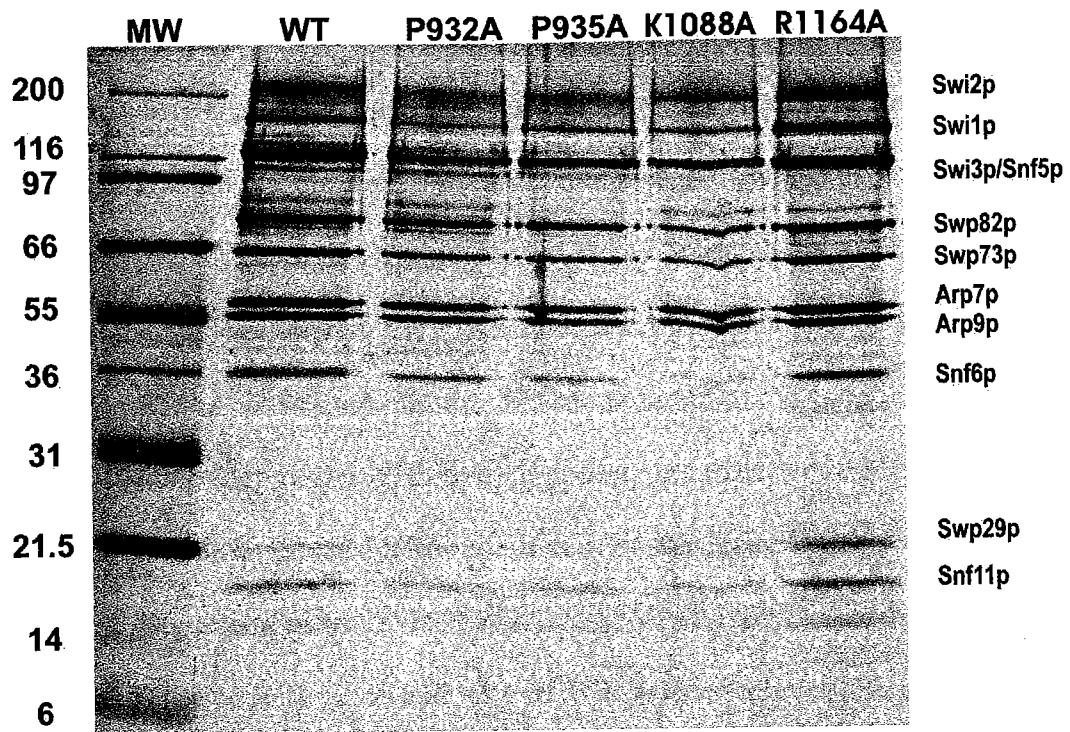
Figure 19. Silver Stain of SWI/SNF complexes containing Swi2p amino acid substitutions. This panel represents the results of a selection of the complexes that were subjected to silver stain. The individual complexes were subjected to SDS-PAGE on 10% polyacrylamide gels. The gels were then silver stained using standard protocols. This panel is representative of repeated results seen from separate preparations of the individual complexes.

ATPase activity of the various Swi2p amino acid substitution-containing complexes.

I first investigated the effect of substitutions within ATPase motifs on ATPase activity and kinetics of purified SWI/SNF complexes. Swi2p, as mentioned in the Introduction chapter, is a DNA-stimulated ATPase. The dsDNA-stimulated ATPase activity of the various altered SWI/SNF complexes is illustrated in Figure 20. The substitution, K798A is in motif I, the Walker A motif (or P-loop), which is the γ-phosphate binding loop of the ATP binding pocket. As expected, a K798A substitution within motif I that houses a highly conserved P-loop lysine ablates ATPase activity altogether. Alterations in motif Ia (P824A) and VI (R1986K) also have very severe effects on ATPase activity (13% and ~3% of WT, respectively). Both of these residues appear to be crucial for the formation of the ATP binding pocket. These results are consistent with studies of other helicases and ATPases as predicted by crystal structures contacts between ATP and these motifs (Caruthers and McKay, 2002).

Motif III is the only major motif found in the ATPase hydrolysis subdomain (subdomain I) of the helicase region that does not have a well defined role in general other than being involved in the ATPase reaction (Hall and Matson, 1999). Both motif III substitutions (P932A and W935A) have an intermediate effect on the ATPase activity (~60% and ~80% of WT respectively, Figure 20) of the variant SWI/SNF complexes.

The substitutions H1061A and K1088A are located in the SWI2-family specific sub-domain of SWI2/SNF2 ATPases (see Figure 16) and both of these mutations have very severe effects on ATPase activity (12% of WT activity in H1061A and no detectable

activity in the case of K1088A, see Figure 20). This region of Swi2p might be important for nucleosome and/or DNA substrate binding. Insertions of enzyme-specific subdomains into the canonical beta-alpha repeat pattern of helicases has been noted for a number of different enzymes including PcrA and HCV (see Figure 15) These non-conserved regions are hypothesized to confer distinct substrate specificity to SF2 members (Caruthers and McKay, 2002).

The remainder of the examined amino acid substitutions occurs in the less well characterized subdomain II of SF2 enzymes. A motif VI alteration, R1196K, has an extreme effect on ATPase activity resulting in only ~3% ATPase activity as compared to WT enzyme (See Figure 20). Substitutions within motif VI (especially for the conserved arginines) have been found to have ATP binding defects in other helicases, and these residues are believed to be involved in receiving the phosphate group during the helicase domain conformation change during ATPase hydrolysis reaction. The reception of the phosphate is believed to be partially responsible for the transduction of ATP hydrolysis information in SF2 helicases (Caruthers and McKay, 2002; Hall and Matson, 1999).

Motif V (R1164A and ΔSTRAGGLG) alterations have either intermediate (R1164A ~60% of WT) or no effect on DNA-stimulated ATPase activity (ΔSTRAGGLG ~100% WT) respectively (Figure 20). Of all the motifs found in SF2 helicase/ATPases, motif V is the least understood. It appears from the little data gleaned from mutational studies and crystal data that the role of this motif is not well conserved between enzymes; it may be that this motif's function is specific to individual classes of SF2 enzymes. In

SWI/SNF this motif might be involved in transducing ATP hydrolysis into the mechanism of chromatin remodeling
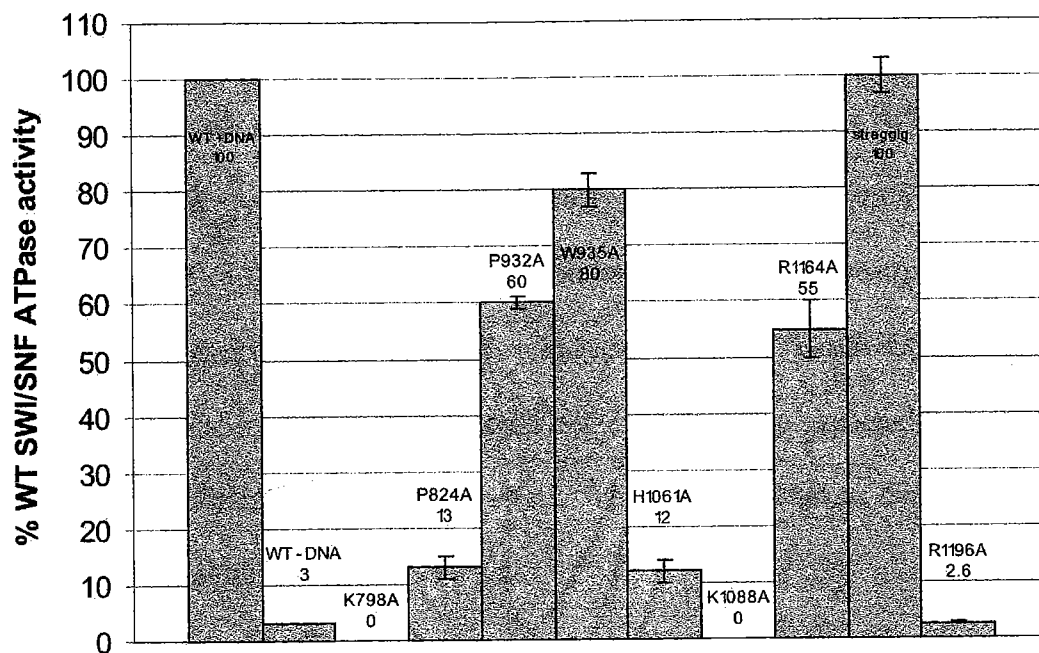
Figure 20. Relative ATPase activity of Swi2p amino acid substitution containing SWI/SNF complexes. Nanomolar quantities of mutant complexes were tested for ATPase activity and compared to WT SWI/SNF to determine relative ATPase activity. This graph represents numerous trials from 2-4 preparations of each of the various SWI/SNF complexes. All experiments were conducted in the presence of dsDNA and ATP in excess to enzyme. The only exception was the WT(-) DNA sample, which was performed in the absence of DNA, to illustrate the DNA stimulation of WT SWI/SNF. Error bars represent the standard deviation for the total trials for each individual complex.

Kinetic analysis of SWI/SNF complexes containing ATPase domain amino acid substitutions.

Following initial ATPase characterization, I conducted a more thorough kinetic analysis of each SWI/SNF variant. The kinetic parameters for ATP hydrolysis, K_m and K_{cat}, were determined by non-linear fitting to the Michaelis-Menten equation for a range of ATP concentrations (2 μM – 750 μM) in the presence of DNA cofactor (Figure 21). These results are summarized in Table 1. The two substitutions, K798A (Motif I) and K1088A (SWI2 specific region) were not analyzed since they do not hydrolyze ATP. Interestingly, most of the mutations result in kinetic defects that correspond well with their *in vivo* phenotypes (see Table 1). Two exceptions are ΔSTRAGGLG and R1164A which do not seem to have as severe a kinetic defect as would be expected from previous *in vivo* results (Richmond and Peterson, 1996). These two alterations display wild type ATPase activity, but fail to remodel *in vivo*.

Effects on both ATP binding and hydrolysis were observed in this analysis: P824A, H1061A, R1164A, and R1196K substitutions have moderate effects on K_m (up to 1.5 - 2.5 fold higher). The turnover rate (K_{cat}) effects were a little more severe especially in P824A (4x lower), H1061A (~10x lower) and R1196K (300-400x lower).
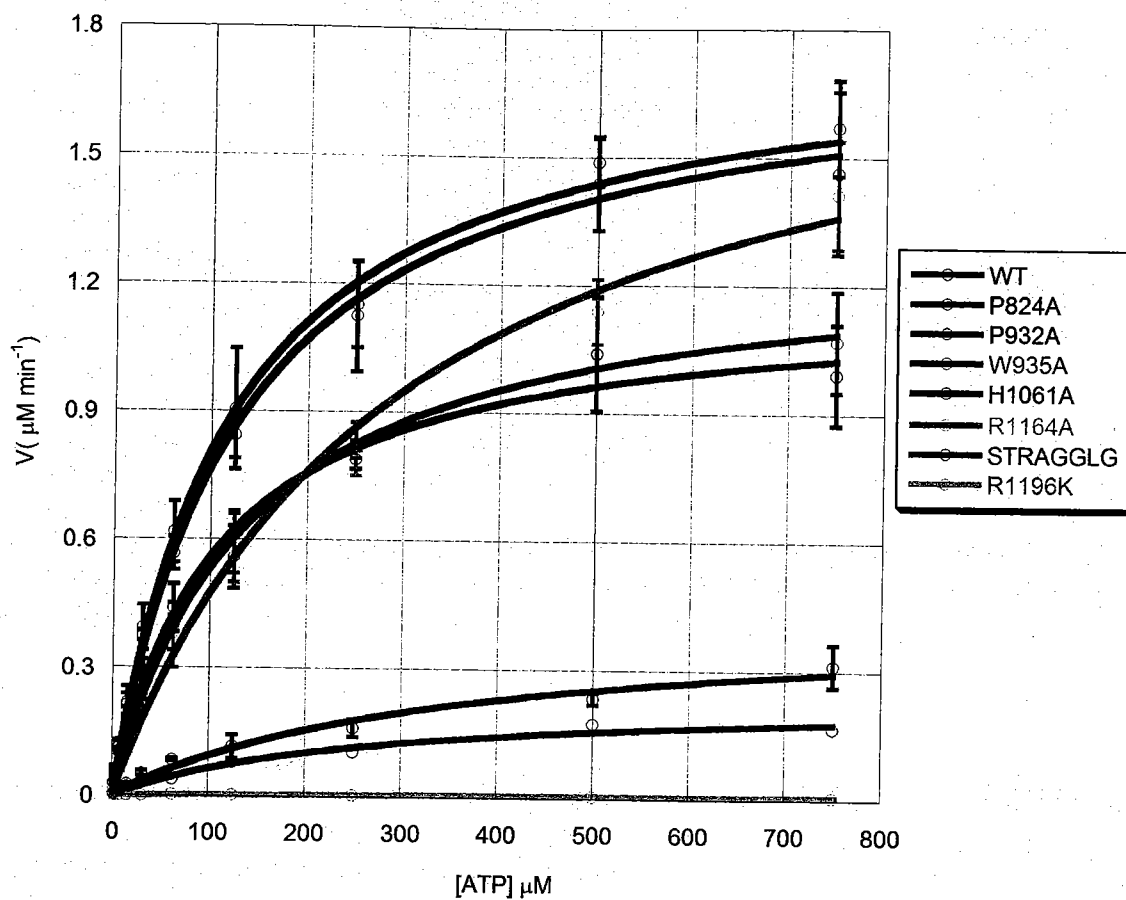
Figure 21. ATPase kinetics for Swi2p ATPase-defective complexes. Kinetic parameters were determined for TAP tagged WT SWI/SNF and the various SWI/SNF complexes harboring Swi2p ATPase amino acid substitutions. Initial velocities were determined from multiple time courses over time ranges giving linear hydrolysis of ATP at each individual ATP concentration. Velocities were plotted as a factor of ATP concentration and fitted to the Michaelis-Menten equation (see Equation 1 in Materials and Methods). The error bars represent the standard deviation of at least 3 separate trials for each ATP concentration.

Table 1: SWI/SNF complex kinetic parameters

	WT	P824A	P932A	W935A
K_m (µM)	152 ± 18	406 ± 76	113 ± 13	172 ± 20
V_{max} (µM/min)	$1.90 \pm .07$	$0.46 \pm .04$	$1.18 \pm .04$	$1.41 \pm .05$
k_{cat} (min^{-1})	632 ± 23	154 ± 14	394 ± 13	471 ± 17
k_{cat}/K_m (M^{-1} s^{-1})	6.8×10^4	6.3×10^3	5.8×10^4	4.5×10^4
r value	0.996	0.994	0.996	0.996
In vivo phenotype[*]	+++	+	+++	++
	H1061A	**R1164A**	**ΔSTRAGGLG**	**R1196K**
K_m (µM)	262 ± 46	332 ± 35	125 ± 6	234 ± 45
V_{max} (µM/min)	$0.24 \pm .02$	$2.00 \pm .08$	$1.81 \pm .03$	$0.01 \pm .001$
k_{cat} (min^{-1})	79 ± 5	669 ± 27	604 ± 8	2 ± 0.5
k_{cat}/K_m (M^{-1} s^{-1})	$5.0E \times 10^3$	1.7×10^4	8.1×10^4	1.4×10^2
r value	0.993	0.999	0.998	0.992
In vivo phenotype[*]	++	+	-	-

[*]*in vivo* phenotype adapted and representative of data from (Richmond and Peterson, 1996)
Neither K798A or K1088A containing complexes hydrolyze ATP and were no scored for ATPase kinetic parameters

Characterization of chromatin remodeling activities of ATPase variant SWI/SNF complexes in the Sal I-coupled remodeling assay.

In light of the ATPase results, chromatin remodeling was assayed using a Sal I chromatin remodeling assay previously developed in our laboratory (Logie and Peterson, 1997). A 2.3 kb fragment of DNA containing 11 tandem 208bp 5S rDNA repeats (208-11) was used to create *in vitro* assembled nucleosomal arrays with purified chicken histones by salt dialyses. These templates can be used to generate rotationally positioned nucleosomal arrays (Carruthers et al., 1999).. The central nucleosome of the 11mer array contains a unique Sal I restriction site that in the absence of chromatin remodeling is inaccessible to the restriction enzyme. When these arrays are incubated with both SWI/SNF and ATP, the central nucleosome is remodeled allowing accessibility to the Sal

I restriction site (See Figure 22a). The kinetics of remodeling was measured by the rate of Sal I digestion.

The various SWI/SNF complexes were incubated with equimolar concentrations of nucleosomal array to test for their ability to remodel chromatin (See Figure 22b, c). Three substitutions, K798A, H1061A, and K1088A, resulted in loss of remodeling. The R1196K complex has very little remodeling activity as compared to WT SWI/SNF (~3-4%); although this residual activity is reproducible. The P824A, P932A and W935A complexes all had intermediate activities that correlate well with their ATPase activity. Interestingly, the ΔSTRAGGLG complex had approximately a two fold decrease in remodeling as compared to WT, despite its near wild-type hydrolysis of ATP (Figure 22c). This partial uncoupling of ATP hydrolysis and chromatin remodeling suggested a more thorough characterization of the ΔSTRAGGLG complex could be informative.

The ΔSTRAGGLG complex was subjected to a multiple round Sal I chromatin remodeling assay to determine if the amino acid substitution impaired new substrate recognition (Logie and Peterson, 1997). Every hour fresh 208-11 template was added to the standard Sal I remodeling reaction to see if ΔSTRAGGLG complex had a defect in the ability to engage fresh substrate (Figure 23). The rate of Sal I cleavage remained constant after each addition of substrate indicating no change in the enzyme's ability to recognize new substrate. Taking into account the ΔSTRAGGLG complex's decrease in Sal I accessibility, there appears to be no additional defect in the ability of the ΔSTRAGGLG complex to accept new substrate or release from previously remodeled chromatin.
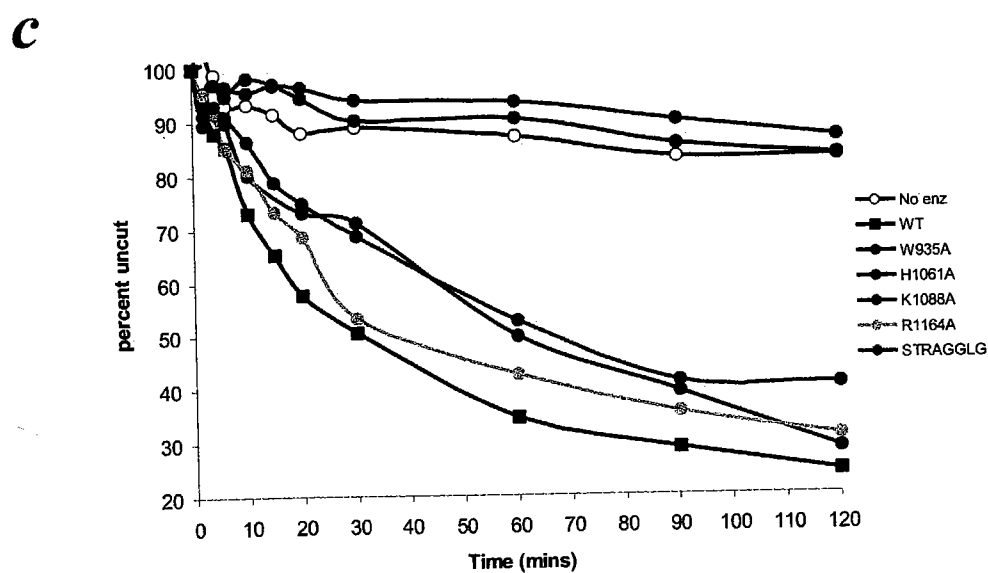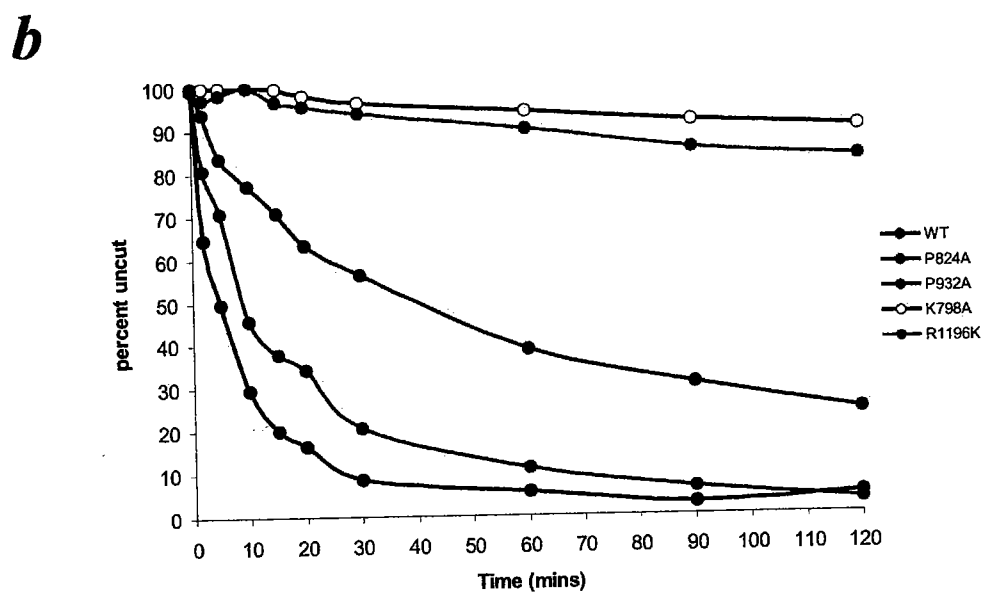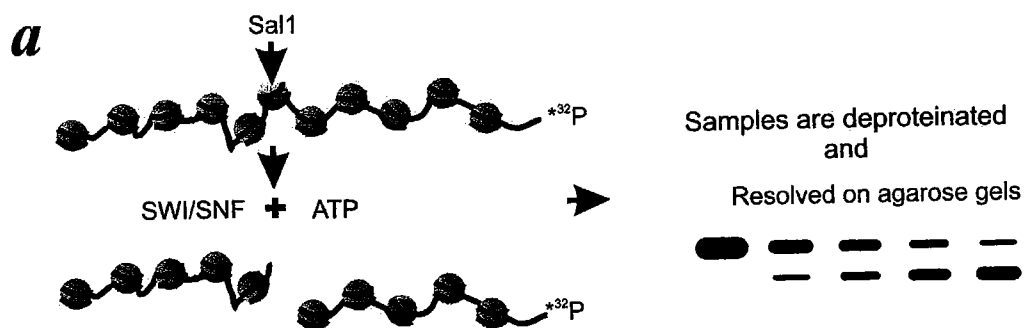
a

Sal1

SWI/SNF + ATP

Samples are deproteinated
and

Resolved on agarose gels

b

- WT
- P824A
- P932A
- K798A
- R1196K

c

- No enz
- WT
- W935A
- H1061A
- K1088A
- R1164A
- STRAGGLG

Figure 22. Sal I coupled chromatin remodeling results for Swi2p ATPase defective SWI/SNF complexes. The ability of SWI/SNF complexes containing Swi2p ATPase amino acid substitutions to remodel nucleosomal arrays was assayed by Sal I accessibility. (*a*) The chromatin substrate used in these experiments consists of a linear array of 11 tandem 208 bp 5S rDNA sequences from sea urchin which are radiolabeled on one end. The central repeat contains a Sal I restriction enzyme site which is inaccessible when incorporated into a nucleosome. In the presence of a remodeling enzyme and ATP this unique site becomes accessible and chromatin remodeling is scored by measuring the percentage of Sal I restriction fragments generated. Deproteinated samples were electrophoresis on 1% agarose gels and quantified for digestion. (*b,c*) Remodeling results of various ATPase-altered SWI/SNF complexes compared to WT SWI/SNF and no enzyme containing reactions. (*b*) 2 nM SWI/SNF complex (WT or variant complex) was incubated with 1 nM 208-11 array (α^{32}P-end labeled), 1 mM ATP, and 150 U Sal I restriction enzyme. (*c*) 1nM SWI/SNF complex (WT or variant complex) was incubated with 1 nM 208-11 array (α^{32}P-end labeled), 1 mM ATP, 150 U Sal I restriction enzyme in these reactions. Note: 100% denotes substrate uncleaved during SalI preincubation (see Materials and Methods). Timepoints were taken over a 120-minute period. These data are representative of at least three trials.
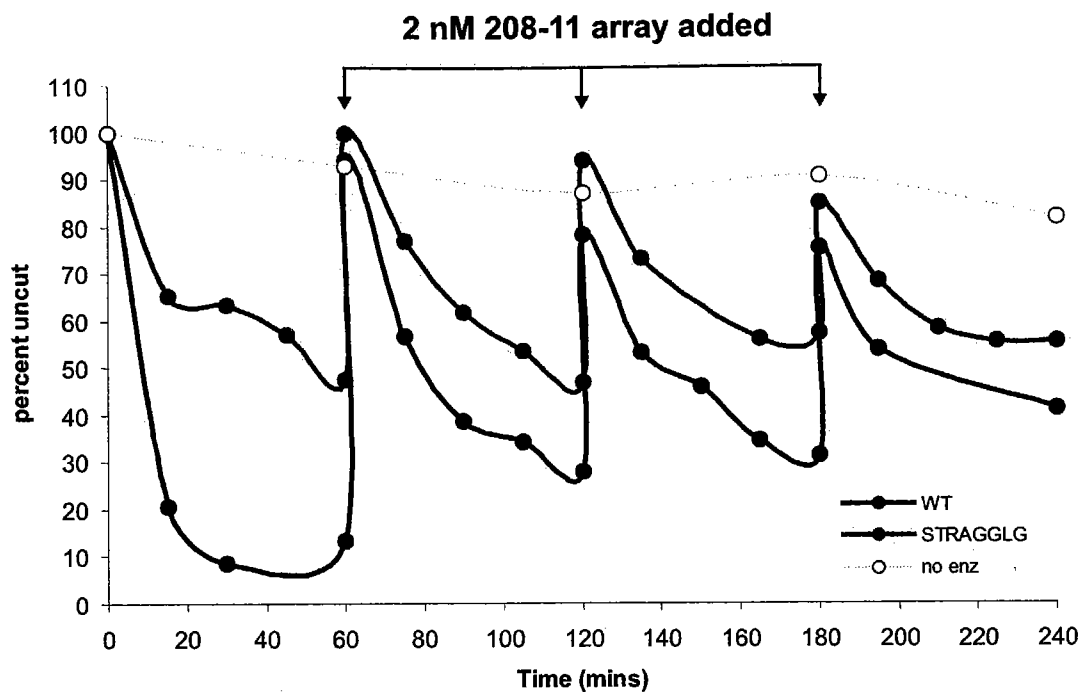
Figure 23. The ΔSTRAGGLG complex functions catalytically to remodel nucleosomal arrays similar to WT SWI/SNF. The ability of ΔSTRAGGLG to engage new nucleosomal array was tested in a multiple round experiment. Initially 2 nM of 208-11 array was incubated with 4 nM of either WT (●) or ΔSTRAGGLG (●) SWI/SNF complex with 1 mM ATP and 150 U of Sal I. At each hour an additional 2 nM array was added to the reaction. The same reaction without enzyme was run as a baseline (○).

Amino acid substitutions in ATPase domain motif V affect the ability of the SWI/SNF enzyme to generate superhelical torsion on DNA substrates.

Another hallmark of the Swip2 subfamily of ATPases is the ability to generate superhelical torsion in DNA (Havas et al., 2000; Jaskelioff et al., 2003). One current model for how SWI/SNF remodels chromatin involves the creation of torsion as a potential mechanism to elicit movement of DNA relative to histones on the surface of the nucleosome. I was therefore interested in investigating the effects the various ATPase domain alterations would have in the generation of torsion. In order to measure torsion generation, a cruciform extrusion assay was employed (Havas et al., 2000). For these experiments, a linear 3.8 kb piece of DNA containing an inverted $[AT]_{34}$ was used as a remodeling template. When this fragment of DNA is subjected to a reduction of superhelicity the $[AT]_{34}$ repeat is extruded as a cruciform. In the assay the DNA fragment is incubated with chromatin remodeling enzyme and T4 Endonuclease VII. If the complex creates a reduction in superhelicity a cruciform will be extruded and cleaved by Endonuclease VII into two smaller DNA fragments (See Figure 24a). As expected, complexes crippled for ATPase activity have no ability to create torsion in DNA (Figure 24b). Likewise, complexes that have intermediate ATPase defects also have corresponding defects in torsion generation (Figure 24b). Surprisingly both R1164A and ΔSTRAGGLG (in motif V) complexes are completely defective in their ability to generate torsion on DNA templates.
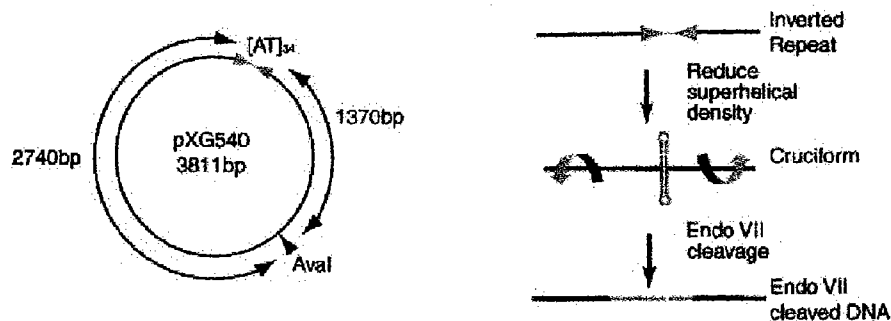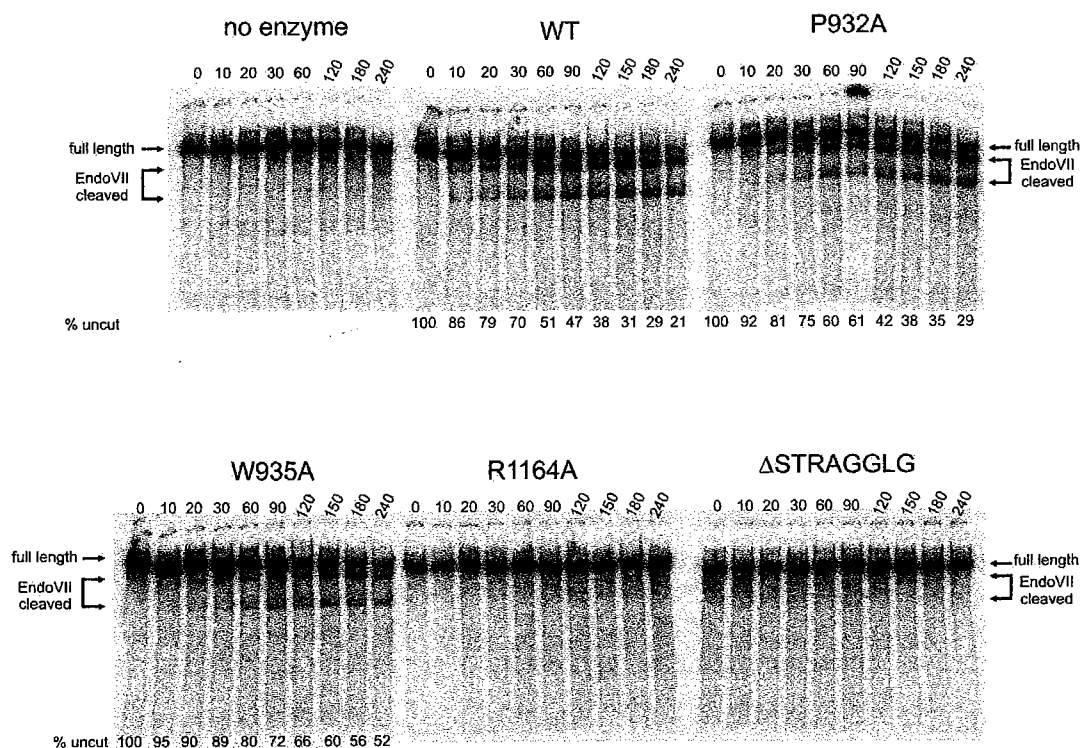
Figure 24. Torsion generation by motif III and motif V alterations. (a) The ability to generate DNA superhelical torsion was tested on a linearized (AvaI digested) pXG540 template which contains an inverted [AT]$_{34}$ repeat. In the presence of an enzyme (SWI/SNF) that can create superhelical torsion the cruciform resolving nuclease T4 Endonuclease VII will cleave the cruciform created by extrusion of the [AT]$_{34}$ repeat. (b) Reactions containing 8 ng of AvaI-linearized pXG540, 1.5 nM SWI/SNF (WT or variant), 3 mM ATP, and 0.15 ug/mL Endo VII were incubated for 4 hours. Samples were taken at the denoted times, quenched, deproteinated and run on 4% native PAGE gels.

Discussion

In this chapter I examined how Swi2p ATPase domain amino acid substitutions disrupt ATPase and chromatin remodeling activities. Swi2p substitutions were identified that disrupt ATP binding, catalysis and generation of superhelical torsion on DNA.

Effects of Swi2p ATPase substitutions on the activity of SWI/SNF.

Substitutions in subdomain I of the ATPase domain of Swi2p yielded results comparable to those seen in other SF2 ATPases/helicases. The best characterized motif in all ATPases (as well as GTPases) is motif I (P-loop or Walker A box), which contains an invariant lysine residue critical for proper ATP γ-phosphate binding. Substitution of this conserved lysine with an alanine results in the predicted loss of ATP hydrolysis. This mutation has been used to show that chromatin remodeling of SWI/SNF is ATP dependent (Cote et al., 1994). Similarly, substitutions in both motifs Ia (P824A) and III (P932A and W935A) appear to agree with established or theorized roles for these motifs.

Motif Ia has been implicated in interacting with oligonucleotide substrate as seen in the crystal structures of the helicases HCV and PcrA (Caruthers and McKay, 2002). Disruption of motif Ia in Swi2p leads to a 3-4 fold decrease in both the affinity of SWI/SNF for ATP (K_m increased) and the turnover rate (K_{cat} decreased). This phenotype is consistent with an alteration that would affect DNA binding in a DNA-stimulated enzyme. Yeast SWI/SNF ATPase activity in the absence of DNA has a 30 fold reduction to that of DNA stimulated, (Figure 20) and (Cote et al., 1994). Thus, a defect in

interaction with DNA could lead to the decreased activity seen with the motif Ia alteration

Motif III shows significant divergence in both length and amino acid sequence among helicase subfamilies. This motif is involved in a number of different specific interactions among SF2 member enzymes. Crystal structures of PcrA and Rep bound to various nucleotide analogs and oligonucleotide substrates point to a role for this motif in recognition of the gamma phosphate of ATP in the binding cleft. In PcrA a glutamine residue in motif III has been proposed to act as a sensor for the presence of the γ-phosphate of ATP (Caruthers and McKay, 2002). This sensor motif might trigger allosteric changes in the enzyme depending on the state of the bound nucleotide. In this study, both of the motif III alterations (P932A and W935A) have a 25-33% decrease in ATP turnover without a significant effect on ATP affinity. These results from Swi2p appear to correlate with the sensor model derived from PcrA and Rep.

The subdomain I amino acid substitutions have defects in chromatin remodeling that correlate with their defects in ATP binding and hydrolysis. The accumulated data on subdomain I of SF1 and SF2 helicases points to a major function in the ATP hydrolysis cycle (Caruthers and McKay, 2002). The data from this study reinforces this role.

The Swi2p specific spacer domain plays an important role in the ATPase activity of the enzyme.

In all SF1 and SF2 enzymes except chromatin remodeling members, the subdomains I and II are only separated by a short flexible loop that keep the two

subdomains in close proximity to each other (see schematic in Figure 15). The yeast initiation factor eIF4a, for example, has only 11 residues between the two subdomains (Figure 25*a*) and (Caruthers et al., 2000). In contrast, the ATPase subdomains I and II in Swi2p are separated by a significant (>100 amino acid) spacer region containing numerous potential alpha helices (see Figure 25*c*). This region is highly conserved in the SWI2/SNF2 family of chromatin remodeling enzymes suggesting that it could be a chromatin remodeling enzyme specific subdomain within the ATPase domain.

The alterations in this Swi2p spacer region, H1061A and K1088A, were found to have severe effects in their ability to hydrolyze ATP. The K1088A substitution results in no discernable ATP hydrolysis while H1061A had a 10x lower ATP turnover rate and a ~1.5x fold decrease in ATP affinity. In addition, both of these substitutions led to SWI/SNF complexes that were inactive in chromatin remodeling as well.

Without structural information on this region of Swi2p, it is impossible to know what role these residues play in chromatin remodeling. This domain might play a similar role in Swi2p that the two extension domains Ib and IIb play in PcrA (see Figure 15, blue and green domains in PcrA structure). In PcrA two subdomains (Ib and IIb) that loop out of subdomains I and II appear to coordinate the oligonucleotide substrate (see Figure 25*b*) and mutations in these PcrA specific subdomains have significant effects on PcrA helicase activity (Soultanas et al., 2000). Both of the Swi2p mutations in the Swi2-specific subdomain had severe effects on ATPase activity and thus chromatin remodeling. Thus, it could be possible that this spacer region in Swi2p acts to coordinate

substrate (DNA or chromatin) into a specific position in order to facilitate chromatin remodeling. This hypothesis will be expanded upon in Chapter V, perspectives.

Further evidence for a role of motif VI in coordinating the γ-phosphate of ATP

In some helicases, motif VI appears to play a role in interacting with the γ-phosphate of ATP. In the crystal structures of a number of helicases (including PcrA and NS3), motif VI is located down near the ATP binding cleft (see Figure 37c in chapter VI). The key residues in this motif are a triplet of highly conserved arginine residues. Substitution of one of these residues in Swi2p, R1196K, results in severe defects in ATP hydrolysis and chromatin remodeling. While ATP hydrolysis is very low in this substitution it does display limited chromatin remodeling activity (~2-3% of WT). Motif VI appears to play an important role in connecting subdomain I to subdomain II through the ATP binding pocket. This connection could behave as a pivot, allowing large conformational changes in the enzyme. This model is supported by the differences in the conformation of PcrA crystal structures solved with Adenosine 5'-(β,γ-imido)triphosphate (AMPPNP) versus a sulfate ion (mimicking a free phosphate) (Velankar et al., 1999). This complex containing the R1196K substitution might be very useful in the future to slow chromatin remodeling and more closely examine the mechanics of this rather rapid enzymatic event since there is a hundred fold reduction in ATP utilization.

a

b

c

951 KSFDEWFNTPFANTGGQDKIELSEEETLLVIRRLHKVLRPFLLRRLKKDVEKELPD 1005

1006 KVEKVVKCKMSALQQIMYQQMLKYRRLFIGDQNNKKMVGLRGFNNQIMQLKKICNH 1061
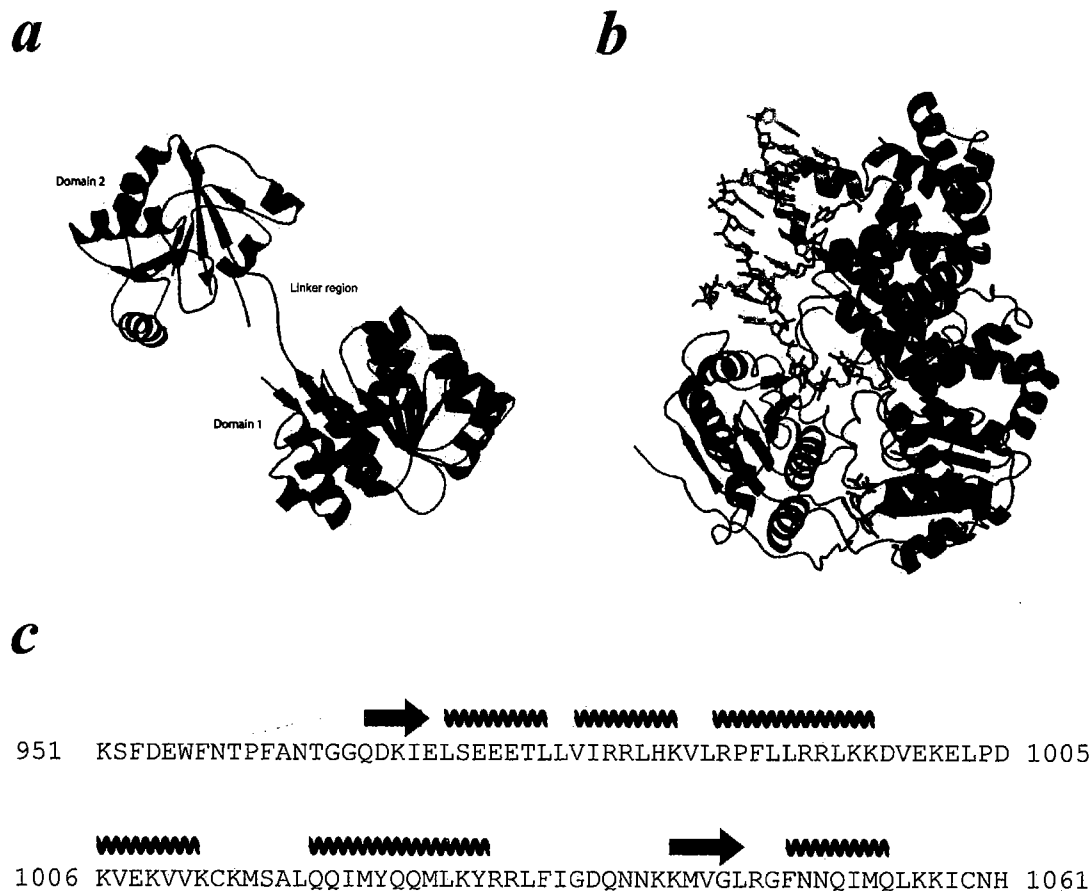
Figure 25. Swi2p specific ATPase linker region. The linker region of Swi2p is significantly larger than those found in SF1 and SF2 helicases. (*a*) Crystal structure of yeast intitation factor eIF4a. The linker region between subdomain I and II of the ATPase is only 11 residues long (figure adapted from (Khorasanizadeh, 2004). (*b*) Structure of PcrA coupled to dsDNA oligo and AMPPNP. PcrA contains two specific subdomains Ib and IIb which loop out of subdomain I and II respectively. These alpha helical regions fold together to form a scaffold for dsDNA contacts leading outside of the canonical ATPase domain pocket. (*c*) The linker region between subdomain I and II in Swi2p is over 100 amino acids in length. This region contains six predicted alpha helices and two predicted beta sheets. Residue H1061 is one of the residues investigated in this study. Panel *b* was rendered by Eric Merithew using PyMOL.

Motif V couples ATPase activity to chromatin remodeling activity.

In contrast to other motifs in SF1 and SF2 helicases, the role of motif V is not well understood. Like motif III, this motif shows considerable variability in length and composition as well as a hypothesized role in different helicase-like proteins. This domain in Swi2p is predicted to be in a large loop which contains the amino acid sequence STRAGGLG (see Figure 16). So far, no general role has been attributed to this motif in helicases (Caruthers and McKay, 2002). One feature of note for this motif is that in a number of helicases this loop makes contacts with both ATP and the oligonucleotide.

In this study I showed that while ATP binding and turnover remains mostly unaffected by amino acid substitutions in this motif, generation of torsion is severely affected and generation of enzyme accessibility on nucleosomal arrays is partially impaired. Both the in vivo phenotype and torsion generation effects suggest that motif V might play an important role in the process of ATP-dependent chromatin remodeling. In the next chapter I will present a more thorough study that suggests a mechanistic role for motif V in chromatin remodeling.

Materials and Methods

Purification of SWI/SNF complexes. Diploid *S. cerevisiae* strains containing both wild type and various SWI2/SNF2-TAP alleles were generated for expression and purification of SWI/SNF complexes. WT SWI2-TAP generation and purification was performed as previously described (Smith et al., 2003; Smith and Peterson, 2003). Mutant SWI2/SNF2 genes were tagged in diploids cells to ease generation of constructs and purification of protein. Haploid strains (see yeast strain list, Table A1 in Appendix) containing various *swi2*-HA6HIS alleles (MATα *swi2*) were crossed with strain CY297 (MATa SWI2) to create diploids. Primer sets were generated to replace the C-terminal *swi2*-HA6His tag with a Tandem 4xProteinA-CBD tag (Puig et al., 2001). Primers used to produce these mutant tagged alleles were: tF-swi2XHO [ACTTCAAGCGTGGCTGAATCTTTCAC AGATGAAGCGGACCGGATCCCCGGGTTAATTAA] and tR-SWI2H6H [GTGATG ATGGCTCGAAGCGTAATCTGGAACATCATATGGGTAGCTCGAGAATTCGAG C GTTTAAAC]. Purification of TAP tagged SWI/SNF strains were purified using established protocols (Smith et al., 2003; Smith and Peterson, 2003). Concentrations of SWI/SNF complexes were determined by comparative western blots to WT SWI/SNF using antibodies (Santa Cruz) to various SWI/SNF subunits and by silver staining.

ATPase assay and ATP hydrolysis kinetics. All ATPase assays were performed using standard conditions as previously described (20 mM Tris pH 8.0, 5 mM $MgCl_2$, 0.1 mg/ml BSA, 5% glycerol, and 0.2 mM DTT) (Logie and Peterson, 1999). DNA (208-11

template containing plasmid) or nucleosomal arrays, was added to a final concentration of 13nM. Reactions were conducted at 30 °C. Rates of hydrolysis were measured by spotting time points on PEI-cellulose and resolving released γ-labeled phosphate from ATP in 750 mM potassium phosphate pH 3.5. Analysis of hydrolysis rates was performed using a Molecular Dynamics PhosphorImager and Imagequant v1.2 (Amersham). For kinetic experiments, velocities were determined over time ranges that gave linear ATP hydrolysis rates for ATP concentrations ([S] 2 μM - 1 mM) for the various complexes. Kinetic parameters K_m, V_{max}, and K_{cat} were determined from non-linear fitting to the Michaelis-Menten equation (Equation 1) using KaleidaGraph v3.6 (Synergy Software), where v is velocity, K_m is the Michaelis constant, [S] is substrate concentration, and V_{max} is maximum reaction velocity.

$$v = \frac{V_{max}[S]}{K_m + [S]} \ \textit{(Equation 1)}$$

Sal I coupled chromatin remodeling assays. Sal I-coupled chromatin remodeling assays were performed in 1x 5-50 buffer (10 mM Tris pH 8.0, 50 mM NaCl, 5 mM MgCl₂, 1 mM DTT, and 0.1 mg/ml BSA) as previously described (Logie and Peterson, 1999). Reactions containing reaction buffer, 1 mM ATP, and 1 nM α^{32}P-end labeled 208-11 array, and 150 U of Sal I restriction enzyme were pre-incubated at 30 °C for 20 minutes prior to addition of SWI/SNF enzymes in order to cleave substrate with an accessible Sal I restriction site. The remodeling reactions were started by the addition of the SWI/SNF

enzyme and the incubation continued at 30 °C. Time points were taken at various intervals, quenched and deproteinated by vortexing briefly in 10 µL of TE pH 8.0 and 20 µL of phenol/chloroform. For multiple round experiments additional 208-11 array was added to a final concentration of 2 nM at each hour, and time courses were allowed to proceed for four hours.

Cruciform formation assays. DNA cruciform formation assays were performed in 30 µL reactions containing 1x 5-50 remodeling buffer, 3 mM ATP, 0.15 µg/ml Endonuclease VII, 8 ng AvaI-linearized α^{32}P-dCTP end labeled pXG540 DNA (CP894), and 1.5 nM SWI/SNF complex. Rates of cruciform extrusion were measured over 240 minutes at 25 °C. 3 µL aliquots, at the indicated times, were taken and quenched by the addition of 2x Stop buffer (10 mM Tris pH 8.0, 0.6% SDS, 40 mM EDTA, 5% glycerol, and 0.1 mg/ml Proteinase K). Quenched reactions were incubated at 50 °C for 20 minutes to deproteinate samples. Samples were then resolved on 4% 1xTBE native acrylamide gels and imaged using a Molecular Dynamics PhosphorImager. Percentage of pXG540 fragment cut was determined by using Imagequant v1.2 (Amersham).

CHAPTER IV

A MOTIF WITHIN THE SWI2P ATPASE DOMAIN CRITICAL FOR COUPLING ATP HYDROLYSIS TO CHROMATIN REMODELING

Summary

Determining how ATP hydrolysis is coupled to the mechanism of ATP-dependent chromatin remodeling is an important part of determining how chromatin remodeling works. In this chapter I will present evidence suggesting that motif V of the Swi2p ATPase domain plays a critical role in the chromatin remodeling reaction. Amino acid substitutions in motif V lead to defects in the generation of superhelical torsion. The data also suggests that these same motif V defects have adverse effects on chromatin remodeling as illustrated by the inability of motif V substitutions R1164A and ΔSTRAGGLG to generate nucleosome mobility and accessibility to restriction enzyme sites within a nucleosome. This suggests that proper generation of torsion is important for chromatin remodeling. Interestingly, mutations within motif V of human BRG1, a SWI2 homolog is commonly found in human cancer cell lines and carcinomas. The *in vitro* effects of amino acid substitutions described here could also explain why mutations in and around motif V have been found in both colon cancer cell lines and lung carcinomas.

The data presented in this chapter are being prepared for publication. The plasmid pGEMZ-lowerstrand-601 (CP1024) was received from Blaine Bartholomew. I would

like to acknowledge Pedro Medina for sharing unpublished data on the Brg1 mutations found in patient lung carcinomas. I also would like to thank Eric Merithew for generating the PyMOL structures in Figure 37.

Introduction

In the last chapter (Chapter III), I investigated how specific alterations in Swi2p ATPase domain affected ATPase and chromatin remodeling activities. Of particular significant were alterations in motif V that did not alter ATPase kinetics but did lead to defects in nucleosomal array remodeling and the generation of superhelical torsion. In this chapter I explore in more detail how alterations in motif V disrupt chromatin remodeling.

Motif V is the least understood of the helicase motifs in the SF1 or SF2 families. Both of these subfamilies contain significantly different consensus sequences and varying lengths in this specific motif (Caruthers and McKay, 2002; Hall and Matson, 1999). In Swi2p-like enzymes the amino acid sequence STRAGGLG appears to exist in a loop between two alpha helices by secondary structure prediction (see Figure 17 in chapter III).

From the structures of the various helicases solved to date the relative position of motif V appears to be highly conserved yet the biochemical role(s) of this motif appears be variable in different helicase enzymes (Hall and Matson, 1999). In NS3 and UvrB, residues of motif V interact with ssDNA (Hsu et al., 1995; Moolenaar et al., 1994; Yao et al., 1997). In contrast, alterations within motif V of the CI RNA helicase exhibit no oligonucleotide binding defect but have reduced ATPase and helicase activities (Fernandez et al., 1997). PcrA motif V, is an example of a third case in which contacts between AMPPNP are mediated through the motif V residue E571 and the residue H565

interacts with DNA (Velankar et al., 1999). The differences between the enzymes have led to the hypothesis that motif V might be involved in coupling ATPase activity to the specific function of the individual enzyme.

A popular current model for the mechanism of SWI/SNF on chromatin involves the generation of torsion to produce twist defects in DNA with the alleviation of these twist defects resulting in either slippage of DNA around the histone octamer or formation of transient bulges of DNA writhing around the nucleosome (see Figure 5 in Introduction). In the past it has been shown that the SWI/SNF complex generates superhelical torsion on both naked DNA and chromatin substrates (Havas et al., 2000). SWI/SNF, unlike ISWI and Mi-2 family chromatin remodeling enzymes, needs only DNA in order to have robust ATPase activity and torsion generation. This has led to the possibility that the SWI/SNF complex may not sense chromatin structure through Swi2p, but rather acts directly on DNA in the context of nucleosomes.

In this chapter I will expand on the phenotypes seen for the motif V altered complexes characterized in Chapter III. The data presented here suggests that motif V plays an important part in coupling the hydrolysis of ATP to the mechanism of chromatin remodeling. The evidence also suggests a model where residues in this loop are responsible for recognizing intact nucleosome core particles in chromatin and that it is this substrate and not DNA alone that is the proper template for SWI/SNF *in vivo*.

Results

The *swi2*ΔSTRAGGLG mutant results in severe growth phenotypes on carbon sources.

Prior to beginning mechanistic studies of motif V, I decided to confirm the severity of the *swi2*ΔSTRAGGLG mutant *in vivo*. Initially our laboratory had characterized the phenotype of *swi2* ATPase mutants at a number of inducible genes. I was interested in determining if the motif V mutants had a traditional *swi⁻* phenotype. One of the hallmarks of *snf* mutants is a defect in growth on various alternative carbon sources (see Introduction, Chapter I). Strains harboring the mutations *swi2ΔSTRAGGLG* (CY519) and *swi2R1164A* (CY458) were tested for the ability to grow on different carbon sources (Figure 26). The carbon source growth phenotypes of the motif V mutants were compared to those of isogenic strains containing either a WT copy of SWI2 (CY396), a deletion of the SWI2 gene (CY120) and the catalytically dead mutant, *swi2K798A* (CY397). The *swi2ΔSTRAGGLG* mutant had a severe growth phenotype at least as strong as or stronger than *swi2K798A* as seen on all tested carbon sources. On normal YEPD (glucose) plates the *swi2ΔSTRAGGLG* mutant had a more severe phenotype than the *swi2K798A* strain. The *swi2R1164A* mutant only displayed a minor growth phenotype on ethanol/glycerol media. The growth phenotype for the *swi2ΔSTRAGGLG* mutant further illustrates the severity of this defect for SWI/SNF function *in vivo* as the mutant displays a null phenotype on all alternative carbon sources

YEP + Glucose

YEP + Galactose

WT

Swi2Δ

Swi2K798A

Swi2ΔSTRAGGLG

Swi2R1164A

WT

Swi2Δ

Swi2K798A

Swi2ΔSTRAGGLG

Swi2R1164A

Ethanol/glycerol

YEP + Raffinose

WT

Swi2Δ

Swi2K798A

Swi2ΔSTRAGGLG

Swi2R1164A

WT

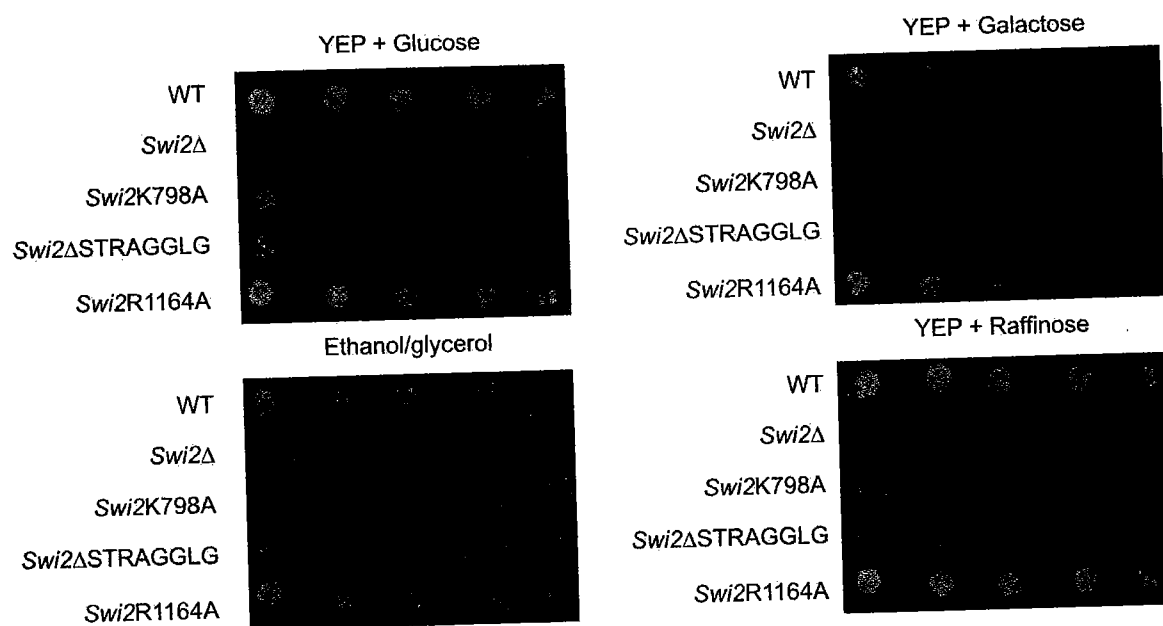Swi2Δ

Swi2K798A

Swi2ΔSTRAGGLG

Swi2R1164A

Figure 26. Carbon source growth phenotypes of *SWI2*-ATPase motif V mutants. Strains containing WT SWI2 (CY396), *swi2Δ* (CY120), *swi2K798A* (CY397), *swi2R1164A* (CY458), and *swi2ΔSTRAGGLG* (CY519) were plated on various carbon sources and tested for the ability to grow. Each spot represents a 5 fold serial dilution, starting with ~5000 cells.

Generation of superhelical torsion on chromatin substrates by Swi2p-motif V alterations indicate direct interactions between the Swi2p ATPase domain and chromatin.

To further analyze the role of motif V in the activity of ATP-dependent chromatin remodeling, nucleosomal arrays were constructed with the cruciform extrusion template in order to measure the ability of the motif V altered complexes to generate torsion on chromatin. In the data presented in the previous chapter, I showed that alterations in motif V eliminate torsion generation on naked DNA. Comparisons between naked DNA and chromatin templates have performed in the past and it was found that ISWI and Mi-2 family members need the presence of nucleosomes on DNA template in order to produce superhelical torsion (Havas et al., 2000). In contrast SWI/SNF generated superhelical torsion of either nucleosomes or naked DNA. To study the effect motif V alterations had on torsion generation, templates were generated to make both saturated (1 nucleosome per 200 bp DNA) and partially saturated (1 nucleosome per 400 bp DNA) nucleosome templates.

When cruciform extrusion experiments were conducted with the chromatin templates several striking results were seen (Figure 27). First, WT SWI/SNF displayed an increase in the ability to generate superhelical torsion on chromatin (3-4 fold increase) as compared to torsion generation on the DNA template alone. Second, on the chromatin substrate the R1164A complex only exhibited a two fold reduction in the ability to generate superhelical torsion as compared to WT SWI/SNF complex (see Figure 27a and b). Finally, the ΔSTRAGGLG complex showed a greater than ten fold

defect in its ability to create torsion as compared to the WT SWI/SNF complex (Figure 27b). Thus assembly of DNA into chromatin creates a better substrate for SWI/SNF, and furthermore chromatin partially suppresses the defects due to alterations in motif V. Notably, the ΔSTRAGGLG complex remains highly defective for torsion generation, consistent with the strong swī⁻ phenotype of the mutant *in vivo* (Table 1). The comparable torsion generation between sub-saturated and saturated arrays suggests that high order chromatin structure is not playing a role in generation of superhelical torsion in this assay (compare black symbols with grey symbols in Figure 27b).

I also tested whether nucleosome assembly might suppress the defective ATPase activity of the R1164A complex. As mentioned earlier, in the presence of DNA, R1164A has an ATPase activity ~60% of that of WT. In the presence of nucleosomal DNA, the ATPase activity of the R1164A complex is increased such that it is more comparable to the ATPase activity of the WT SWI/SNF complex (Figure 28). This is the first time that significant nucleosomal stimulation has been seen in the case of ySWI/SNF. These data, in combination with the superhelical torsion assays suggests that the residues within motif V of the ATPase domain might play a role in orienting the motif V loop to allow proper oligonucleotide contacts in the context of nucleosomes.

a
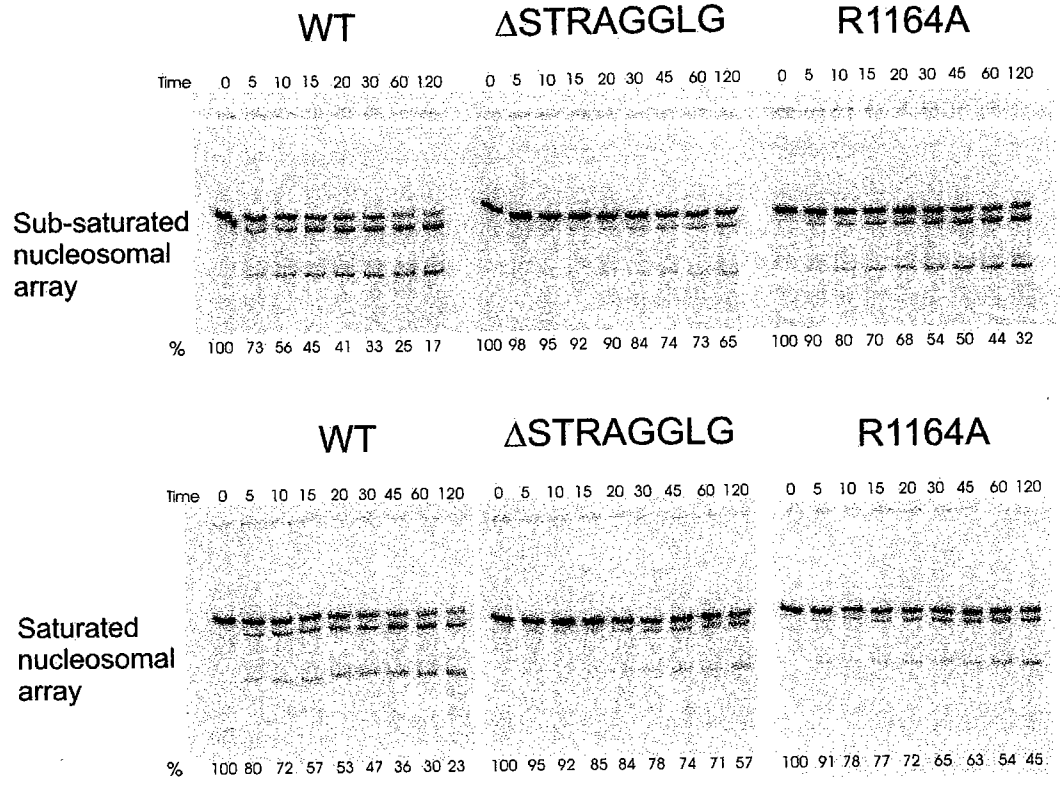
b
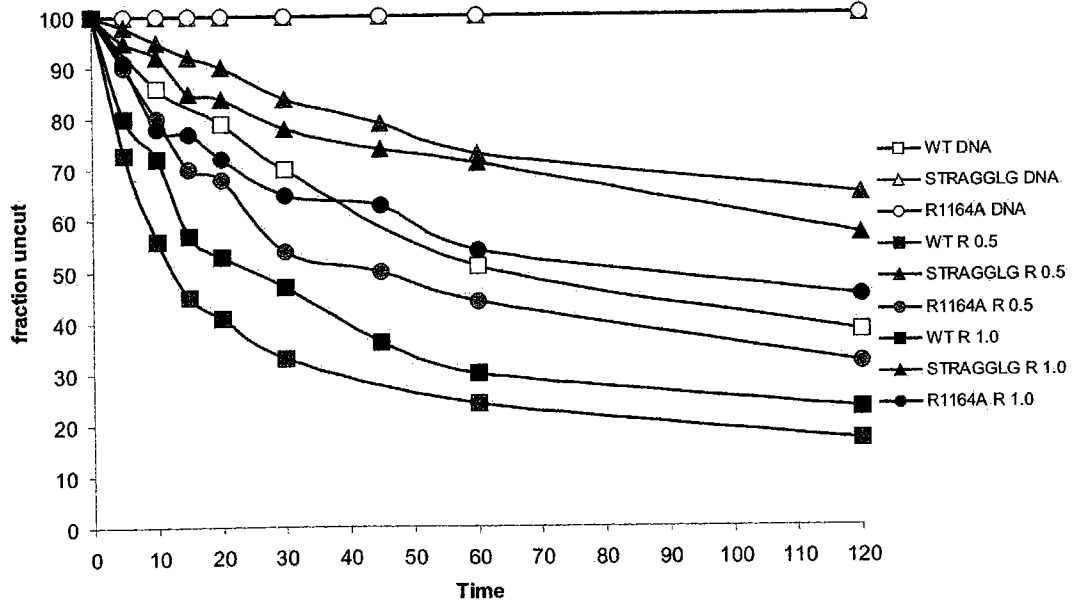
Figure 27. Motif V alterations affect torsion generation on chromatin substrates. SWI/SNF complexes were assayed for their ability to create torsion on cruciform templates. The AvaI-pXG540 linear dsDNA fragment was used as a template to generate nucleosomal arrays by salt dialysis. R1164A (circles), ΔSTRAGGLG (triangles), and WT SWI/SNF (squares) were tested on saturated (R1.0, 1 nucleosome per 200 bp of DNA) and half saturated templates (R0.5, 1 nucleosome per 400 bp of DNA). 1.5 nM SWI/SNF was incubated with 8 ng chromatin cruciform template or 8 ng DNA template, 0.15 ug/ml Endonuclease VII and 3 mM ATP. Time course was run for 2 hrs with samples taken as indicated, quenched, deproteinated and run on 4% native TBE PAGE gels. (*a*) Raw data. (*b*) Graphical representation of data from previous panel showing percentage template uncut. Black filled symbols are the results for saturated templates and grey symbols represent half-saturated templates.
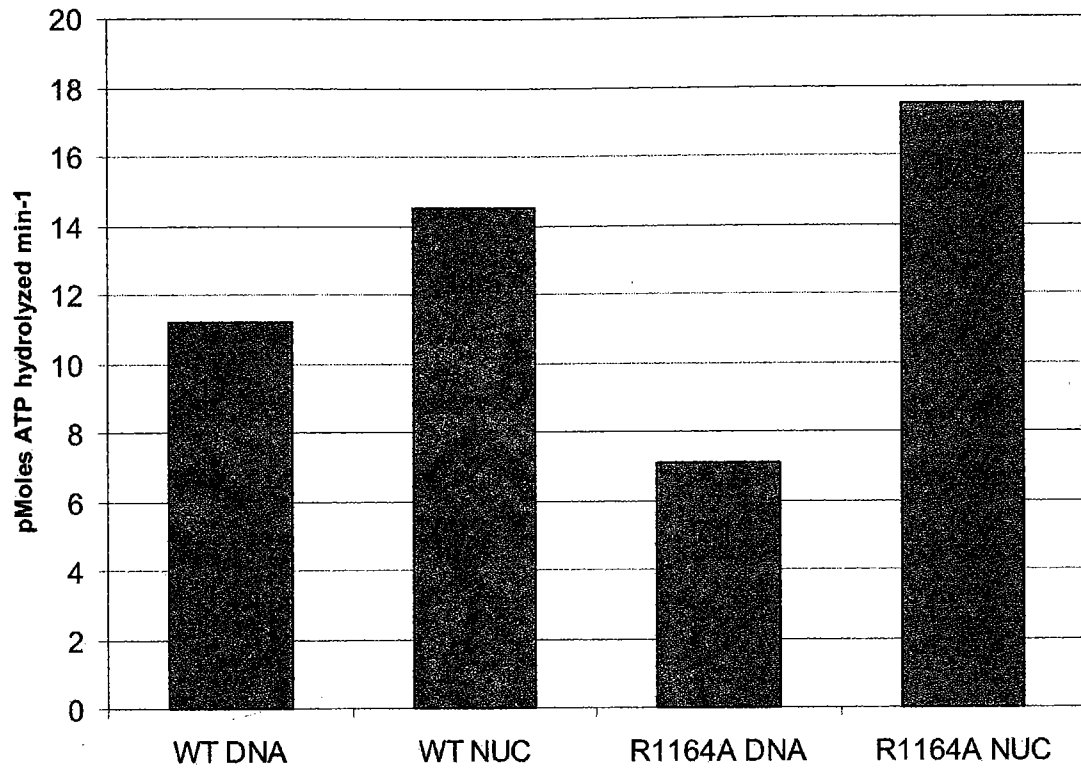
Figure 28. **Nucleosomal substrates rescue the R1164A ATPase defect.** ATPase activity of 4 nM WT or Swi2R1164A SWI/SNF complexes tested with 13 nM dsDNA or 13 nM nucleosomal DNA and 100 uM ATP in a standard ATPase reaction buffer. Hydrolysis rates were determined over a 15 minute time period.

Generation of torsion by SWI/SNF is sensitive to the presence of histone N-terminal tails.

The data shows that nucleosome assembly suppresses the defects in ATPase and torsion generation by the R1164A complex, suggesting that motif V may sense nucleosome structure. I decided to investigate which features of the nucleosome are important. Next, I tested whether the histone N-terminal tails functionally interact with

motif V. In order to look at tail-dependent effects on ATPase motif, torsion assay templates were generated with naked DNA, WT recombinant (*Xenopus laevis*) octamers, tailless recombinant octamers (lacking all histone N-terminal domains), or recombinant $(H3-H4)_2$ tetramers (see Materials and Methods for substrate assembly and evaluation).

These alternate chromatin substrates were then used to look at the generation of torsion with both WT SWI/SNF and the R1164A complexes (Figure 29). WT SWI/SNF was able to create superhelical torsion on all substrates (Figure 29*b*), although the generation of torsion was much lower on both the tailless and tetramer templates (Figure 29*c* dark grey squares and grey squares with dashed lines respectively) compared to intact octamer templates (Figure 29*c* black squares). Interestingly, the results of torsion generation by the WT SWI/SNF on tailless octamers and tetramers were very similar to levels of torsion generation on naked DNA.

The R1164A complex was able to generate little superhelical torsion on the tailless template (dark grey circles) as compare to intact octamers (black circles). In contrast to WT SWI/SNF, the R1164A complex was very ineffective at generation of torsion on the tetramer substrate (circles with dashed line), and this defect was similar to that seen with naked DNA. These data suggest that the histone tails and/or proper nucleosome structure might play a role in coordinating motif V action on the chromatin substrate.

a
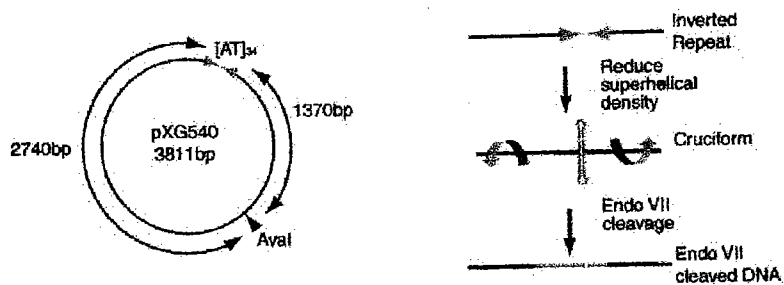
b
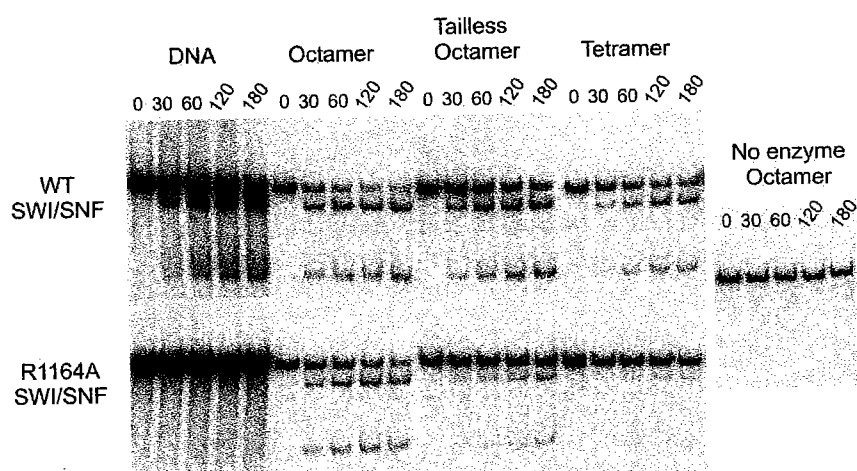
c
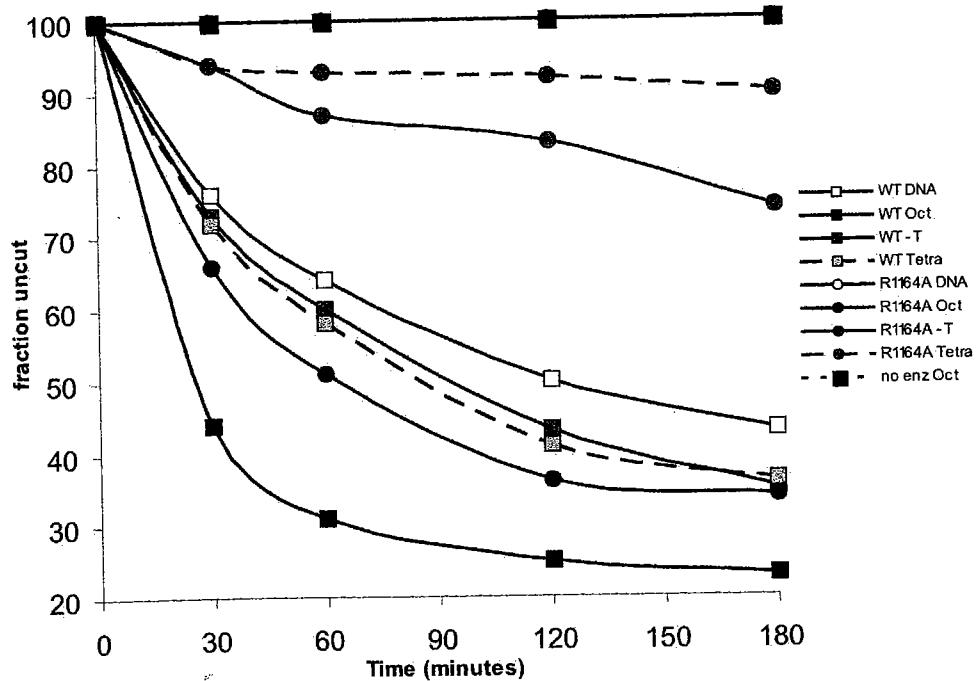
Figure 29. Defections in the generation of torsion by disruption of motif V is further exacerbated on nucleosomal arrays lacking histone N-termini. The rates of torsion generation by WT and R1164A complexes were assayed on chromatin templates containing intact octamers (*black symbols*), tailless octamers (*dark grey symbols*), or (H3-H4)$_2$ tetramers (*light gray symbols*). 1.5 nM SWI/SNF was incubated with 8 ng chromatin cruciform template or 8 ng DNA template, 0.15 ug/ml Endonuclease VII and 3 mM ATP. (*a*) Schematic of torsion assay. (*b*) Raw data from tailless octamer and tetramer torsion assay experiments. (*c*) Graphical representation of data from previous panel. WT SWI/SNF data is represented as squares and R1164A is represented by circles.

Mobilization of nucleosomes requires an intact motif V.

Since disrupting motif V has a major effect on the generation of torsion, I wanted to next see if this translated into a defect in mobilization of nucleosomes on DNA. To test this hypothesis, I decided to use a mononucleosome template containing a very strong nucleosome positioning sequence to create a centrally positioned nucleosome. The mononucleosome used contains a 340 bp fragment of DNA with a "601" positioning element located in the center of the DNA fragment with nearly 100 bp of DNA to either side (Figure 30a). The 601 element was originally isolated in a screen to select for DNA sequences that bind nucleosomes very tightly (Lowary and Widom, 1998). As a result this sequence has much higher affinity for nucleosomes than the 5S rDNA sequences (Anderson and Widom, 2000). This positioning element also differs from the 5S repeat used in the Sal I assay in that the 601 element has only one major nucleosome translational positioning frame (Lowary and Widom, 1998). The 5S repeat has one translational position that is occupied 60% of the time as well as two other translational positioning sequences that are occupied the remaining 40% (Dong et al., 1990). Similar highly positioned nucleosomes have been used for mobility shift experiments by other groups (Flaus and Owen-Hughes, 2003).

Motif V altered SWI/SNF complexes were tested for mobility defects on centrally positioned mononucleosomes on native PAGE gels. Mononucleosomes for mobility studies were generated using the chicken oligonucleosome transfer method (Owen-Hughes et al., 1999). Prior to incubation with SWI/SNF, >95% of the mononucleosomes migrate as a single species on native PAGE gels (Figure 30b, zero minute time point).

WT SWI/SNF complex is able to shift this positioned nucleosome to a set of faster migrating species and after 90 minutes some DNA that co-migrates with free DNA is generated (see the key in Figure 30*b* for theoretical nucleosome positions). The ΔSTRAGGLG complex, in stark contrast, is almost completely defective for mobilization on the nucleosome, similar to its torsion phenotype (Figure 30*b*). The R1164A complex has similar activity to WT SWI/SNF for the mobilization of mononucleosomes on this template except for the generation of the fastest migrating species and an accumulation of a species of nucleosomes that migrates slightly slower then the initial positioned nucleosome. This defect by motif V altered complexes in the mobilization of mononucleosomes correlates well with their defects in generating torsion.

Next mobility was confirmed by Exonuclease III mapping of nucleosome positions on the mononucleosome. There is a possibility that the apparent mobility on the native PAGE gels reflects mononucleosomes that have created stable remodeled products containing small bulges or loops of DNA. These products would migrate fastest then the initial mononucleosome as the linker DNA would be spooled into the nucleosome at the entry/exit sites. To confirm whether the remodeled mononucleosomes were sliding or generating alterative nucleosomes I created mononucleosomes that could only be digested with Exo III from the Eco RI end of the mononucleosome. Exo III digestion can be used map the boundaries of nucleosomes on a fragment of DNA with 5'-overhang (Hamiche et al., 1999; Li and Wrange, 1993; Li and Wrange, 1995; Li and Wrange, 1997). I used Exo-III to map the nucleosome boundary relative to the Eco RI restriction site on the DNA template (see Figure 31*a*). As the R1164A defect is more

subtle compared to WT SWI/SNF, only the ΔSTRAGGLG complex was used in this assay. After incubation of the mononucleosomes with the different SWI/SNF complexes the reactions were treated with Exo III for 10 minutes (times in figure reflect total remodeling time plus Exo III treatment). In the absence of chromatin remodeling (no enzyme, lane 3 Figure 31b) a clear Exo III stop can be seen representing a nucleosome with a boundary near the Nsp I site. Wild-type SWI/SNF is able to disrupt this nucleosome boundary in less then 10 minutes (lane 4). The WT SWI/SNF complex also generates a repetitive digestion pattern different from the DNA digest or the no enzyme reaction. Disruption of the nucleosome boundary is not seen with ΔSTRAGGLG SWI/SNF complex until 100 minutes (lane 18, Figure 31b). These data suggest that the nucleosomes are sliding on the 601 DNA fragment as the nucleosome boundary is disrupted upon remodeling by WT SWI/SNF. If novel bulge containing nucleosomes were generated by SWI/SNF then the doublet corresponding to the nucleosome boundary would migrate at a higher base pair position and the repetitive digestion pattern in the WT reactions would not be seen. Thus, it appears that SWI/SNF is disrupting nucleosomes by a sliding mechanism.

a
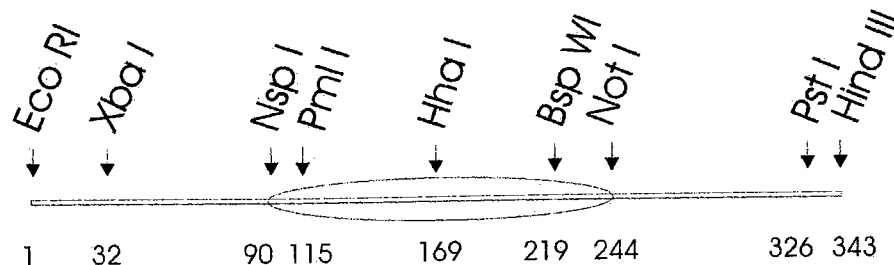
b
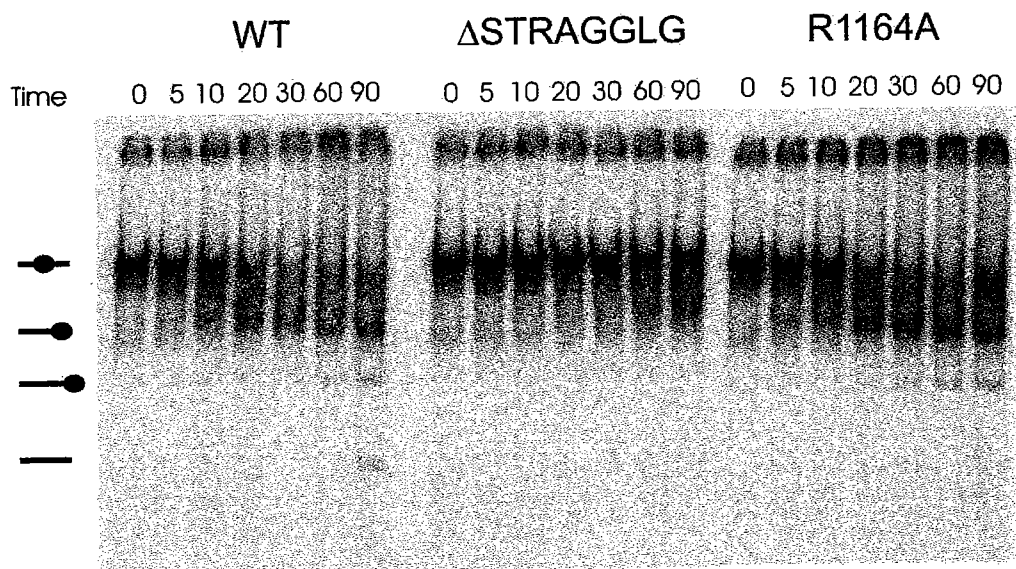
Figure 30. Nucleosome mobility by motif V altered SWI/SNF complexes. Native PAGE analysis of 601-340 bp mononucleosomes incubated with WT, ΔSTRAGGLG or R1164A SWI/SNF complexes. (*a*) Schematic of the 340 bp 601 DNA fragment. (*b*) Samples were taken from the reactions at indicated time and incubated with excess dsDNA and glycerol to remove SWI/SNF and quenched on ice. Samples were electrophoresed on 4% TBE PAGE gels. Left hand bars represent theoretical nucleosome positions.

a
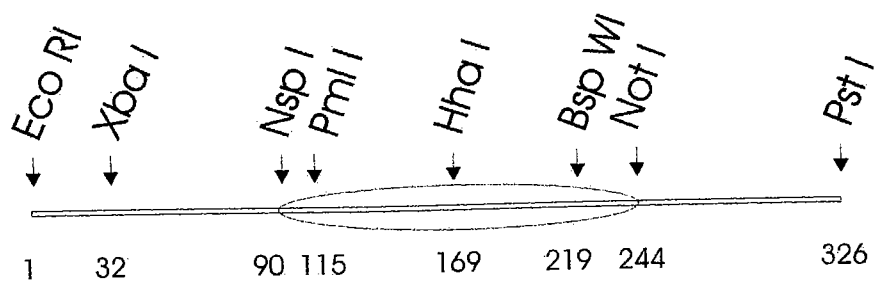
b
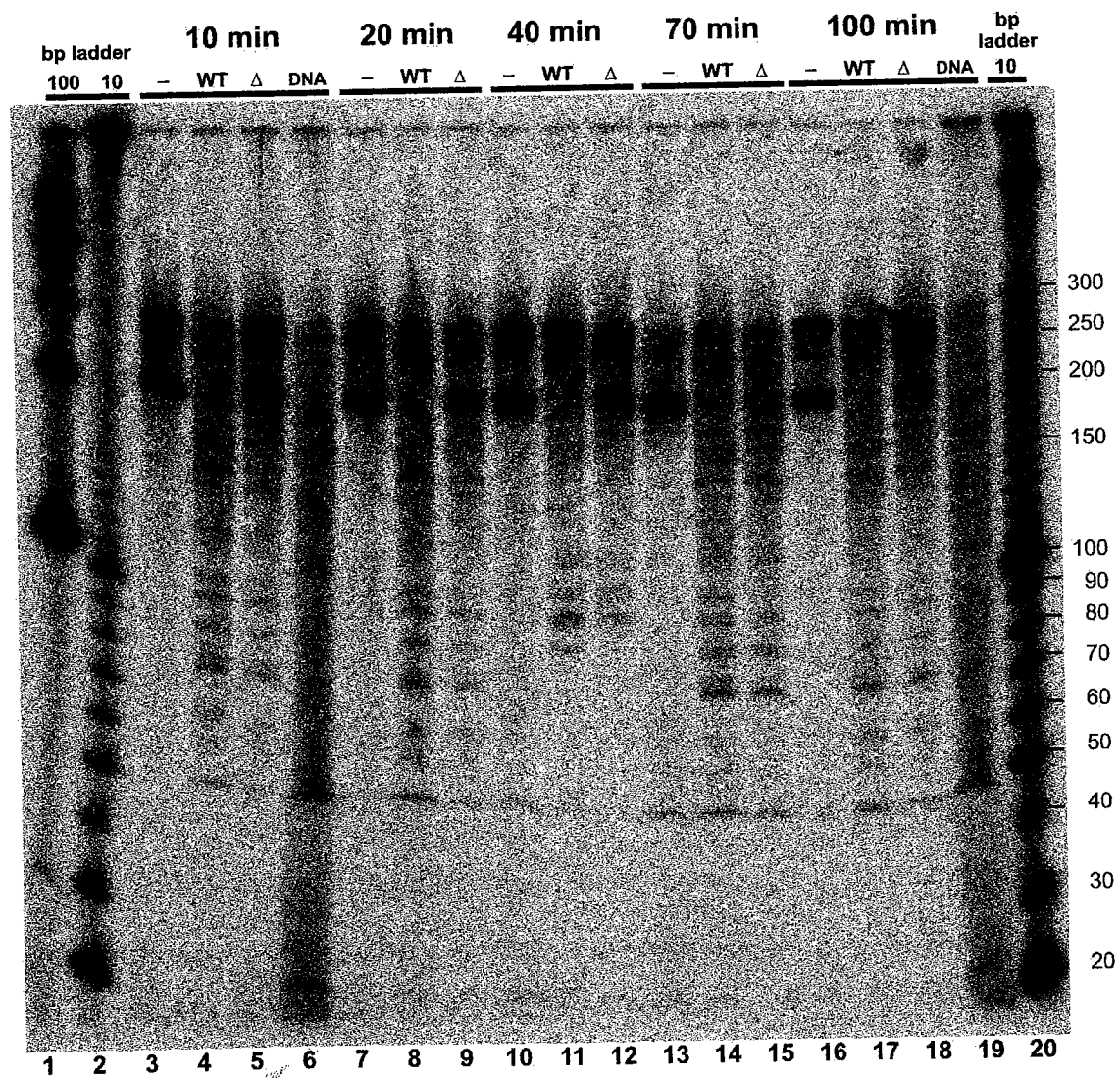
Figure 31. Exo III mapping of nucleosome positions after SWI/SNF remodeling.
Nucleosome boundary positions were mapped with Exonuclease III to confirm
mobility of the nucleosomes on the 601 substrate. (*a*) Schematic of the 601 sequence
used for Exo III mapping. (*b*) 3 nM Eco RI fragments labeled at the Pst I site were
incubated with 3 nM SWI/SNF complex (WT or ΔSTRAGGLG), and 3 mM ATP in
1x 5-50 buffer. At (t-10) minutes, 5 U of Exo III was added to the reaction and
digestion was allowed to occur for 10 minutes. Exo III digestion was stopped by the
addition of 2x Stop buffer. After a 20 minute deproteination, samples were boiled in
formamide loading buffer and loaded onto DNA sequencing gels. Lanes marked
(WT) correspond to WT SWI/SNF, (-) represent reactions without remodeling enzyme
and (Δ) denotes ΔSTRAGGLG complex. Ten and 100 bp ladders are indicated on the
gel.

SWI/SNF is not able to create restriction enzyme accessibility on mononucleosomes in the absence of torsion generation.

One hallmark of SWI/SNF action is the ATP-dependent increase in restriction enzyme accessibility of mononucleosomes. In principle, this accessibility could result from either movement of nucleosomes or changes in histone-DNA contacts resulting in loops or bulges of DNA forming on the surface of the nucleosome. In the latter model, SWI/SNF may facilitate restriction enzyme accessibility movement of the nucleosome (Peterson, 2002b). As the small deletion (ΔSTRAGGLG) within motif V cripples nucleosome mobilization, I sought to test whether there was also a defect in remodeling assayed by restriction enzyme accessibility. The "601"-DNA positioning fragment used for the mobility experiments was used for these assays as well since it has a number of convenient restriction enzyme sites that are useful for monitoring chromatin remodeling in a similar manner as the Sal I remodeling assay (see Figure 32a). Accessibility was monitored with two different restriction enzymes, Pml I and Hha I. On the 340 bp centrally positioned mononucleosome, the Pml I restriction site is located 25 bp from one DNA entry/exit site on the nucleosome, while the Hha I site is near the dyad axis of the 601 nucleosome sequence (see Figure 32a). Remodeling by the WT SWI/SNF complex leads to rapid ATP-dependent accessibility to the Pml I site; where 65% of the Pml I sites are accessible in 20 minutes (Figure 32b and c). The ΔSTRAGGLG complex shows drastically decreased activity. Less than 10% of the template was cleaved in 20 minutes (Figure 32b and c). Accessibility at the dyad axis (as illustrated by Hha I accessibility), is nearly abolished in the ΔSTRAGGLG complex while accessibility with WT SWI/SNF

shows a linear increase that appears to have similar kinetics to the mobilization results. Hha I cleavage is nearly 50% in 90 minutes with WT SWI/SNF while ΔSTRAGGLG complex only allows access to >5% of the Hha I sites in 90 minutes. Thus, these data indicate that the decrease in nucleosome mobilization directly correlates with the enhancement of restriction enzyme accessibility.

Next, restriction enzyme accessibility on an end positioned nucleosome was tested to further address if mobilization of nucleosomes was separable from restriction enzyme accessibility (Figure 33a). This substrate was generated using the same "601" sequence (CP1024), except that the restriction fragment Eco RI – Not I was used to produce a 240 bp, end positioned mononucleosome with a 100 bp linker on only one side (Figure 33a). Previous studies have shown that while SWI/SNF can move nucleosomes from the middle of DNA fragments to the end, it cannot move an end positioned nucleosome to the center of the DNA (Becker and Horz, 2002). Consistent with these previous data, I found that remodeling by WT SWI/SNF results in much less accessibility on the end-positioned nucleosomes than with centrally positioned mononucleosomes (compare results from Figure 32c and Figure 33c). The ΔSTRAGGLG complex resulted in a ~3 fold decrease (compared to WT SWI/SNF) in accessibility at the entry edge of the nucleosome as illustrated by Pml I accessibility (Figure 33c). Also consistent with previous data, I found that neither WT SWI/SNF nor the ΔSTRAGGLG complex could generate significant Hha I accessibility on the 240 bp, end-positioned mononucleosome (Figure 33b). It appears that in the absence of linker DNA on both sides of the nucleosome core particle, little accessibility can occur with ΔSTRAGGLG. In contrast to

WT enzyme, this phenomenon is observed at both the entry/exit and dyad axis position within the nucleosome.

The apparent rate of accessibility appears different on these 601 mononucleosomes as compared to the results with the Sal I assay (Chapter 3, Figure 22). In the case of the Sal I digestion of nucleosomal arrays, disruption of motif V led to only an approximate two fold decrease in remodeling activity. In order to address the inherent differences between these assays, 5S rDNA mononucleosomes were constructed using the Sal I containing 5S rDNA repeat from the central nucleosome on the 208-11 template. When 5S mononucleosomes are treated with Sal I there is much more cleavage in the absence of remodeling enzyme, compared to similar experiments with "601" mononucleosomes, reflecting the greater heterogeneity of translational positions of the DNA template (see Figure 34a). In the presence of WT SWI/SNF, Sal I accessibility is increased, and disruption of motif V leads to a three fold decrease in Sal I digestion rate (Figure 34b and c). The WT complex can remodel >60% of the substrate in 20 minutes while either motif V disrupted complex results in ~20% of the substrate being remodeled. These defects are more in line with the results seen in the Sal I nucleosomal array assay from Chapter III. This is easily explained by the fact that in nearly 40% of the mononucleosome incorporated in the 5S rDNA sequence the Sal I site is going to be closer to the entry/exit sites and further away from the dyad axis of the nucleosome.
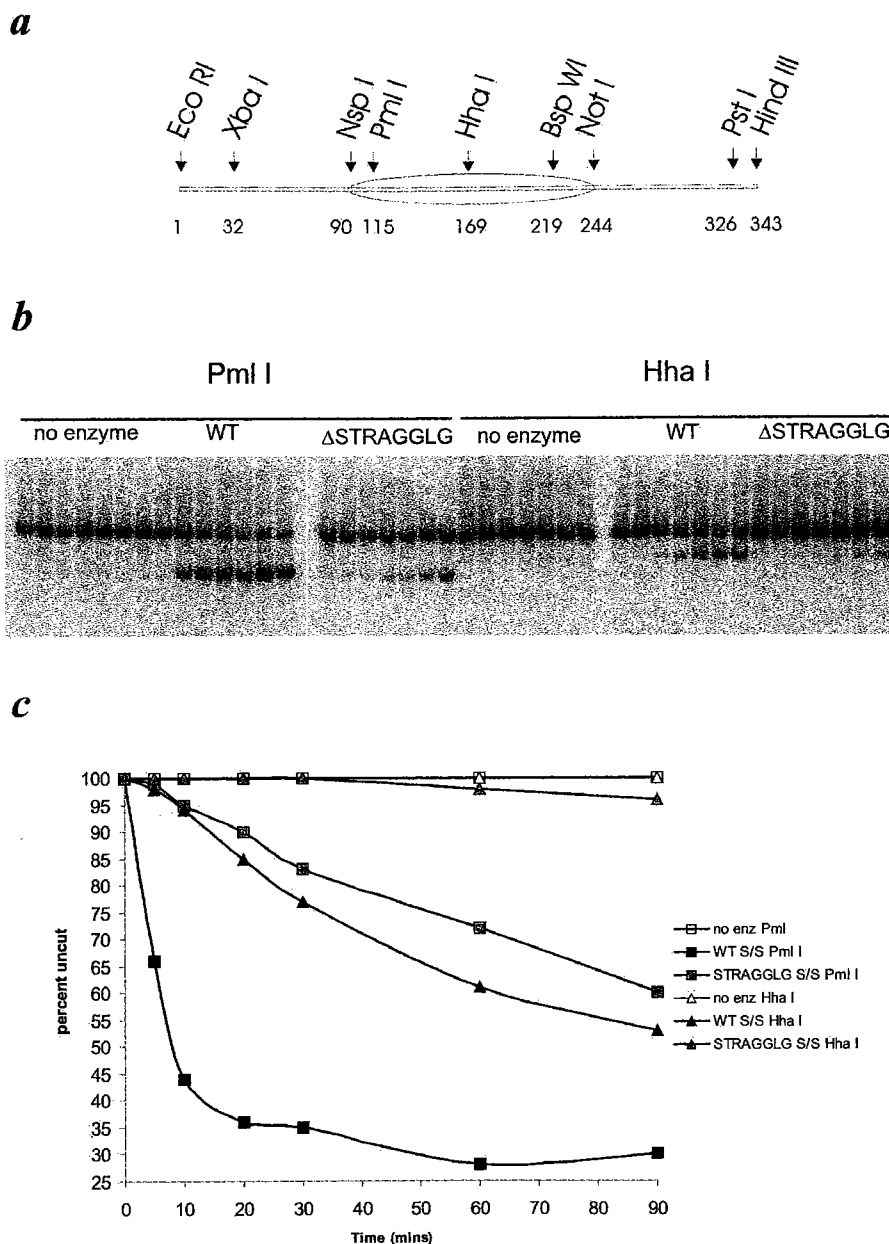
Figure 32. Motif V is required for enhanced restriction enzyme accessibility on mononuclesosomes. (*a*) Schematic of the 340 bp 601 DNA fragment. (*b*) 1.0 nM WT (black symbols) and ΔSTRAGGLG (grey symbols) SWI/SNF were incubated with 130 ng total nucleosomes (0.3 ng 601-mononucleosomes), 3 mM ATP and 40U of restriction enzyme (Hha I-triangles or Pml I-squares). Reactions containing no enzyme are represented by open symbols. Samples were removed from the reactions at given times, quenched and deproteinated. Samples were resolved on 8% TBE native PAGE gels. (*c*) Graphical representation of data from panel *b*.

a

Eco RI
Xba I
Nsp I
Pml I
Hha I
Bsp WI
Not I

1   32   90 115   169   219 244

b

Hha I digest

WT   ΔSTRAGGLG

Time   0 5 10 20 30 60 90   0 5 10 20 30 60 90

c

Pml I digest

WT

ΔSTRAGGLG

Time   0   20 30 40 60 70 90 100 120

fraction uncut

120

100

80

60

40

20

0

0   20   40   60   80   100   120
Time (mins)

ΔSTRAGGLG

WT
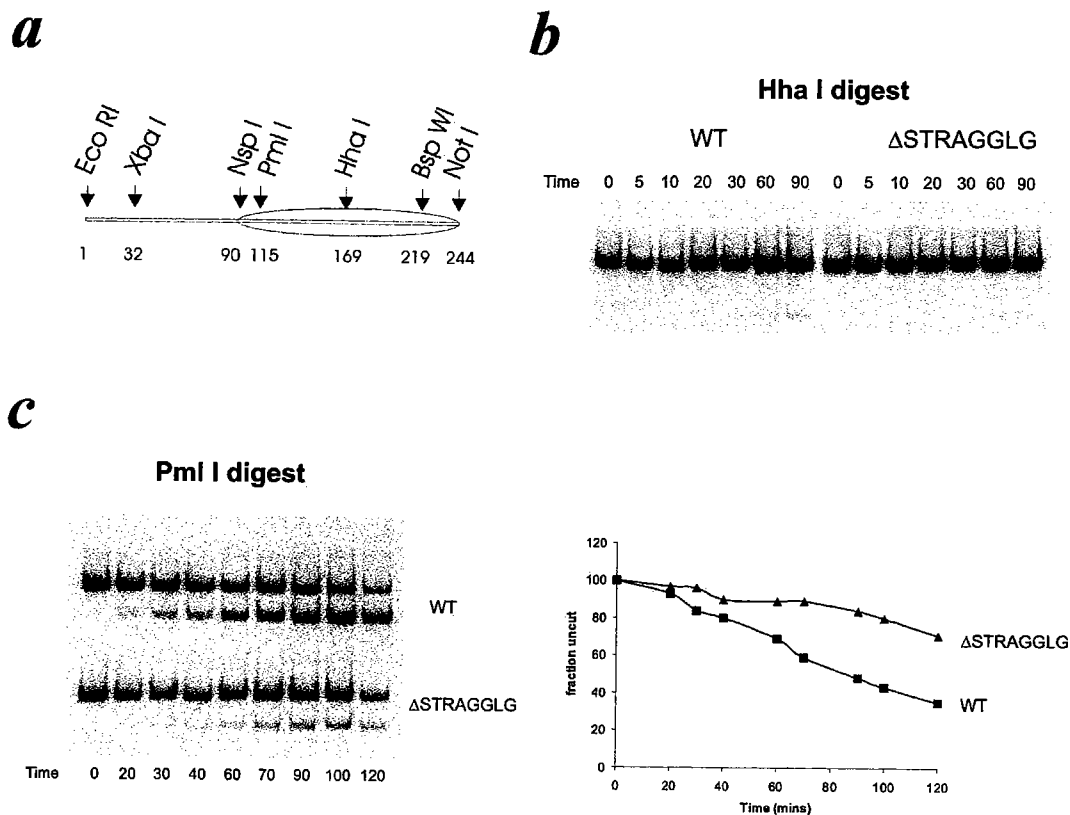
Figure 33. SWI/SNF enzyme accessibility on end-positioned nucleosomes. (*a*) 601 mononucleosomes were generated with linker DNA on only one end. These mononucleosomes were used to test restriction enzyme accessibility with both WT and ΔSTRAGGLG SWI/SNF complexes. (*b*) Hha I accessibility on end positioned mononucleosomes. Note that WT SWI/SNF does create ~2% Hha I cleavage at 90 minutes while ΔSTRAGGLG SWI/SNF complex creates less virtually no Hha I cleavage during this timecourse. (*c*) Pml I accessibility on end positioned nucleosome. Reactions contained 130 ng nucleosomes (0.5 ng labeled), 1.0 nM SWI/SNF, 3 mM ATP and 40 U of restriction enzymes.
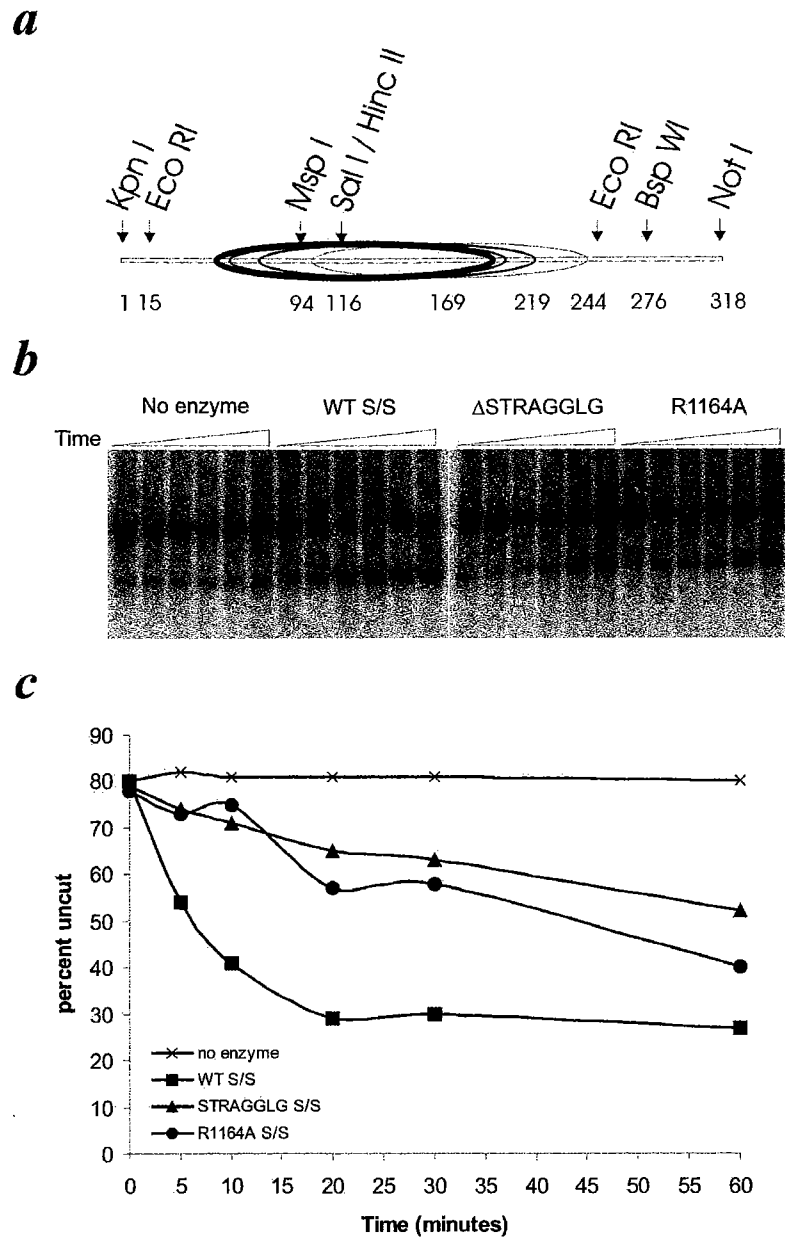
Figure 34. **SWI/SNF remodeling of 5S rDNA mononucleosomes.**
Restriction enzyme accessibility of the Sal1 5S mononucleosome remodeled
with SWI/SNF complexes. (*a*) Schematic of 5S DNA mononucleosome
illustrating the major and minor nucleosome positions in this DNA fragment
(thickness of oval represent relative strength of positioning elements. (*b*) raw
data for Sal I accessibility. (*c*) Graphical representation of data from panel *b*.
Reactions contained 130 ng nucleosomes (0.5 ng labeled), 1.0 nM SWI/SNF,
3 mM ATP and 150 U of Sal I restriction enzyme.

Impaired remodeling of chromatin substrates lacking histone N-termini.

Using the same recombinant octamers generated for the torsion assays, mononucleosomes were constructed to test restriction enzyme accessibility on intact or tailless nucleosomal substrates. Recombinant mononucleosomes were made by stepwise salt dialysis with α^{32}P-dCTP end-labeled 601 DNA fragments and recombinant histones (see Materials and Methods for description of reagent generation). Figure 35 shows the results of the mononucleosome reconstitutions. Intact recombinant octamers assembled as expected with >95% of the nucleosomes migrating as a discrete species on native PAGE. The tailless octamers on the other hand generated three species with discreet mobility patterns. None of these species corresponds to free DNA, indicating that assembly of the labeled 601 fragment into the mononucleosomes was complete (see Figure 35).

These mononucleosomes were used to examine Hha I accessibility (the restriction site near the dyad axis, Figure 36a). In the case of the WT SWI/SNF complex, the absence of the N-terminal tails leads to a defect in remodeling, reflected by a 3-fold slower rate of Hha I accessibility; it takes three times as long to get to 50% accessibility at the dyad axis on tailless octamers versus intact octamers (24 minutes versus 8 minutes Figure 36b, c). In the case of the R1164A enzyme there is a much greater defect (6 fold or greater) observed on tailless nucleosomes relative to intact nucleosomes. The ΔSTRAGGLG complex was not tested since HhaI accessibility is negligible on intact mononucleosome substrates. The results of the accessibility experiments correlate very well with the results seen on the tailless cruciform arrays (compare Figures 34 and 36).

Since, the absence of the N-terminal histone tails exacerbates the defects seen with the disruptions of motif V, it appears that the histone tails and/or the presence of an intact octamer play an important role in interactions with the ATPase domain of Swi2p or are crucial for proper chromatin remodeling by the SWI/SNF complex.
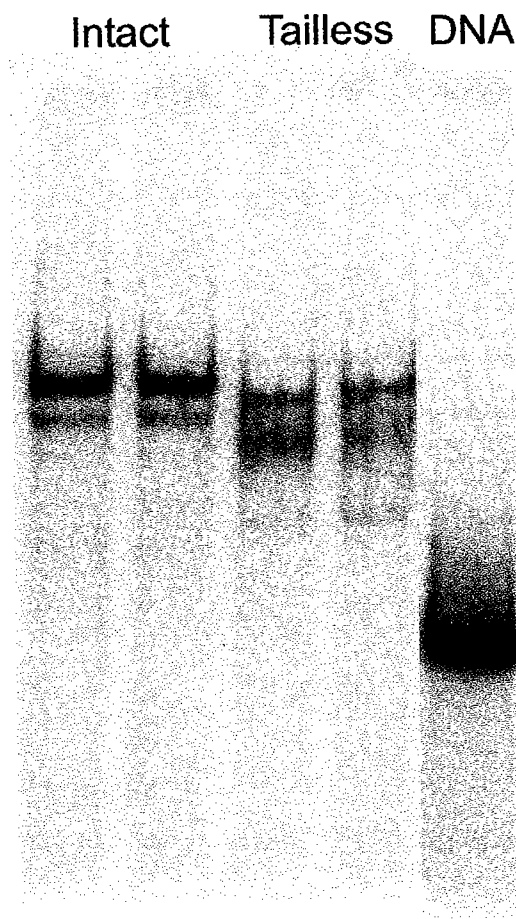
Figure 35. Generation of recombinant xenopus mononucleosomes with and without histone tails. Recombinant xenopus histones were used to construct intact tailless octamers. These octamers were used to produce mononucleosomes on 340 bp 601 DNA fragments. Mononucleosomes were created by salt dialysis as described in the Materials and Methods section.

a

Eco RI   Xba I   Nsp I   Pml I   Hha I   Bsp WI   Not I   Pst I   Hind III

1   32   90   115   169   219   244   326   343

b

Intact Octamer   Tailless Octamer
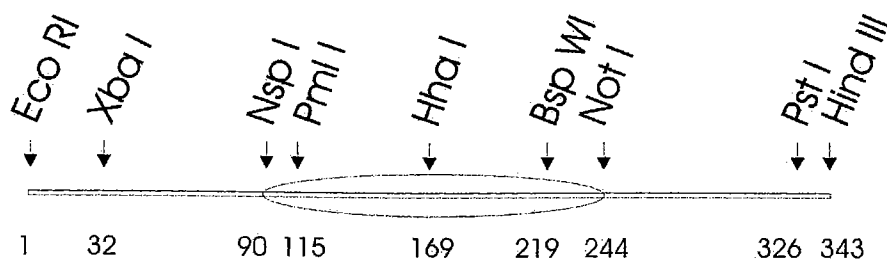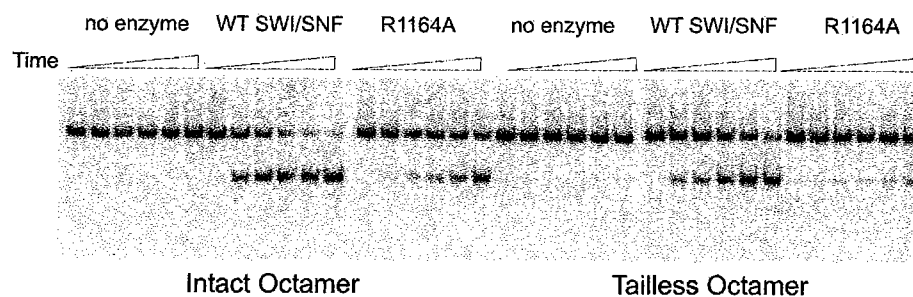
c
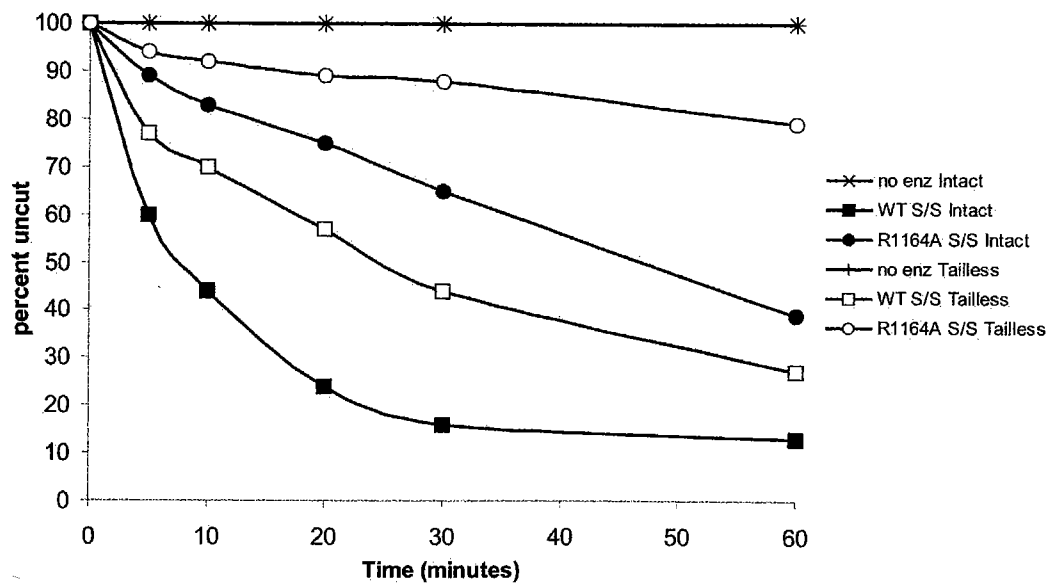
Figure 36. Restriction enzyme accessibility on histone tailless octamers. The ability of WT and R1164A SWI/SNF complexes to create restriction enzyme accessibility (Hha I) was tested on mononucleosomes with intact and tailless octamers. (*a*) Schematic of 601 mononucleosome. (*b*) Raw data for Hha I accessibility. 1.0 nM SWI/SNF (WT or R1164A) was incubated with 1 nM mononucleosomes, 3 mM ATP and 40 U Hha I. Samples were removed from the reaction at specific time points over 1 hour and prepared as described in the methods. (*c*) Graphical representation of data from accessibility experiment. WT S/S reactions are represented by squares and R1164A reactions are represented as circles. Intact octamers are represented as filled symbols and Tailless octamers are represented as open symbols.

Discussion

In this chapter I examined the role of motif V within the ATPase/helicase domain of Swi2p on the ATPase activity and chromatin remodeling capabilities of SWI/SNF complex. In this study I found that key ATPase residues in motif V play a chromatin-specific role in the function of SWI/SNF *in vitro* on assembled chromatin substrates. The *in vitro* data presented here shows strong biochemical significance for the severity of motif V mutations in ySWI/SNF. I will also discuss recent evidence linking specific amino acid substitutions in and around motif V of the Swi2p human homolog Brg1 that are found to be specific mutations in both colon cancer cell lines and lung carcinomas.

Motif V uncouples ATPase activity from chromatin remodeling activity in SWI/SNF.

As mentioned earlier, the specific role of motif V in SF1 and SF2 helicases is not well understood. Motif V, like motif III discussed in Chapter III, shows considerable sequence variability in different helicase-like proteins. This domain in Swi2p contains a large predicted loop that contains the amino acid sequence STRAGGLG (see Figure 17). One feature of note for this motif is that this loop in some helicases, like PcrA (Figure 37c), makes contacts with both ATP and the oligonucleotide (Velankar et al., 1999). The sequence of motif V is highly conserved among ATP-dependent chromatin remodeling enzymes (Table 2). Among the more closely related Swi2/Snf2 homologs the conservation of this motif is very high (85% or better). The conservation of this motif is

also high in the ISWI and Mi-2 subfamilies of ATP-dependent chromatin remodeling enzymes. The Swi2p-like repair proteins are weakly conserved in this portion of the ATPase domain (Table 2: see ATRX, Rad54b, and ERCC, for examples).

In this study I used a deletion of eight residues (ΔSTRAGGLG) which contains two invariant motif V consensus residues (outlined in red), as well as a single amino acid substitution at R1164 (R1164A). Evidence from the helicases PcrA, NS3, and the repair protein CSB illustrates the importance of the terminal glutamine residue for biochemical contacts and for *in vivo* function (respectively) in this stretch of amino acids (Caruthers and McKay, 2002; Muftuoglu et al., 2002). *In vivo*, the deletion of STRAGGLG resulted in a phenotype similar to a complete deletion of SWI2 (Figure 26) and (Richmond and Peterson, 1996). In yeast, the expression of a number of SWI/SNF specific genes are reduced either 2 to 3 fold in the case of the R1164A mutant, or greater than ten fold in the ΔSTRAGGLG mutant. The results of the carbon source plate assays also illustrate the consequence of the loss of motif V function in yeast (see Figure 26).

Deletion of these eight amino acids in ΔSTRAGGLG has no effect on the ATPase kinetics of SWI/SNF (Figures 20, 21 and Table 1). However, defects are apparent in various chromatin remodeling assays. While the defect in nucleosomal array remodeling assay (e.g. Sal I accessibility) was only reduced two fold, the severity of the substitution in the generation of torsion was significantly higher (compare Figures 23 and 24). On DNA templates, the ΔSTRAGGLG substitution was not able to generate superhelical

Table 2: Motif V alignment within the SWI2/SNF2 ATPase family

NAME	ORGANISM	MOTIF	SEQUENCE	IDENTITY
Snf2p	Saccharomyces cerevisiae	V	FILSTRAGGLGLNLQTADTVI	100%
Brg1p	Tetrahymena thermophila	V	FILSTRAGGLGLNLQTADTVI	100%
SPCC1620.14c	Schizosaccharomyces pombe	V	FMLSTRAGGLGLNLQTADTVI	95%
Sth1p	Saccharomyces cerevisiae	V	FLLSTRAGGLGLNLQTADTVI	95%
MG06388.4	Magnaporthe grisea 70-15	V	FLLSTRAGGLGLNLQTADTVI	95%
PSA-4	Caenorhabditis elegans	V	FMLSTRAGGLGLNLQTADTVI	95%
hypothetical protein	Neurospora crassa	V	FLLSTRAGGLGLNLQTADTVI	95%
SPCC830.01c	Schizosaccharomyces pombe	V	FMLSTRAGGLGLNLQTADTVI	95%
BRAHMA	Caenorhabditis elegans	V	FMLSTRAGGLGLNLQTADTVI	95%
SPAC1250.01	Schizosaccharomyces pombe	V	FLLSTRAGGLGLNLQTADTVI	95%
BRAHMA	Drosophila melanogaster	V	FLLSTRAGGLGLNLQTADTVV	90%
ENSANGP	Anopheles gambiae	V	FLLSTRAGGLGLNLQTADTVV	90%
SNF2-BETA	Homo sapiens	V	FLLSTRAGGLGLNLQSADTVI	90%
SMARCA4-1	Homo sapiens	V	FLLSTRAGGLGLNLQSADTVI	90%
BRG1	Homo sapiens	V	FLLSTRAGGLGLNLQSADTVI	90%
BRG1	Gallus gallus	V	FLLSTRAGGLGLNLQSADTVI	90%
SMARCA4-2	Homo sapiens	V	FLLSTRAGGLGLNLQSADTVI	90%
SMARCA4-1	Mus Musculus	V	FLLSTRAGGLGLNLQSADTVI	90%
SMARCA4-2	Mus Musculus	V	FLLSTRAGGLGLNLQSADTVI	90%
BRM	Gallus gallus	V	FLLSTRAGGLGLNLQAADTVI	90%
Hrp1	Schizosaccharomyces pombe	V	FLLSTRAGGLGINLNTADTVI	85%
HBRM	Homo sapiens	V	FLLSTRAGGLGLNLQAADTVV	85%
Mi-2b	Mus Musculus	V	FILSTRAGGLGINLATADTVI	85%
INO80	Saccharomyces cerevisiae	V	FILSTRAGGLGINLTAADTVI	81%
ISW1	Saccharomyces cerevisiae	V	FLLTTRAGGLGINLTSADVVV	71%
ATRX	Homo sapiens	V	FIISTKAGSLGINLVAANRVI	62%
RAD54b	Gallus gallus	V	FLLSSKAGGVGLNLVGASHLI	57%
ERCC-6 (CSB)	Homo sapiens	V	FLLTTRVGGLGVNLTGANRVV	57%

CONSENSUS		V	FLLSTRAGGLGLNLQTADTVI	
Key SF2 family residues		V	T G D	
			S S N	

torsion. On a template incorporated into chromatin, the enzyme was able to generate some torsion, but levels were greater than 10 fold lower than WT SWI/SNF. This led me to explore the idea that this motif might be responsible for the transduction of ATP hydrolysis into the generation of superhelical torsion and therefore the generation of mobility and restriction enzyme accessibility of DNA on nucleosomes.

The results of the mobility assay on the 601 mononucleosome clearly indicate that the ΔSTRAGGLG complex has a severe defect in the mobilization of nucleosomes. Furthermore, the ΔSTRAGGLG complex was also severely defective in generating enhanced enzyme accessibility to restriction enzymes on the 601 mononucleosome substrate. The rate of WT SWI/SNF-induced Hha I accessibility on the 601 mononucleosome (Figure 32c, WT Hha I accessibility) correlates remarkably well with the emergence of the fastest migrating species in the mobility assays (Figure 30 WT SWI/SNF 60 and 90 minutes). The strong correlation between the mobility results and the Hha I kinetics suggest that the Hha I site remains occluded until the nucleosome has "slid" past the restriction site. This model explains why incubation with ΔSTRAGGLG results in very little stimulation of Hha I accessibility, since the enzyme also fails to slide nucleosomes.

The results of the restriction enzyme experiments on the 240 bp end-positioned nucleosome also support a defect for ΔSTRAGGLG in the ability to generate remodeling in a mobility-independent manner. Previously, it was concluded that SWI/SNF can generate enzyme accessible sites on DNA incorporated into a nucleosome in the absence of mobility (Fan et al., 2003). In the case of the 240 bp 601 mononucleosome used here,

accessibility of DNA near the dyad axis remains occluded even in the presence of the WT enzyme (Hha I site, see Figure 33*a* and *b*). These results seem to disagree with previously published results showing that human SWI/SNF can create restriction enzyme accessibility on mononucleosomes (Aoyagi et al., 2002). This could be due to the strength of the positioning element used in this study compared to the other study. It is also possible that there is a fundamental difference between yeast and human SWI/SNF complexes.

In the absence of superhelical torsion generation, both mobility and restriction enzyme accessibility are severely decreased. This suggests that restriction enzyme accessibility may be dependent on the mobility of mononucleosomes. These results also support the model that chromatin remodeling results from the generation of an under-wound twist defect in the DNA duplex (van Holde and Yager, 2003). This twist defect could then be propagated along the surface of the nucleosome resulting in small ~1 base pair slippage of DNA per ATPase cycle.

The results of the Exonuclease III mapping of nucleosome position after remodeling reinforces the model that SWI/SNF primarily slides nucleosomes on strong DNA positioning sequences. The loss of the strong exonuclease stop in the Exo III experiments suggests that either nucleosomes are lost or are slide on the DNA sequence. The change in the Exo III digest pattern after remodeling indicates that nucleosomes are still present since the pattern is clearly different than Exo III digested naked DNA. The distract decrease in mobility rate by ΔSTRAGGLG complex compared to WT SWI/SNF is mirrored in the Exo III mapping.

Motif V plays an important role in the mechanism of SWI/SNF chromatin remodeling.

The data presented in this chapter indicate that motif V within Swi2p couples ATP hydrolysis to the molecular mechanism of chromatin remodeling. The motif V loop appears to be crucial for the proper generation of superhelical torsion on a nucleosomal DNA substrate. It is interesting to note that the ability to generate torsion on DNA is stimulated by chromatin even for the WT SWI/SNF enzyme. While deletion of the STRAGGLG amino acid results in a severe effect in torsion generation on both DNA and chromatin, the single amino acid substitution (R1164A) has only a two fold effect on torsion generation on chromatin, yet no ability to create torsion on DNA. So it appears that the defect of the R1164A substitution in motif V is partially relieved in the context of a chromatin substrate. This chromatin stimulation was confirmed by comparing the ATP hydrolysis rates of R1164A to WT SWI/SNF in the presence of nucleosomes and DNA. The R1164A complex had a 2.5 fold defect when DNA was used as a co-factor, but incorporation of this DNA into nucleosomes completely alleviates the defect. This suggests that R1164A might be involved in orientating the motif V loop in response to DNA thereby allowing the transduction of the ATP hydrolysis event into remodeling.

How could motif V couple ATP hydrolysis to the mechanism of remodeling?

Sequence threading of Swi2p ATPase motifs onto the crystal structure of PcrA illustrates important contacts in the ATPase domain that might explain the role of motif V

(Figure 37*c*). The STRAGGLG residues of motif V are highlighted in pink in Figure 37c and illustrate a potential connection made between ATP and the oligonucleotide substrate. At the C-terminus of the loop (middle of frame), the Gln251 (in PcrA) is seen to make contacts with the γ-phosphate of ATP (Velankar et al., 1999). At the N-terminus of the loop (near the beta sheet) PcrA makes contacts with ssDNA (see Figure 37*a* and 37*c*). In Swi2p this loop might play a similar role coupling changes in hydrolysis state with generation of torsion and therefore movement of the DNA through the ATPase domain. From this threading of Swi2p onto PcrA, R1164A appears to be at the top of the motif V loop. This arginine residue might be involved in structuring the loop to allow contact between ATP and the glutamine residue at the C-terminus of the STRAGGLG motif (Gln1169), and positioning the N-terminus of the loop to make contacts with oligonucleotide in a manner similar to other helicases. This model could explain the phenotypes seen *in vivo* as well as the results from the *in vitro* experiments presented here.
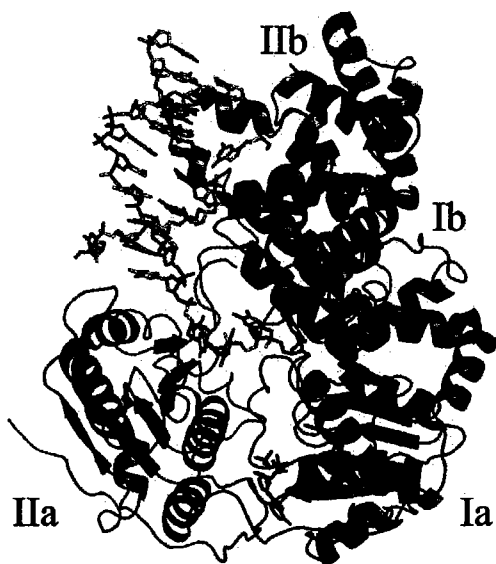
Figure 37. Theoretical modeling of Swi2p ATPase motifs. Swi2p ATPase motifs were modeled on the crystal structure of PcrA to illustrate possible interactions between oligonucleotide and ATP and the individual ATPase motifs. (*a*) Crystal structure of PcrA. Subdomain I (blue) and Subdomain II (green) are colored separately to aid visualization. AMPPNP is colored red and the ds/ssDNA oligonucleotide is colored gold. Numerals Ia and IIa represent the canonical domains found in SF1 and SF2 helicase. Ib and IIb represent folds that are specific to PcrA that fold out of subdomains Ia and IIa respectively. (*b*) Rotation of the PcrA structure in panel *a* 90° on the Z axis to illustrate the ATP binding cleft of the enzyme. (*c*) Magnification of the ATP-binding cleft of PcrA with the Swi2p ATPase motifs threaded onto the structure. Motifs are color coded according to the key on the side of the illustration. PcrA (PDB code 3PJR) structure (Velankar et al., 1999) was rendered with PyMOL, Delano software (Delano, 2002). Special thanks to Eric Merithew for rendering PcrA.

The N-terminal histone tails are important for proper remodeling by SWI/SNF and disruption of the nucleosome core particle exacerbates the defects of motif V amino acid substitutions.

As seen in Figures 34 and 36 the SWI/SNF complex appears to have reduced remodeling activity on tailless octamers as assayed by the ability to generate superhelical torsion and restriction enzyme accessibility. This defect was even more severe with the R1164A complex than with WT (2 fold reduced in WT and 5-8 fold reduced in the R1164A complex). The data suggest that the histone tails might interact directly with the Swi2p ATPase domain or that the tails are responsible for the correct positioning of the DNA on the octamer face to facilitate Swi2p interaction. The significance of these results will be further addressed in Chapter V.

The results with tetramer substrates also suggest that nucleosome integrity is essential for interactions with motif V. In the superhelical torsion assay, wild-type SWI/SNF exhibits little difference on either tetramer or tailless arrays. In contrast, the R1164A complex generated less superhelical torsion on tetramer arrays than tailless arrays. In either case disruption of the nucleosome results in torsion generation more akin to that seen on naked DNA.

Specific amino acid substitutions in motif V of hBRG1 (human Swi2p) result in both lung and colon carcinomas in culture and in patients.

One of the human homologs of SWI2, hBRG1, has been the focus of numerous recent studies due to an apparent connection to cancer in mammals (Roberts and Orkin,

2004). Recently, a number of studies have found mutations in the ATPase domain of hBRG1 that are in a number of different forms of cancers (Table 3). A recent study of 76 different tumor cell lines isolated a colon cancer cell line HCT-116 with a leucine to proline substitution in residue L1164 of hBrg1 (Wong et al., 2000). Another recent study of lung carcinomas from patients reveals two separate amino acid substitutions G1160R and S1176C, found in or around motif V, (personal communication and (Medina et al., 2004)). These amino acid substitutions further illustrate the importance of motif V in the function of the SWI/SNF complex *in vivo*.

Table 3: Cancer mutations found in the ATPase motif V of hBRG1

Isoform	Motif V Sequence	Notes
WT BRG1	FILSTRAGGLGLNLQTADTVIIFDS	WT Brg1
L1164P	FILSTRAGGLGPNLQTADTVIIFDS	HCT-116, colon cancer cell line (Wong et al., 2000)
G1160R	FILSTRAGRLGLNLQTADTVIIFDS	G1160R lung carcinoma from patient (Medina et al., 2004)
S1176C	FILSTRAGGLGLNLQTADTVIIFDC	S1176C lung carcinoma from patient (Medina et al., 2004)

Together these data point to an important role for motif V of the SWI2/SNF2 family of ATPases in the mechanism of ATP-dependent chromatin remodeling. This is the first case for a Swi2p specific role for any ATPase motif in the functionality of SWI/SNF chromatin remodeling. The study also suggests that N-terminal histone tails play a role in SWI/SNF chromatin remodeling that is related to motif V function. The results of the *in vitro* remodeling assays also suggest why amino acid residues in motif V

have been discovered in carcinogenic cells. These results begin to shed light on how Swi2p uses the hydrolysis of ATP to create nucleosome mobility and enzyme accessibility on chromatin.

Materials and Methods

Carbon source phenotype growth assay. Strains CY396 (WT), CY120 (*swi2Δ)* CY397 (*swi2K798A*), CY458 (*swi2R1164A*), and CY519 (*swi2ΔSTRAGGLG*) were used to study carbon growth phenotypes of motif V mutants. Serial dilutions of each strain (starting with 5000 cells and diluting 5x for each sequential spot) were plated on YEP media supplemented with either 2% glucose, 2% galactose, 2% ethanol and 2% glycerol, or 2% raffinose. Plates were incubated at 30 °C and photographed after the colonies had grown to sufficient size.

Generation of nucleosomal cruciform templates. Nucleosome templates for chromatin torsion assays were generated by mixing purified chicken histone octamers with pXG540 α^{32}P-dCTP labeled DNA (CP894) as well as 208-11 DNA. AvaI linearized pXG540 was treated like 208-11 chromatin arrays for the purpose of chromatin assembly and the protocol for 208-11 template generation was used to generate pXG540-chromatin substrate. Nucleosome concentrations were used to generate templates containing either 1 nucleosome per 200 bp of DNA (R=1.0, saturated) or 1 nucleosome per 400 bp of DNA (R=0.5, half saturated). Briefly 2 μg of 208-11 DNA and 0.5 μg of α^{32}P-dCTP labeled pXG540 was mixed with either 1 (R 0.5) or 2 μg (R 1.0) of chicken histones in 2 M NaCl. Chromatin array template was generated as previously described (Logie and Peterson, 1999). The addition of the 208-11 template into the reactions made it possible to analyze chromatin saturation of these reconstituted arrays by Eco RI digestion analysis

(Logie and Peterson, 1999). Eco RI analysis was used to estimate the incorporation of chromatin into pXG540 template. DNA:nucleosome ratios were chosen to give arrays which were not oversaturated.

Torsion assays with DNA versus chromatin substrates. Torsion assays were performed in the same manner as with naked DNA substrates (See Methods in Chapter III). Chromatin cruciform formation assays were performed in 30 μL reactions containing 1x 5-50 remodeling buffer, 3 mM ATP, 0.15 μg/ml Endonuclease VII, 8 ng (DNA concentration) of α^{32}P-dCTP pXG540 DNA or chromatin assembled pXG540, and 1.5 nM SWI/SNF complex. Rates of cruciform extrusion were measured over 120 minutes at 25 °C. 3 μl aliquots, at the indicated times, were taken, quenched and deproteinated by the addition of 2x Stop buffer (10 mM Tris pH 8.0, 0.6% SDS, 40 mM EDTA, 5% glycerol, and 0.1 mg/ml Proteinase K). Quenched reactions were incubated at 50 °C for 20 minutes to deproteinate samples. Samples were then resolved on 4% 1xTBE native acrylamide gels and imaged using a Molecular dynamics PhosphorImager. Percentage of pXG540 fragment cut was determined by using Imagequant v1.2 (Amersham).

Generation of "601" mononucleosomes substrates for mobility and restriction enzyme assays. Mononucleosomes for mobilization and restriction enzyme accessibility studies were generated as follows. The 343 or 244 bp mononucleosome DNA fragments were generated by digesting plasmid CP1024 (pGEMZ-lowerstrand "601") with either Eco RI and Hind III (343 bp fragment) or Eco RI and Not I (244 bp fragment). Fragments were

gel purified and labeled with α^{32}P-dCTP in a standard Klenow reaction. Labeled DNA fragments were used to generate mononucleosomes by oligonucleosome transfer. In these nucleosome reconstitutions, 2.5 μg of chicken oligonucleosomes (Yager et al., 1989) were mixed with 5.0 ng of labeled DNA fragments and reconstituted by stepwise serial dilution as previously described (Owen-Hughes et al., 1999). Native PAGE gels were used to determine the integrity of the arrays.

Generation of "601" mononucleosomes for Exo III mapping. Mononucleosomes for Exonuclease III mapping were generated as follows. The 326 bp mononucleosome DNA fragment was generated by digesting plasmid CP1024 (pGEMZ-lowerstrand "601") with both Eco RI and Pst I. Fragments were gel purified and labeled with γ^{32}P-dATP in a partial denaturing T4-PNK reaction. Pst I end labeled DNA fragments were used to generate mononucleosomes by salt dialysis. A total 4 μg chicken octamers were mixed with 4.9 μg of unlabeled 208-11 DNA template (to act as a histone sink) and 90 ng γ^{32}P-dATP labeled 326 bp "601" DNA fragments. Mononucleosome reconstitutions were assembled by stepwise salt dialysis as previously described for 208-11 chromatin arrays (Logie and Peterson, 1999). Incorporation of labeled "601" DNA fragment was assayed by native gel shift on 4% TBE polyacrylamide gels.

Generation of 5s mononucleosomes. Mononucleosomes containing a single Sal I 5S rDNA repeat were generated as follows. CP881 (pBluescript-5S Sal I) was digested sequentially with Kpn I then Not I. Fragments were gel purified and labeled with α^{32}P-

dCTP in a standard Klenow reaction. Mononucleosomes were generated in the same manner as described under "601" mononucleosomes.

Nucleosome mobilization assay. 340 bp mononucleosomes were used to assay SWI/SNF-induced nucleosome mobilization. 30 µl reactions containing 0.3 ng labeled mononucleosomes (130 ng total oligonucleosomes) were incubated at 30 °C with 3nM SWI/SNF complex (WT or), and 3mM ATP, in 5-50 remodeling buffer over 90 minutes. 4.0 µl fractions were taken at various times and quenched with 2xGD buffer (20% glycerol and 600 ng/µl plasmid DNA) and place on ice. Fractions were resolved on 4% native TBE polyacrylamide gels for 90 minutes at 150 volts. Gels were dried and imaged using a Molecular Dynamics PhosphorImager.

Exo III mapping of nucleosome boundaries. 30 µl reactions containing 3 nM mononucleosomes or naked DNA were incubated with 3 nM SWI/SNF, 3 mM ATP, in 5-50 remodeling buffer at 30 °C. At each timepoint (t-10 minutes) 5 µl Time points were taken and incubated with 5 U of Exo III. After 10 more minutes at 30 °C reactions were quenched in 2x Stop buffer and incubated at 50 °C for 20 minutes to deproteinate samples. Deproteinated samples were boiled in an equal volume of formamide buffer (80% w/v deionized formamide, 10 mM EDTA, 1 mg/ml xylene cyanol FF, and 1 mg/ml bromophenol blue) resolved on 6% sequencing gels (27.1:1 acrylamide: bisacrylamide, w/w) containing 7M urea which were ran in 1x TBE for 55 minutes at 650 volts. Gels were dried and imaged using a Molecular Dynamics PhosphorImager (Amersham).

Mononucleosome restriction enzyme accessibility assays. 30 µl reactions containing 130 ng (0.3 ng labeled) mononucleosomes (either 240 bp or 340 bp) were incubated with 1.0 nM SWI/SNF complex (WT or variant), 3 mM ATP, and 40 U of restriction enzyme (Hha I or Pml I) in 5-50 remodeling buffer at 30 °C. 3-4 µl Time points were taken as indicated and quenched in 2x Stop buffer. Reactions were incubated at 50 °C for 20 minutes to deproteinate samples. Deproteinated samples were resolved on 8% native TBE polyacrylamide gels. Gels were dried and imaged using a Molecular Dynamics PhosphorImager (Amersham).

Construction of recombinant histone octamer and tetramers. Recombinant histone octamers were expressed and purified as previously described (Luger et al., 1999). Briefly WT or tailless octamers were generated by mixing equimolar amounts of lyophilized *Xenopus laevis* recombinant histones H2A, H2B, H3 and H4 (either intact or lacking N-termini) in unfolding buffer (7 M guanidinium-HCl, 20 mM Tris-HCl, pH 7.5, 10 mM DTT) for 2-4 hours at room temperature and then subjecting the histone mixture to dialysis into refolding buffer (2 M NaCl, 10 mM Tris-HCl, pH 7.5, 1 mM EDTA, and 5 mM 2-mercaptoethanol) overnight with multiple buffer changes at 4 °C. The refolded octamers were then separated from unincorporated histones on an S-200HR gel filtration column. Fractions containing octamers were determined by coomassie staining, pooled and concentrated. Concentrations were determined using molar extinction coefficients

and octamers were stored at 4 °C until use (Luger et al., 1999). Tetramers were purified in the same manner except only histones H3 and H4 were used to generate tetramers.

Generation of tailless and tetramer cruciform templates. Cruciform templates were generated in the same fashion as chicken histone pXG540-linearized templates except recombinant intact octamers, tailless octamers or tetramers were used to construct the templates. Cruciform assays were conducted as described above under the torsion assay heading.

Generation of recombinant wild type and tailless mononucleosomes. Mononucleosomes for tail effect studies were generated in the following manner. A total 3.6 µg or 5.2 µg of recombinant intact or tailless octamers (respectively) were mixed with 4.9 µg of unlabeled 208-11 DNA template (to act as a histone sink) and 90 ng α^{32}P-dCTP labeled 340 bp "601" DNA fragments. Mononucleosome reconstitutions were assembled by stepwise salt dialysis as previously described for 208-11 chromatin arrays (Logie and Peterson, 1999). Incorporation of labeled "601" DNA fragment was assayed by native gel shift on 4% TBE polyacrylamide gels.

CHAPTER V

Perspectives

The SWI/SNF complex uses the energy derived from ATP hydrolysis to disrupt histone-DNA contacts and thus "remodel" chromatin. But what is chromatin remodeling and how do these enzymes facilitate the reaction? Over the last ten years different observations have been made of the action of these enzymes on different chromatin substrates (Peterson, 2002b). Chromatin remodeling enzymes have been shown to facilitate restriction enzyme accessibility to sites occluded by nucleosomes. They also appear to be able to mobilize nucleosomes either randomly (SWI/SNF) or into more ordered positions (ISWI containing complexes). *In vitro*, these enzymes can catalyze the transfer of an octamer from one DNA fragment onto another. Recently, these enzymes have also been found to be able to transfer H2A-H2B dimers from one octamer to another (Krogan et al., 2003; Mizuguchi et al., 2004). In some cases this histone transfer involves the replacement of one histone variant with another (e.g. Ino80 complex). How do all these activities fit together and is there a single mechanism to explain how these enzymes function in remodeling? In this chapter I will discuss how ATP-dependent remodeling might work at the molecular level and how this relates to the role of these enzymes *in vivo*.

Swi2p: the motor under the hood of SWI/SNF.

The ATP-dependent chromatin remodeling enzymes all share a subunit belonging to the SF2 family of helicases, yet none of the ATPases have helicase-like activities. From the numerous studies of these catalytic subunits it is obvious that they are the motor behind the complex. How do these enzymes use the energy from ATP hydrolysis to remodel nucleosomes?

Swi2p and its homologs all share high homology to the SF2 helicases and contain all the conserved motifs found in these enzymes yet little was known about the specific roles these domains play in the remodeling reaction. The work presented in Chapter III and Chapter IV shows that a number of the motifs of subdomain I (I-III) along with motif VI (in subdomain II) play direct roles in ATP hydrolysis or ATP binding.

Motif V on the other hand seems to have a more specific role in the function of the *S. cerevisiae* SWI/SNF complex. As illustrated in Chapter IV, it appears that motif V (in subdomain II) of the ATPase domain plays a critical role in coupling ATP hydrolysis to the mechanism of remodeling. Intact SWI/SNF complexes harboring amino acid substitutions in this motif were shown to have a drastic defect in the generation of superhelical torsion and the generation of remodeled products as compared to WT SWI/SNF complex while still retaining WT levels of ATPase activity. In Chapter IV the data suggests that motif V may require canonical nucleosomal structure. This was illustrated by the fact that on naked DNA alone the substitutions in motif V render SWI/SNF completely defective for the generation of torsion and only a complete

nucleosome core particle is sufficient for even partial torsion generation by these altered complexes.

Motif V is highly conserved among canonical chromatin remodeling enzymes as would be expected for a motif critical for the transduction of the ATP hydrolysis cycle into the mechanism of remodeling. As seen in Table 2 in Chapter 4 this loop is only strongly conserved in the three major chromatin remodeling families, SWI2/SNF2, ISWI, and Mi2/CHD but not in the SWI-like repair proteins (Rad54p ATRX, etc). Interestingly Ino80, which has been recently shown to perform H2A-H2B dimer exchange, has a highly conserved motif V (see Figure 17).

The SWI2 family was the only class of remodeling enzymes that did not display nucleosome-specific stimulation of ATPase or torsion activities. ISWI and Mi-2 complexes show vastly higher ATPase activity in the presence of chromatin versus naked dsDNA (Becker and Horz, 2002). These complexes also show chromatin dependence in the generation of superhelical torsion. In Chapter IV, I found evidence that the ability of ySWI/SNF complex to create torsion is in fact stimulated on chromatin relative to DNA and that this stimulation is dependent on both an intact nucleosome and motif V of the ATPase domain of Swi2p. Substrate specificity in helicase-like enzymes has been documented in the past. Mot1p is stimulated by interaction with TBP (Auble et al., 1997) and chromatin specificity of the ATPase subunit has been proposed to be a defining feature of chromatin remodeling enzymes (Flaus and Owen-Hughes, 2001).

The Swi2p specific subdomain might be vital to the recognition of nucleosomal DNA versus naked dsDNA. No known helicase to date has an extended linker between

subdomains I and II of the helicase fold (compare Figure 15 with Figure 25). Unique subdomains have been discovered in other helicases and they play a significant role in orienting the oligonucleotide substrate into the helicase subdomains (see Figure 37a). The Swi2p-like enzymes might have evolved this specific region to contend with the nucleosomal DNA structure that makes up its native substrate. This might be an interesting avenue to explore in the future.

What is chromatin remodeling?

The ATP-dependent under-winding of DNA leads to the creation of superhelical torsion in the DNA duplex on the surface of the nucleosome. The result of this under-winding leads to a twist defect that then must be relieved (see Figure 38). The relief of this twist defect could result in a number of potential outcomes. In the absence of any constraint the defect could diffuse back to it original conformation (Nucleosome I converted to II then rapidly converted back to I, Figure 38a). Two possible models have been proposed lead to "remodeling"; these are the twisting or writhing models (see Figure 38b). In the twisting model the duplex is under-wound yet remains in contact with the histones in the region of the twist defect. This defect is relieved by a slipping event where the DNA corkscrews along the surface contacts in the nucleosome resulting in small base pair steps and ultimately movement of the DNA relative to the histone octamer (Nucleosome I becoming converted finally to nucleosome III, Figure 38a). The second model involves a writhe of DNA becoming dissociated from the surface of the octamer and moving in a bulge migration or inchworm fashion. It has been proposed that

the writhing model could explain the ability of some chromatin remodeling enzymes to move the histone octamer off the end of a short DNA fragment. Recapture of a free DNA end might lead to the generation of a novel mononucleosome as illustrated in Figure 5c.

It is possible that both models are actually occurring *in vivo*. The twist model might be the result of nucleosomes having sufficient free linker DNA regions to one or both sides of the nucleosome core particle that allow the chromatin remodeling enzyme to mobilize the nucleosome (Nucleosome **I** remodeled to **III**). This has been well documented in the case of the ISWI complexes. ISWI alone or in complexes remodels chromatin by translocating nucleosomes relative to DNA (Fan et al., 2003; Langst and Becker, 2001b).

In a constrained system that does not allow nucleosome sliding, the process of creating torsion on the DNA duplex might result in a writhe becoming free thus allowing access to DNA without actual translocation of the nucleosome (remodeling results in nucleosome **II**). This has been seen for Brg1 and hSWI/SNF on nucleosomes when the histone octamer is cross-linked to DNA, thereby preventing movement (Aoyagi et al., 2002). ISWI, in contrast, needs free ends to mobilize DNA and does not appear to create writhe on trapped nucleosomes (Fan et al., 2003; Narlikar et al., 2001). Brg1 and human SWI/SNF are believed to create enzyme accessible remodeling products on mononucleosomes with little to no linker regions to (nucleosome **II**, Figure 38b) and it is believed that these nucleosomes are not remodel via sliding (nucleosome **III**). It is possible that enzyme accessibility might be generated by pushing a remodeled nucleosome into the first gyre of a neighboring nucleosome.

a
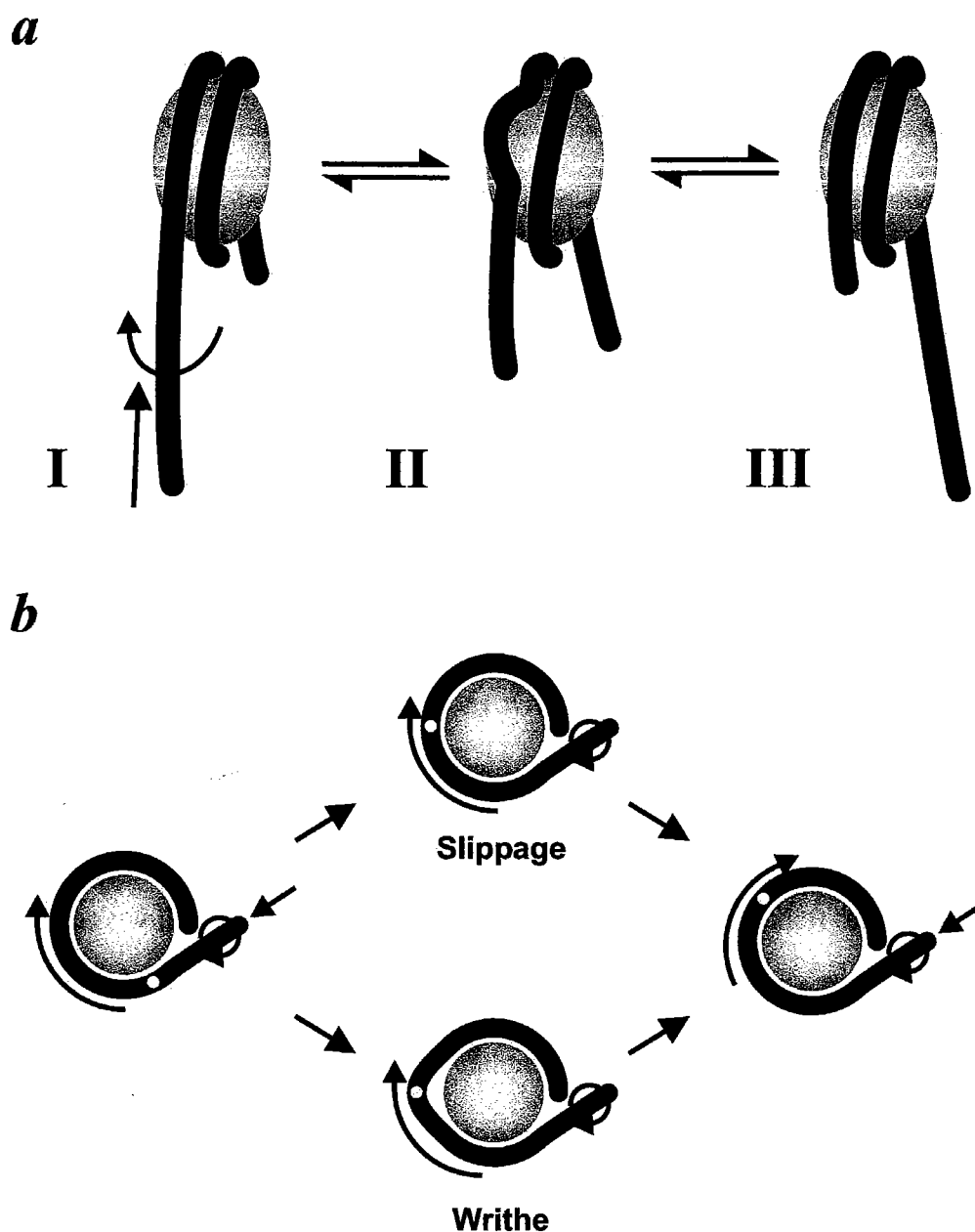

I   II   III

b

Slippage

Writhe

Figure 38. Torsion models for chromatin remodeling. This figure shows a few potential models for chromatin remodeling via relief of torsional twist defects. (*a*) A cartoon illustrating how intermediates (**II**) might lead to accessibility without DNA translocation. (*b*) Cartoon depicting how twist or writhe could lead to remodeling.

A model for ATP-dependent chromatin remodeling.

The data presented here illustrates a possible mechanism for the activity of the *S. cerevisiae* SWI/SNF complex. Combining the structural EM data from Chapter II with the functional analysis in Chapters III and IV we can make some predictions about the function of SWI/SNF on nucleosomes.

From the 3D-EM reconstructions of ySWI/SNF, it is clear that SWI/SNF has a large depression or cavity approximately the same dimensions as a nucleosome (see Chapter II and Figure 39). From the initial Cryo-EM structure it is easy to see that the nucleosome core particle would fit nicely into this central cavity. It appears that there are two projections, one to either side of this cavity, which could play a role in stabilizing the nucleosome, optimizing Swi2p interactions with nucleosomal DNA. These projections could represent the Swi3p subunits which were shown to be present in two copies in the complex (Chapter II). These subunits might interact with histone tails through the SANT domain, thus stabilizing the nucleosome core particle in the active cleft (see Figure 39).

I believe that the bottom of this cavity is an attractive site for the location of Swi2p (see Figure 39). Modeling of the nucleosome core particle into the 3D-EM reconstruction data also suggests the nucleosome core particle only fits into this cavity in specific orientations. The favored orientation of the core particle has the H3 tail protruding away from the cavity and into solution. This would leave the dyad axis of symmetry solution exposed. I believe that Swi2p might act on the DNA near the entry/exit sites. Other subunits (Swi3p) might stabilize the nucleosome allowing optimal

under-winding of DNA by Swi2p. The relief of the resulting DNA twist defect could then translate into remodeling.

I believe that the EM data as well as the motif V data from Chapters III and IV suggest that the primary method of remodeling by the yeast SWI/SNF complex involves the translocation of the nucleosome relative to the DNA molecule. On end-positioned nucleosomes yeast SWI/SNF does not appear to create restriction enzyme accessibility at the dyad axis. It might be that the entry/exit sites were not as accessible to Swi2p or that they do not form the proper interface on these mobility-constrained nucleosomes. The Exonuclease III mapping also supports that, at least on strong positioning sequences, SWI/SNF primarily mobilizes nucleosomes. These data taken together suggests that at least in the case of yeast SWI/SNF that chromatin remodeling results primarily in mobility when no constraint is placed on nucleosome translocation.

How does Swi2p act on the nucleosome? Experiments from Chapter IV suggest that in the absence of histone terminal domains the defect in chromatin remodeling of motif V altered complexes is further exacerbated. This data coupled with the hypothesis that Swi3p is stabilizing the nucleosome suggests that Swi3p might hold the nucleosome into the "active cleft" allowing Swi2p to act on the DNA gyres on the surface of the nucleosome (see Figure 39). Furthermore, it is possible that the linker region between subdomain I and II of the ATPase domain in Swi2-like enzymes gives the enzyme it characteristic DNA torsion ability. This unique subdomain might explain Swi2p's difference from canonical helicases. Swi2p might then act on one of the entry/exit DNA

gyres and push and/or twist the DNA toward the dyad axis. Relief of the resulting twist defect could be relieved by sliding the DNA while holding the nucleosome in place.

This model leaves a number of testable hypotheses. In the future both Swi3p-SANT (histone tail interaction domain?) and Swi2p-motif V alterations could be used to look at the histone-tail stability model. If histone tails were responsible for optimal remodeling, purified SWI/SNF containing both Swi3p-SANT deletions and a Swi2p-R1164A substitution might display the same *in vitro* characteristics that Motif V alterations coupled with tailless histone octamers. A refined EM structure of SWI/SNF containing the location of various subunits as well as a bound nucleosome would also greatly aid our understanding of the enzyme-nucleosome interface and prove that the cleft seen in the EM structures is the active site of the enzyme. The work presented in this thesis establishes a solid framework to test how SWI/SNF interacts with nucleosomal-level chromatin structure.

Determining how remodeling works in vivo

The biggest questions unanswered are still the questions that are the most interesting: what do chromatin remodeling enzymes do *in vivo*? As discussed above, the SWR1 complex appears to exchange histone H2AZ-H2B dimers *in vivo* and this seems to be functionally important. But what role does ATP-dependent nucleosome mobilization or formation of DNA loops play *in vivo*? Most *in vivo* studies of chromatin remodeling have used restriction enzymes or other nucleases like MNase to probe chromatin structure. However, these reagents only show that DNA accessibility has been altered;
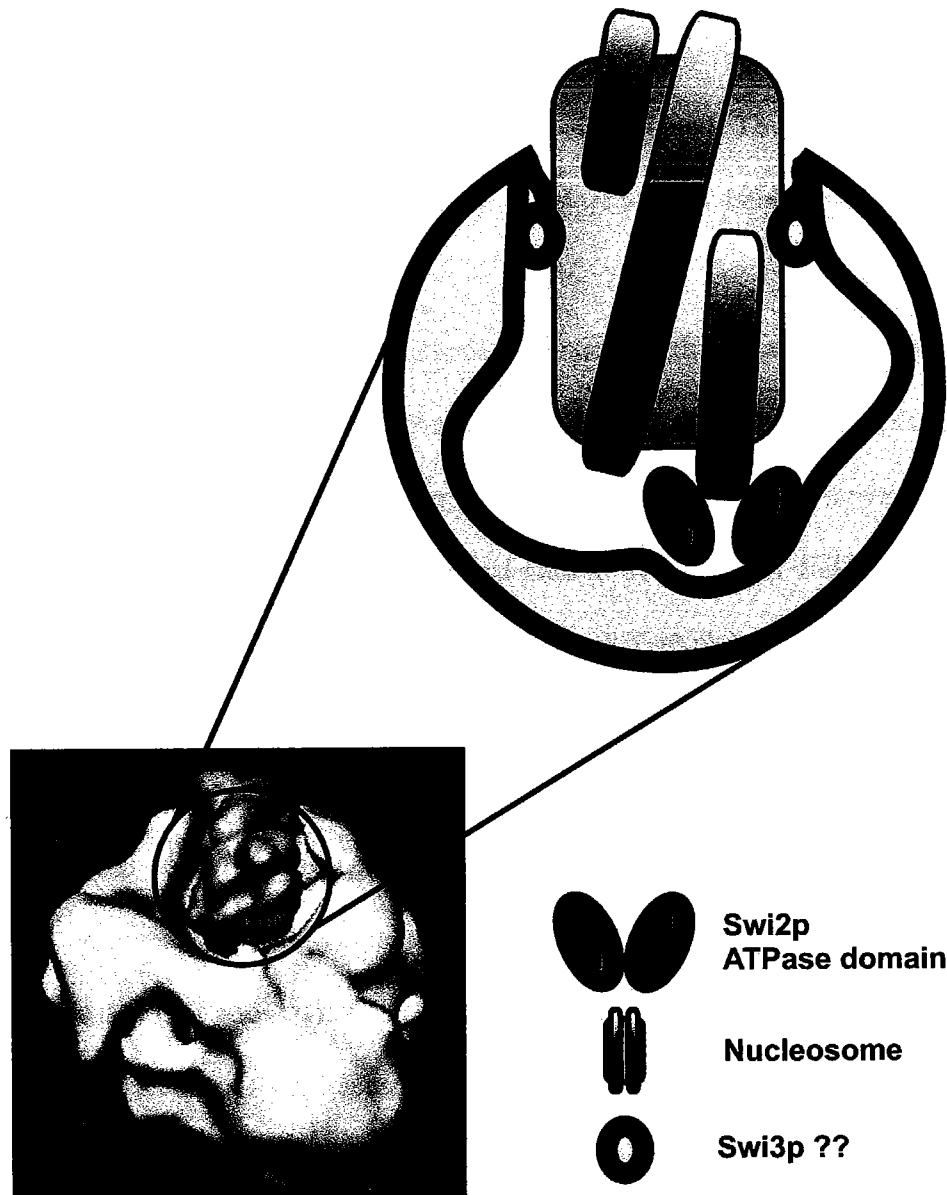
Figure 39. Model for how SWI/SNF interacts with nucleosomes. This cartoon depicts a possible model for how Swi2p could interact with the nucleosome core particle. The expanded view shows the prospective "catalytic" cleft of SWI/SNF. The blue ovals represent the two subdomains of the Swi2p ATPase domain. Swi3p (yellow circles to either side of the cleft) is illustrated as a possible subunit for SWI/SNF specific interactions with the histone octamer stabilizing the nucleosome core particle. The H3 truncated tail is seen coming straight out of the nucleosome core particle of the cryo-EM construct.

the mechanism is not clear. Furthermore, it is important to note that none of the nuclease reagents are able to detect changes in higher-order chromatin folding. Thus, a potential role for remodeling enzymes cannot yet be assayed *in vivo*. Thus, what seems to be lacking in the *in vivo* analysis are actually development of better methodologies for studying chromatin in cells.

Even with the application of nuclease digestion methods, a number of labs have found that chromatin remodeling appears to be distinct at different gene loci. At some genes chromatin remodeling appears to involve the mobilization or removal of multiple nucleosomes near the promoter, as illustrated earlier by the yeast *POT1* and *REC104* promoter regions after remodeling by Isw2 (Fazzio and Tsukiyama, 2003). In contrast at the mouse mammary tumor virus (MMTV) promoter, mobilization or removal of nucleosomes is not necessary for chromatin remodeling. Indeed, in this case it appears that a nuclear hormone receptor (glucocorticoid receptor; GR) recruits SWI/SNF which then enhances the accessibility of a promoter bound nucleosome without induced or nucleosome loss (Fryer and Archer, 1998; Truss et al., 1995). At the MMTV promoter, a nucleosome, referred to as nucleosome B, spans an important DNA sequence for hormone receptor binding sites known as the hormone responsive region (HRR) (Richard-Foy and Hager, 1987). Changes in DNase I sensitivity at nucleosome B suggest that chromatin remodeling is necessary for remodeling at this particular nucleosome to allow *cis*-acting elements to occupy the HRR (Truss et al., 1995). The nuclear hormone receptor GR recruits hSWI/SNF and other co-activators (P300/CBP for example)to the MMTV promoter facilitating chromatin remodeling and transcriptional activation (Fryer

and Archer, 1998). More recently a requirement for an ATP-dependent chromatin remodeling activity has been shown on MMTV promoters in *Drosophila* extracts (Di Croce et al., 1999). While these and other studies begin to shed light on the differences in chromatin remodeling at different genomic loci they only begin to address how chromatin remodeling works *in vivo*. In the case of MMTV, this may be a candidate for ATP-dependent DNA loop formation or perhaps a role for ATP-dependent dimer loss.

Remodeling at the fiber level

One important point that needs to be addressed is the differences between mononucleosomes and nucleosomal arrays. *In vitro* the SWI/SNF complexes are able to move nucleosomes well off the end of a short fragment of DNA resulting in a stable remodeled state. Also Brg1 experiments mentioned above show evidence for a stable remodeled nucleosome with enzyme accessible DNA loops. In contrast on nucleosomal arrays chromatin remodeling appears to be reversible in a short period of time. *In vivo* chromatin exists as large 100 - 400 nm fibers that are not only highly condensed but contain many non-histone proteins as well. Indeed, incorporation of a linker histone into a nucleosomal array substrate blocks the *in vitro* remodeling activities of most all ATP-dependent remodeling enzymes (Hill and Imbalzano, 2000; Horn et al., 2002). *In vivo* however, H1 is present at nearly every nucleosome (Hansen, 2002). How do these enzymes modulate chromatin at the fiber level? Are loops of DNA removed from the surface of the nucleosome *in vivo*? Are minor histone-DNA contact disruptions enough to facilitate the processivity of large enzymes like holoenzyme?

Some chromatin remodeling enzymes might be acting at the fiber level as well as the nucleosomal level. As mentioned earlier one of the first links between SWI/SNF and chromatin came from the genetic observations that *Sin⁻* mutants restore transcription in *Swi⁻* and *Snf* mutants. One prediction of these genetic studies was that *Sin⁻* chromatin might mimic the SWI/SNF remodeled state (Wechser et al., 1997). A recent *in vitro* study demonstrated that *Sin⁻* versions of histone H4 eliminate the cation dependent intramolecular folding of nucleosomal arrays (Horn et al., 2002). Thus, these data suggest that chromatin remodeling may not only act at the nucleosomal array level but might also affect chromatin at the fiber level.

Concluding Remarks

The study of chromatin biology has come a long way but there are still a lot of unanswered questions. We now have a better feeling for the dynamics involved at the simplest levels of chromatin structure (nucleosomal arrays) and how chromatin remodeling enzymes see and act on these substrates. The work of numerous groups has attempted to elucidate the function of chromatin modifying enzymes and their affect on chromatin. In the future we need to get a better understanding of how these enzymes behave *in vivo*. We are starting to get an idea for how ATP-dependent enzymes behave on short chromatin fragments but chromatids are more complex then those modeled in the laboratory. We also have a basic understanding of the function of the ATPase subunits of these enzymes but we are just beginning to scratch the surface of understanding why some of these complexes have numerous subunits. In the future experimental approaches will have to be designed to address how chromatin remodeling enzymes deal with the higher order structure of chromatids. It is at the level of the compact chromatin fiber that we believe that the true differences between the different enzymes will be revealed.

References

Adam, M., Robert, F., Larochelle, M., and Gaudreau, L. (2001). H2A.Z is required for global chromatin integrity and for recruitment of RNA polymerase II under specific conditions. Mol Cell Biol *21*, 6270-6279.

Ahmad, K., and Henikoff, S. (2001). Centromeres are specialized replication domains in heterochromatin. J Cell Biol *153*, 101-110.

Ahmad, K., and Henikoff, S. (2002). Histone H3 variants specify modes of chromatin assembly. Proc Natl Acad Sci U S A *99 Suppl 4*, 16477-16484.

Alexeev, A., Mazin, A., and Kowalczykowski, S. C. (2003). Rad54 protein possesses chromatin-remodeling activity stimulated by the Rad51-ssDNA nucleoprotein filament. Nat Struct Biol *10*, 182-186.

Alexiadis, V., and Kadonaga, J. T. (2002). Strand pairing by Rad54 and Rad51 is enhanced by chromatin. Genes Dev *16*, 2767-2771.

Anderson, J. D., Thastrom, A., and Widom, J. (2002). Spontaneous access of proteins to buried nucleosomal DNA target sites occurs via a mechanism that is distinct from nucleosome translocation. Mol Cell Biol *22*, 7147-7157.

Anderson, J. D., and Widom, J. (2000). Sequence and position-dependence of the equilibrium accessibility of nucleosomal DNA target sites. J Mol Biol *296*, 979-987.

Aoyagi, S., and Hayes, J. J. (2002). hSWI/SNF-catalyzed nucleosome sliding does not occur solely via a twist-diffusion mechanism. Mol Cell Biol *22*, 7484-7490.

Aoyagi, S., Narlikar, G., Zheng, C., Sif, S., Kingston, R. E., and Hayes, J. J. (2002). Nucleosome remodeling by the human SWI/SNF complex requires transient global disruption of histone-DNA interactions. Mol Cell Biol *22*, 3653-3662.

Aravind, L., and Landsman, D. (1998). AT-hook motifs identified in a wide variety of DNA-binding proteins. Nucleic Acids Res *26*, 4413-4421.

Arents, G., Burlingame, R. W., Wang, B. C., Love, W. E., and Moudrianakis, E. N. (1991). The nucleosomal core histone octamer at 3.1 A resolution: a tripartite protein assembly and a left-handed superhelix. Proc Natl Acad Sci U S A *88*, 10148-10152.

Asturias, F. J., Chung, W. H., Kornberg, R. D., and Lorch, Y. (2002). Structural analysis of the RSC chromatin-remodeling complex. Proc Natl Acad Sci U S A *99*, 13477-13480.

Auble, D. T., Wang, D., Post, K. W., and Hahn, S. (1997). Molecular analysis of the SNF2/SWI2 protein family member MOT1, an ATP-driven enzyme that dissociates TATA-binding protein from DNA. Mol Cell Biol *17*, 4842-4851.

Bazett-Jones, D. P., Cote, J., Landel, C. C., Peterson, C. L., and Workman, J. L. (1999). The SWI/SNF complex creates loop domains in DNA and polynucleosome arrays and can disrupt DNA-histone contacts within these domains. Mol Cell Biol *19*, 1470-1478.

Becker, P. B., and Horz, W. (2002). ATP-dependent nucleosome remodeling. Annu Rev Biochem *71*, 247-273.

Bednar, J., Horowitz, R. A., Dubochet, J., and Woodcock, C. L. (1995). Chromatin conformation and salt-induced compaction: three-dimensional structural information from cryoelectron microscopy. J Cell Biol *131*, 1365-1376.

Bouazoune, K., Mitterweger, A., Langst, G., Imhof, A., Akhtar, A., Becker, P. B., and Brehm, A. (2002). The dMi-2 chromodomains are DNA binding modules important for ATP-dependent nucleosome mobilization. EMBO J *21*, 2430-2440.

Boyer, L. A., Latek, R. R., and Peterson, C. L. (2004). The SANT domain: a unique histone-tail-binding module? Nat Rev Mol Cell Biol *5*, 158-163.

Boyer, L. A., Logie, C., Bonte, E., Becker, P. B., Wade, P. A., Wolffe, A. P., Wu, C., Imbalzano, A. N., and Peterson, C. L. (2000a). Functional delineation of three groups of the ATP-dependent family of chromatin remodeling enzymes. J Biol Chem *275*, 18864-18870.

Boyer, L. A., Shao, X., Ebright, R. H., and Peterson, C. L. (2000b). Roles of the histone H2A-H2B dimers and the (H3/H4)$_2$ tetramer in nucleosome remodeling by the SWI-SNF complex. J Biol Chem *275*, 11545-11552.

Bozhenok, L., Wade, P. A., and Varga-Weisz, P. (2002). WSTF-ISWI chromatin remodeling complex targets heterochromatic replication foci. EMBO J *21*, 2231-2241.

Brehm, A., Langst, G., Kehle, J., Clapier, C. R., Imhof, A., Eberharter, A., Muller, J., and Becker, P. B. (2000). dMi-2 and ISWI chromatin remodelling factors have distinct nucleosome binding and mobilization properties. EMBO J *19*, 4332-4341.

Brower-Toland, B. D., Smith, C. L., Yeh, R. C., Lis, J. T., Peterson, C. L., and Wang, M. D. (2002). Mechanical disruption of individual nucleosomes reveals a reversible multistage release of DNA. Proc Natl Acad Sci U S A *99*, 1960-1965.

Bruno, M., Flaus, A., Stockdale, C., Rencurel, C., Ferreira, H., and Owen-Hughes, T. (2003). Histone H2A/H2B dimer exchange by ATP-dependent chromatin remodeling activities. Mol Cell *12*, 1599-1606.

Cairns, B. R., Erdjument-Bromage, H., Tempst, P., Winston, F., and Kornberg, R. D. (1998). Two actin-related proteins are shared functional components of the chromatin-remodeling complexes RSC and SWI/SNF. Mol Cell 2, 639-651.

Cairns, B. R., Henry, N. L., and Kornberg, R. D. (1996a). TFG/TAF30/ANC1, a component of the yeast SWI/SNF complex that is similar to the leukemogenic proteins ENL and AF-9. Mol Cell Biol 16, 3308-3316.

Cairns, B. R., Kim, Y.-J., Sayre, M. H., Laurent, B. C., and Kornber, R. D. (1994). A multisubunit complex containing the SWI1/ADR6, SWI2/SNF2, SWI3, SNF5, and SNF6 gene products isolated from yeast. Proc Natl Acad Sci USA 91, 1950-1954.

Cairns, B. R., Levinson, R. S., Yamamoto, K. R., and Kornberg, R. D. (1996b). Essential role of Swp73p in the function of yeast Swi/Snf complex. Genes Dev 10, 2131-2144.

Cairns, B. R., Lorch, Y., Li, Y., Zhang, M., Lacomis, L., Erdjument-Bromage, H., Tempst, P., Du, J., Laurent, B., and Kornberg, R. D. (1996c). RSC, an essential, abundant chromatin-remodeling complex. Cell 87, 1249-1260.

Carruthers, L. M., Bednar, J., Woodcock, C. L., and Hansen, J. C. (1998). Linker histones stabilize the intrinsic salt-dependent folding of nucleosomal arrays: mechanistic ramifications for higher-order chromatin folding. Biochemistry 37, 14776-14787.

Carruthers, L. M., and Hansen, J. C. (2000). The core histone N termini function independently of linker histones during chromatin condensation. J Biol Chem 275, 37285-37290.

Carruthers, L. M., Tse, C., Walker, K. P., 3rd, and Hansen, J. C. (1999). Assembly of defined nucleosomal and chromatin arrays from pure components. Methods Enzymol 304, 19-35.

Caruthers, J. M., Johnson, E. R., and McKay, D. B. (2000). Crystal structure of yeast initiation factor 4A, a DEAD-box RNA helicase. Proc Natl Acad Sci U S A 97, 13080-13085.

Caruthers, J. M., and McKay, D. B. (2002). Helicase structure and mechanism. Curr Opin Struct Biol 12, 123-133.

Citterio, E., Van Den Boom, V., Schnitzler, G., Kanaar, R., Bonte, E., Kingston, R. E., Hoeijmakers, J. H., and Vermeulen, W. (2000). ATP-dependent chromatin remodeling by the Cockayne syndrome B DNA repair-transcription-coupling factor. Mol Cell Biol 20, 7643-7653.

Collins, N., Poot, R. A., Kukimoto, I., Garcia-Jimenez, C., Dellaire, G., and Varga-Weisz, P. D. (2002). An ACF1-ISWI chromatin-remodeling complex is required for DNA replication through heterochromatin. Nat Genet *32*, 627-632.

Collins, R. T., and Treisman, J. E. (2000). Osa-containing Brahma chromatin remodeling complexes are required for the repression of wingless target genes. Genes Dev *14*, 3140-3152.

Corona, D. F., Langst, G., Clapier, C. R., Bonte, E. J., Ferrari, S., Tamkun, J. W., and Becker, P. B. (1999). ISWI is an ATP-dependent nucleosome remodeling factor. Mol Cell *3*, 239-245.

Corona, D. F., and Tamkun, J. W. (2004). Multiple roles for ISWI in transcription, chromosome organization and DNA replication. Biochim Biophys Acta *1677*, 113-119.

Cote, J., Peterson, C. L., and Workman, J. L. (1998). Perturbation of nucleosome core structure by the SWI/SNF complex persists after its detachment, enhancing subsequent transcription factor binding. Proc Natl Acad Sci U S A *95*, 4947-4952.

Cote, J., Quinn, J., Workman, J. L., and Peterson, C. L. (1994). Stimulation of GAL4 derivative binding to nucleosomal DNA by the yeast SWI/SNF complex. Science *265*, 53-60.

de la Serna, I. L., Carlson, K. A., and Imbalzano, A. N. (2001). Mammalian SWI/SNF complexes promote MyoD-mediated muscle differentiation. Nat Genet *27*, 187-190.

Decristofaro, M. F., Betz, B. L., Rorie, C. J., Reisman, D. N., Wang, W., and Weissman, B. E. (2001). Characterization of SWI/SNF protein expression in human breast cancer cell lines and other malignancies. J Cell Physiol *186*, 136-145.

Delano, W. L. (2002). The PyMOL Molecular Graphics System (San Carlos, CA, DeLano Scientific).

Deuring, R., Fanti, L., Armstrong, J. A., Sarte, M., Papoulas, O., Prestel, M., Daubresse, G., Verardo, M., Moseley, S. L., Berloco, M., *et al.* (2000). The ISWI chromatin-remodeling protein is required for gene expression and the maintenance of higher order chromatin structure in vivo. Molec Cell *5*, 355-365.

Dhillon, N., and Kamakaka, R. T. (2000). A histone variant, Htz1p, and a Sir1p-like protein, Esc2p, mediate silencing at HMR. Mol Cell *6*, 769-780.

Di Croce, L., Koop, R., Venditti, P., Westphal, H. M., Nightingale, K. P., Corona, D. F., Becker, P. B., and Beato, M. (1999). Two-step synergism between the progesterone receptor and the DNA-binding domain of nuclear factor 1 on MMTV minichromosomes. Mol Cell *4*, 45-54.

Dong, F., Hansen, J. C., and van Holde, K. E. (1990). DNA and protein determinants of nucleosome positioning on sea urchin 5S rRNA gene sequences in vitro. Proc Natl Acad Sci U S A *87*, 5724-5728.

Du, J., Nasir, I., Benton, B. K., Kladde, M. P., and Laurent, B. C. (1998). Sth1p, a Saccharomyces cerevisiae Snf2p/Swi2p homolog, is an essential ATPase in RSC and differs from Snf/Swi in its interactions with histones and chromatin-associated proteins. Genetics *150*, 987-1005.

Eberharter, A., Ferrari, S., Langst, G., Straub, T., Imhof, A., Varga-Weisz, P., Wilm, M., and Becker, P. B. (2001). Acf1, the largest subunit of CHRAC, regulates ISWI-induced nucleosome remodelling. EMBO J *20*, 3781-3788.

Eisen, J. A., Sweder, K. S., and Hanawalt, P. C. (1995). Evolution of the SNF2 family of proteins: subfamilies with distinct sequences and functions. Nucleic Acids Res *23*, 2715-2723.

Elfring, L. K., Daniel, C., Papoulas, O., Deuring, R., Sarte, M., Moseley, S., Beek, S. J., Waldrip, W. R., Daubresse, G., DePace, A., *et al.* (1998). Genetic analysis of brahma: the Drosophila homolog of the yeast chromatin remodeling factor SWI2/SNF2. Genetics *148*, 251-265.

Elfring, L. K., Deuring, R., McCallum, C. M., Peterson, C. L., and Tamkun, J. W. (1994). Identification and characterization of Drosophila relatives of the yeast transcriptional activator SNF2/SWI2. Mol Cell Biol *14*, 2225-2234.

Fan, H. Y., He, X., Kingston, R. E., and Narlikar, G. J. (2003). Distinct strategies to make nucleosomal DNA accessible. Mol Cell *11*, 1311-1322.

Fan, J. Y., Gordon, F., Luger, K., Hansen, J. C., and Tremethick, D. J. (2002). The essential histone variant H2A.Z regulates the equilibrium between different chromatin conformational states. Nat Struct Biol *9*, 172-176.

Fazzio, T. G., and Tsukiyama, T. (2003). Chromatin remodeling in vivo: evidence for a nucleosome sliding mechanism. Mol Cell *12*, 1333-1340.

Fernandez, A., Guo, H. S., Saenz, P., Simon-Buela, L., Gomez de Cedron, M., and Garcia, J. A. (1997). The motif V of plum pox potyvirus CI RNA helicase is involved in NTP hydrolysis and is essential for virus RNA replication. Nucleic Acids Res *25*, 4474-4480.

Finch, J. T., and Klug, A. (1976). Solenoidal model for superstructure in chromatin. Proc Natl Acad Sci U S A *73*, 1897-1901.

Firman, K., and Szczelkun, M. D. (2000). Measuring motion on DNA by the type I restriction endonuclease EcoR124I using triplex displacement. EMBO J *19*, 2094-2102.

Fischle, W., Wang, Y., and Allis, C. D. (2003). Histone and chromatin cross-talk. Curr Opin Cell Biol *15*, 172-183.

Flaus, A., and Owen-Hughes, T. (2001). Mechanisms for ATP-dependent chromatin remodelling. Curr Opin Genet Dev *11*, 148-154.

Flaus, A., and Owen-Hughes, T. (2003). Dynamic properties of nucleosomes during thermal and ATP-driven mobilization. Mol Cell Biol *23*, 7767-7779.

Fry, C. J., and Peterson, C. L. (2001). Chromatin remodeling enzymes: who's on first? Curr Biol *11*, R185-197.

Fryer, C. J., and Archer, T. K. (1998). Chromatin remodelling by the glucocorticoid receptor requires the BRG1 complex. Nature *393*, 88-91.

Garcia-Ramirez, M., Dong, F., and Ausio, J. (1992). Role of the histone tails in the folding of oligonucleosomes depleted of histone H1. J Biol Chem *267*, 19587-19595.

Garrick, D., Samara, V., McDowell, T. L., Smith, A. J., Dobbie, L., Higgs, D. R., and Gibbons, R. J. (2004). A conserved truncated isoform of the ATR-X syndrome protein lacking the SWI/SNF-homology domain. Gene *326*, 23-34.

Gavin, I., Horn, P. J., and Peterson, C. L. (2001). SWI/SNF chromatin remodeling requires changes in DNA topology. Mol Cell *7*, 97-104.

Gibbons, R. J., Picketts, D. J., Villard, L., and Higgs, D. R. (1995). Mutations in a putative global transcriptional regulator cause X-linked mental retardation with alpha-thalassemia (ATR-X syndrome). Cell *80*, 837-845.

Goldmark, J. P., Fazzio, T. G., Estep, P. W., Church, G. M., and Tsukiyama, T. (2000). The Isw2 chromatin remodeling complex represses early meiotic genes upon recruitment by Ume6p. Cell *103*, 423-433.

Goodwin, G. H., and Nicolas, R. H. (2001). The BAH domain, polybromo and the RSC chromatin remodelling complex. Gene *268*, 1-7.

Grune, T., Brzeski, J., Eberharter, A., Clapier, C. R., Corona, D. F., Becker, P. B., and Muller, C. W. (2003). Crystal structure and functional analysis of a nucleosome recognition module of the remodeling factor ISWI. Mol Cell *12*, 449-460.

Guidi, C. J., Sands, A. T., Zambrowicz, B. P., Turner, T. K., Demers, D. A., Webster, W., Smith, T. W., Imbalzano, A. N., and Jones, S. N. (2001). Disruption of Ini1 leads to peri-implantation lethality and tumorigenesis in mice. Mol Cell Biol *21*, 3598-3603.

Guschin, D., Geiman, T. M., Kikyo, N., Tremethick, D. J., Wolffe, A. P., and Wade, P. A. (2000a). Multiple ISWI ATPase complexes from xenopus laevis. FUNCTIONAL CONSERVATION OF AN ACF/CHRAC HOMOLOG [In Process Citation]. J Biol Chem 275, 35248-35255.

Guschin, D., Wade, P. A., Kikyo, N., and Wolffe, A. P. (2000b). ATP-Dependent histone octamer mobilization and histone deacetylation mediated by the Mi-2 chromatin remodeling complex. Biochemistry 39, 5238-5245.

Hainfeld, J. F., Wall, J. S., and Desmond, E. J. (1982). A small computer system for micrograph analysis. Ultramicroscopy 8, 263-270.

Hake, S. B., Xiao, A., and Allis, C. D. (2004). Linking the epigenetic 'language' of covalent histone modifications to cancer. Br J Cancer 90, 761-769.

Hall, M. C., and Matson, S. W. (1999). Helicase motifs: the engine that powers DNA unwinding. Mol Microbiol 34, 867-877.

Hamiche, A., Kang, J. G., Dennis, C., Xiao, H., and Wu, C. (2001). Histone tails modulate nucleosome mobility and regulate ATP-dependent nucleosome sliding by NURF. Proc Natl Acad Sci U S A 98, 14316-14321.

Hamiche, A., Sandaltzopoulos, R., Gdula, D. A., and Wu, C. (1999). ATP-dependent histone octamer sliding mediated by the chromatin remodeling complex NURF. Cell 97, 833-842.

Hansen, J. C. (2002). Conformational dynamics of the chromatin fiber in solution: determinants, mechanisms, and functions. Annu Rev Biophys Biomol Struct 31, 361-392.

Hansen, J. C., Ausio, J., Stanik, V. H., and van Holde, K. E. (1989). Homogeneous reconstituted oligonucleosomes, evidence for salt-dependent folding in the absence of histone H1. Biochemistry 28, 9129-9136.

Havas, K., Flaus, A., Phelan, M., Kingston, R., Wade, P. A., Lilley, D. M. J., and Owen-Hughes, T. (2000). Generation of superhelical torsion by ATP-dependent chromatin remodeling activities. Cell 103, 1133-1142.

Hill, D. A., and Imbalzano, A. N. (2000). Human SWI/SNF Nucleosome Remodeling Activity Is Partially Inhibited by Linker Histone H1. Biochemistry 39, 11649-11656.

Holstege, F. C., Jennings, E. G., Wyrick, J. J., Lee, T. I., Hengartner, C. J., Green, M. R., Golub, T. R., Lander, E. S., and Young, R. A. (1998). Dissecting the regulatory circuitry of a eukaryotic genome. Cell 95, 717-728.

Horn, P. J., Crowley, K. A., Carruthers, L. M., Hansen, J. C., and Peterson, C. L. (2002). The SIN domain of the histone octamer is essential for intramolecular folding of nucleosomal arrays. Nat Struct Biol 9, 167-171.

Horn, P. J., and Peterson, C. L. (2002). Molecular biology. Chromatin higher order folding--wrapping up transcription. Science 297, 1824-1827.

Hsu, D. S., Kim, S. T., Sun, Q., and Sancar, A. (1995). Structure and function of the UvrB protein. J Biol Chem 270, 8319-8327.

Huang, C., Sloan, E. A., and Boerkoel, C. F. (2003). Chromatin remodeling and human disease. Curr Opin Genet Dev 13, 246-252.

Huang, M., Qian, F., Hu, Y., Ang, C., Li, Z., and Wen, Z. (2002). Chromatin-remodelling factor BRG1 selectively activates a subset of interferon-alpha-inducible genes. Nat Cell Biol 4, 774-781.

Hunter, W. M., and Greenwood, F. C. (1962). Preparation of iodine-131 labelled human growth hormone of high specific activity. Nature 194, 495-496.

Ito, T., Bulger, M., Pazin, M. J., Kobayashi, R., and Kadonaga, J. T. (1997). ACF, an ISWI-containing and ATP-utilizing chromatin assembly and remodeling factor. Cell 90, 145-155.

Jaskelioff, M., Van Komen, S., Krebs, J. E., Sung, P., and Peterson, C. L. (2003). Rad54p is a chromatin remodeling enzyme required for heteroduplex DNA joint formation with chromatin. J Biol Chem 278, 9212-9218.

Jenuwein, T., and Allis, C. D. (2001). Translating the histone code. Science 293, 1074-1080.

Kagalwala, M. N., Glaus, B. J., Dang, W., Zofall, M., and Bartholomew, B. (2004). Topography of the ISW2-nucleosome complex: insights into nucleosome spacing and chromatin remodeling. Embo J 23, 2092-2104.

Kassabov, S. R., Henry, N. M., Zofall, M., Tsukiyama, T., and Bartholomew, B. (2002). High-resolution mapping of changes in histone-DNA contacts of nucleosomes remodeled by ISW2. Mol Cell Biol 22, 7524-7534.

Kassabov, S. R., Zhang, B., Persinger, J., and Bartholomew, B. (2003). SWI/SNF unwraps, slides, and rewraps the nucleosome. Mol Cell 11, 391-403.

Kehle, J., Beuchle, D., Treuheit, S., Christen, B., Kennison, J. A., Bienz, M., and Muller, J. (1998). dMi-2, a hunchback-interacting protein that functions in polycomb repression. Science 282, 1897-1900.

Kelleher, D. J., and Gilmore, R. (1997). DAD1, the defender against apoptotic cell death, is a subunit of the mammalian oligosaccharyltransferase. Proc Natl Acad Sci U S A *94*, 4994-4999.

Kennison, J. A., and Tamkun, J. W. (1988). Dosage-dependent modifiers of polycomb and antennapedia mutations in Drosophila. Proc Natl Acad Sci U S A *85*, 8136-8140.

Khattak, S., Lee, B. R., Cho, S. H., Ahnn, J., and Spoerel, N. A. (2002). Genetic characterization of Drosophila Mi-2 ATPase. Gene *293*, 107-114.

Khavari, P. A., Peterson, C. L., Tamkun, J. W., Mendel, D. B., and Crabtree, G. R. (1993). BRG1 contains a conserved domain of the SWI2/SNF2 family necessary for normal mitotic growth and transcription. Nature *366*, 170-174.

Khorasanizadeh, S. (2004). The nucleosome: from genomic organization to genomic regulation. Cell *116*, 259-272.

Kikyo, N., Wade, P. A., Guschin, D., Ge, H., and Wolffe, A. P. (2000). Active remodeling of somatic nuclei in egg cytoplasm by the nucleosomal ATPase ISWI. Science *289*, 2360-2362.

Kim, J., Sif, S., Jones, B., Jackson, A., Koipally, J., Heller, E., Winandy, S., Viel, A., Sawyer, A., Ikeda, T., *et al.* (1999). Ikaros DNA-binding proteins direct formation of chromatin remodeling complexes in lymphocytes. Immunity *10*, 345-355.

Klochendler-Yeivin, A., Fiette, L., Barra, J., Muchardt, C., Babinet, C., and Yaniv, M. (2000). The murine SNF5/INI1 chromatin remodeling factor is essential for embryonic development and tumor suppression. EMBO Rep *1*, 500.

Kobor, M. S., Venkatasubrahmanyam, S., Meneghini, M. D., Gin, J. W., Jennings, J. L., Link, A. J., Madhani, H. D., and Rine, J. (2004). A Protein Complex Containing the Conserved Swi2/Snf2-Related ATPase Swr1p Deposits Histone Variant H2A.Z into Euchromatin. PLoS Biol *2*, E131.

Koipally, J., Heller, E. J., Seavitt, J. R., and Georgopoulos, K. (2002). Unconventional potentiation of gene expression by Ikaros. J Biol Chem *277*, 13007-13015.

Krebs, J. E., Fry, C. J., Samuels, M., and Peterson, C. L. (2000). Global role for chromatin remodeling enzymes in mitotic gene expression. Cell *102*, 587-598.

Krebs, J. E., and Peterson, C. L. (2000). Understanding "active" chromatin: a historical perspective of chromatin remodeling. Crit Rev Eukaryot Gene Expr *10*, 1-12.

Krogan, N. J., Keogh, M. C., Datta, N., Sawa, C., Ryan, O. W., Ding, H., Haw, R. A., Pootoolal, J., Tong, A., Canadien, V., *et al.* (2003). A Snf2 family ATPase complex required for recruitment of the histone H2A variant Htz1. Mol Cell *12*, 1565-1576.

Kruger, W., and Herskowitz, I. (1991). A negative regulator of HO transcription, SIN1 (SPT2), is a nonspecific DNA-binding protein related to HMG1. Mol Cell Biol *11*, 4135-4146.

Kwon, H., Imbalzano, A. N., Khavari, P. A., Kingston, R. E., and Green, M. R. (1994). Nucleosome disruption and enhancement of activator binding by a human SW1/SNF complex. Nature *370*, 477-481.

Ladurner, A. G. (2003). Inactivating chromosomes: a macro domain that minimizes transcription. Mol Cell *12*, 1-3.

Langst, G., and Becker, P. B. (2001a). ISWI induces nucleosome sliding on nicked DNA. Mol Cell *8*, 1085-1092.

Langst, G., and Becker, P. B. (2001b). Nucleosome mobilization and positioning by ISWI-containing chromatin- remodeling factors. J Cell Sci *114*, 2561-2568.

Langst, G., Bonte, E. J., Corona, D. F., and Becker, P. B. (1999). Nucleosome movement by CHRAC and ISWI without disruption or trans- displacement of the histone octamer. Cell *97*, 843-852.

Laurent, B. C., Treitel, M. A., and Carlson, M. (1991). Functional interdependence of the yeast SNF2, SNF5, and SNF6 proteins in transcriptional activation. Proc Natl Acad Sci U S A *88*, 2687-2691.

Leach, T. J., Mazzeo, M., Chotkowski, H. L., Madigan, J. P., Wotring, M. G., and Glaser, R. L. (2000). Histone H2A.Z is widely but nonrandomly distributed in chromosomes of Drosophila melanogaster. J Biol Chem *275*, 23267-23272.

Li, Q., and Wrange, O. (1993). Translational positioning of a nucleosomal glucocorticoid response element modulates glucocorticoid receptor affinity. Genes Dev *7*, 2471-2482.

Li, Q., and Wrange, O. (1995). Accessibility of a glucocorticoid response element in a nucleosome depends on its rotational positioning. Mol Cell Biol *15*, 4375-4384.

Li, Q., and Wrange, O. (1997). Assays for transcription factors access to nucleosomal DNA. Methods *12*, 96-104.

Licht, C. L., Stevnsner, T., and Bohr, V. A. (2003). Cockayne syndrome group B cellular and biochemical functions. Am J Hum Genet *73*, 1217-1239.

Lilley, D. M., and Kemper, B. (1984). Cruciform-resolvase interactions in supercoiled DNA. Cell *36*, 413-422.

Lo, A. W., Craig, J. M., Saffery, R., Kalitsis, P., Irvine, D. V., Earle, E., Magliano, D. J., and Choo, K. H. (2001). A 330 kb CENP-A binding domain and altered replication timing at a human neocentromere. EMBO J *20*, 2087-2096.

Logie, C., and Peterson, C. L. (1997). Catalytic activity of the yeast SWI/SNF complex on reconstituted nucleosome arrays. EMBO J *16*, 6772-6782.

Logie, C., and Peterson, C. L. (1999). Purification and biochemical properties of yeast SWI/SNF complex. Methods Enzymol *304*, 726-741.

Longtine, M. S., McKenzie, A., 3rd, Demarini, D. J., Shah, N. G., Wach, A., Brachat, A., Philippsen, P., and Pringle, J. R. (1998). Additional modules for versatile and economical PCR-based gene deletion and modification in Saccharomyces cerevisiae. Yeast *14*, 953-961.

Lorch, Y., Cairns, B. R., Zhang, M., and Kornberg, R. D. (1998). Activated RSC-nucleosome complex and persistently altered form of the nucleosome. Cell *94*, 29-34.

Lorch, Y., Zhang, M., and Kornberg, R. D. (1999). Histone octamer transfer by a chromatin-remodeling complex. Cell *96*, 389-392.

Lorch, Y., Zhang, M., and Kornberg, R. D. (2001). RSC unravels the nucleosome. Mol Cell *7*, 89-95.

Lowary, P. T., and Widom, J. (1998). New DNA sequence rules for high affinity binding to histone octamer and sequence-directed nucleosome positioning. J Mol Biol *276*, 19-42.

Ludtke, S. J., Baldwin, P. R., and Chiu, W. (1999). EMAN: semiautomated software for high-resolution single-particle reconstructions. J Struct Biol *128*, 82-97.

Luger, K., Mader, A. W., Richmond, R. K., Sargent, D. F., and Richmond, T. J. (1997). Crystal structure of the nucleosome core particle at 2.8 A resolution. Nature *389*, 251-260.

Luger, K., Rechsteiner, T. J., and Richmond, T. J. (1999). Expression and purification of recombinant histones and nucleosome reconstitution. Methods Mol Biol *119*, 1-16.

Lusser, A., and Kadonaga, J. T. (2003). Chromatin remodeling by ATP-dependent molecular machines. Bioessays *25*, 1192-1200.

Martens, J. A., and Winston, F. (2003). Recent advances in understanding chromatin remodeling by Swi/Snf complexes. Curr Opin Genet Dev *13*, 136-142.

Martinez-Balbas, M. A., Tsukiyama, T., Gdula, D., and Wu, C. (1998). Drosophila NURF-55, a WD repeat protein involved in histone metabolism. Proc Natl Acad Sci U S A *95*, 132-137.

McClellan, J. A., Boublikova, P., Palecek, E., and Lilley, D. M. (1990). Superhelical torsion in cellular DNA responds directly to environmental and genetic factors. Proc Natl Acad Sci U S A *87*, 8373-8377.

McDowell, T. L., Gibbons, R. J., Sutherland, H., O'Rourke, D. M., Bickmore, W. A., Pombo, A., Turley, H., Gatter, K., Picketts, D. J., Buckle, V. J., *et al.* (1999). Localization of a putative transcriptional regulator (ATRX) at pericentromeric heterochromatin and the short arms of acrocentric chromosomes. Proc Natl Acad Sci U S A *96*, 13983-13988.

Medina, P. P., Carretero, J., Mario, F. F., Esteller, M., Sidransky, D., and Sanchez-Cespedes, M. (2004). Genetic and epigenetic screening for gene alterations of the chromatin-remodeling factor, *SMARCA4/BRG1*, in lung tumors. Mol Cell *In press*.

Mello, J. A., and Almouzni, G. (2001). The ins and outs of nucleosome assembly. Curr Opin Genet Dev *11*, 136-141.

Mizuguchi, G., Shen, X., Landry, J., Wu, W. H., Sen, S., and Wu, C. (2004). ATP-driven exchange of histone H2AZ variant catalyzed by SWR1 chromatin remodeling complex. Science *303*, 343-348.

Mizuuchi, K., Kemper, B., Hays, J., and Weisberg, R. A. (1982). T4 endonuclease VII cleaves holliday structures. Cell *29*, 357-365.

Mohrmann, L., Langenberg, K., Krijgsveld, J., Kal, A. J., Heck, A. J., and Verrijzer, C. P. (2004). Differential targeting of two distinct SWI/SNF-related Drosophila chromatin-remodeling complexes. Mol Cell Biol *24*, 3077-3088.

Moolenaar, G. F., Visse, R., Ortiz-Buysse, M., Goosen, N., and van de Putte, P. (1994). Helicase motifs V and VI of the Escherichia coli UvrB protein of the UvrABC endonuclease are essential for the formation of the preincision complex. J Mol Biol *240*, 294-307.

Morillon, A., Karabetsou, N., O'Sullivan, J., Kent, N., Proudfoot, N., and Mellor, J. (2003). Isw1 chromatin remodeling ATPase coordinates transcription elongation and termination by RNA polymerase II. Cell *115*, 425-435.

Muftuoglu, M., Selzer, R., Tuo, J., Brosh, R. M., Jr., and Bohr, V. A. (2002). Phenotypic consequences of mutations in the conserved motifs of the putative helicase domain of the human Cockayne syndrome group B gene. Gene *283*, 27-40.

Muller, C., and Leutz, A. (2001). Chromatin remodeling in development and differentiation. Curr Opin Genet Dev *11*, 167-174.

Muyldermans, S., Lasters, I., Wyns, L., and Hamers, R. (1981). Protection of discrete DNA fragments by the complex H1-octamerhistones or H5-octamerhistones after micrococcal nuclease digestion. Nucleic Acids Res *9*, 3671-3680.

Narlikar, G. J., Phelan, M. L., and Kingston, R. E. (2001). Generation and interconversion of multiple distinct nucleosomal states as a mechanism for catalyzing chromatin fluidity. Mol Cell *8*, 1219-1230.

Neely, K. E., Hassan, A. H., Brown, C. E., Howe, L., and Workman, J. L. (2002). Transcription activator interactions with multiple SWI/SNF subunits. Mol Cell Biol *22*, 1615-1625.

Neely, K. E., and Workman, J. L. (2002). The complexity of chromatin remodeling and its links to cancer. Biochim Biophys Acta *1603*, 19-29.

Neigeborn, L., and Carlson, M. (1984). Genes affecting the regulation of SUC2 gene expression by glucose repression in *Saccharomyces cerevisiae*. Genetics *108*, 845-858.

Noll, M., and Kornberg, R. D. (1977). Action of micrococcal nuclease on chromatin and the location of histone H1. J Mol Biol *109*, 393-404.

Ogas, J., Cheng, J. C., Sung, Z. R., and Somerville, C. (1997). Cellular differentiation regulated by gibberellin in the Arabidopsis thaliana pickle mutant. Science *277*, 91-94.

Ogas, J., Kaufmann, S., Henderson, J., and Somerville, C. (1999). PICKLE is a CHD3 chromatin-remodeling factor that regulates the transition from embryonic to vegetative development in Arabidopsis. Proc Natl Acad Sci U S A *96*, 13839-13844.

Okada, M., and Hirose, S. (1998). Chromatin remodeling mediated by Drosophila GAGA factor and ISWI activates fushi tarazu gene transcription in vitro. Mol Cell Biol *18*, 2455-2461.

Olins, A. L., and Olins, D. E. (1974). Spheroid chromatin units (v bodies). Science *183*, 330-332.

O'Neill, D. W., Schoetz, S. S., Lopez, R. A., Castle, M., Rabinowitz, L., Shor, E., Krawchuk, D., Goll, M. G., Renz, M., Seelig, H. P., *et al.* (2000). An ikaros-containing chromatin-remodeling complex in adult-type erythroid cells. Mol Cell Biol *20*, 7572-7582.

Owen-Hughes, T., and Bruno, M. (2004). Molecular biology. Breaking the silence. Science *303*, 324-325.

Owen-Hughes, T., Utley, R. T., Steger, D. J., West, J. M., John, S., Cote, J., Havas, K. M., and Workman, J. L. (1999). Analysis of nucleosome disruption by ATP-driven chromatin remodeling complexes. Methods Mol Biol *119*, 319-331.

Parker, C. W. (1990). Radiolabeling of Proteins. In Guide to Protein Purification, M. P. Duetscher, ed. (San Diego, Academic Press), pp. 723.

Peterson, C. L. (2002a). Chromatin remodeling enzymes: taming the machines. Third in review series on chromatin dynamics. EMBO Rep *3*, 319-322.

Peterson, C. L. (2002b). Chromatin remodeling: nucleosomes bulging at the seams. Curr Biol *12*, R245-247.

Peterson, C. L., and Cote, J. (2004). Cellular machineries for chromosomal DNA repair. Genes Dev *18*, 602-616.

Peterson, C. L., Dingwall, A., and Scott, M. P. (1994). Five SWI/SNF gene products are components of a large multi-subunit complex required for transcriptional enhancement. Proc Natl Acad Sci USA *91*, 2905-2908.

Peterson, C. L., and Herskowitz, I. (1992). Characterization of the yeast SWI1, SWI2, and SWI3 genes, which encode a global activator of transcription. Cell *68*, 573-583.

Peterson, C. L., Kruger, W., and Herskowitz, I. (1991). A functional interaction between the C-terminal domain of RNA polymerase II and the negative regulator SIN1. Cell *64*, 1135-1143.

Peterson, C. L., and Tamkun, J. W. (1995). The SWI-SNF complex: a chromatin remodeling machine? Trends Biochem Sci *20*, 143-146.

Peterson, C. L., Zhao, Y., and Chait, B. T. (1998). Subunits of the yeast SWI/SNF complex are members of the actin-related protein (ARP) family. J Biol Chem *273*, 23641-23644.

Phelan, M. L., Schnitzler, G. R., and Kingston, R. E. (2000). Octamer transfer and creation of stably remodeled nucleosomes by human SWI-SNF and its isolated ATPases. Mol Cell Biol *20*, 6380-6389.

Prochasson, P., Neely, K. E., Hassan, A. H., Li, B., and Workman, J. L. (2003). Targeting activity is required for SWI/SNF function in vivo and is accomplished through two partially redundant activator-interaction domains. Mol Cell *12*, 983-990.

Puig, O., Caspary, F., Rigaut, G., Rutz, B., Bouveret, E., Bragado-Nilsson, E., Wilm, M., and Seraphin, B. (2001). The tandem affinity purification (TAP) method: a general procedure of protein complex purification. Methods *24*, 218-229.

Quinn, J., Fyrberg, A. M., Ganster, R. W., Schmidt, M. C., and Peterson, C. L. (1996). DNA-binding properties of the yeast SWI/SNF complex. Nature *379*, 844-847.

Redon, C., Pilch, D., Rogakou, E., Sedelnikova, O., Newrock, K., and Bonner, W. (2002). Histone H2A variants H2AX and H2AZ. Curr Opin Genet Dev *12*, 162-169.

Reisman, D. N., Sciarrotta, J., Wang, W., Funkhouser, W. K., and Weissman, B. E. (2003). Loss of BRG1/BRM in human lung cancer cell lines and primary lung cancers: correlation with poor prognosis. Cancer Res *63*, 560-566.

Richard-Foy, H., and Hager, G. L. (1987). Sequence-specific positioning of nucleosomes over the steroid-inducible MMTV promoter. EMBO J *6*, 2321-2328.

Richmond, E., and Peterson, C. L. (1996). Functional analysis of the DNA-stimulated ATPase domain of yeast SWI2/SNF2. Nucleic Acids Res *24*, 3685-3692.

Rider, S. D., Jr., Hemm, M. R., Hostetler, H. A., Li, H. C., Chapple, C., and Ogas, J. (2004). Metabolic profiling of the Arabidopsis pkl mutant reveals selective derepression of embryonic traits. Planta.

Rigaut, G., Shevchenko, A., Rutz, B., Wilm, M., Mann, M., and Seraphin, B. (1999). A generic protein purification method for protein complex characterization and proteome exploration. Nat Biotechnol *17*, 1030-1032.

Roberts, C. W., and Orkin, S. H. (2004). The SWI/SNF complex--chromatin and cancer. Nat Rev Cancer *4*, 133-142.

Roberts, C. W. M., Galusha, S. A., McMenamin, M. E., Fletcher, C. D. M., and Orkin, S. H. (2000). Haploinsufficiency of Snf5 (integrase interactor 1) predisposes to malignant rhabdoid tumors in mice. Proc Natl Acad Sci USA *97*, 13796-13800.

Saha, A., Wittmeyer, J., and Cairns, B. R. (2002). Chromatin remodeling by RSC involves ATP-dependent DNA translocation. Genes Dev *16*, 2120-2134.

Salma, N., Xiao, H., Mueller, E., and Imbalzano, A. N. (2004). Temporal recruitment of transcription factors and SWI/SNF chromatin-remodeling enzymes during adipogenic induction of the peroxisome proliferator-activated receptor gamma nuclear hormone receptor. Mol Cell Biol *24*, 4651-4663.

Santisteban, M. S., Kalashnikova, T., and Smith, M. M. (2000). Histone H2A.Z regulates transcription and is partially redundant with nucleosome remodeling complexes. Cell *103*, 411-422.

Sawa, H., Kouike, H., and Okano, H. (2000). Components of the SWI/SNF complex are required for asymmetric cell division in C. elegans. Mol Cell *6*, 617-624.

Schnitzler, G., Sif, S., and Kingston, R. E. (1998). Human SWI/SNF interconverts a nucleosome between its base state and a stable remodeled state. Cell *94*, 17-27.

Schnitzler, G. R., Cheung, C. L., Hafner, J. H., Saurin, A. J., Kingston, R. E., and Lieber, C. M. (2001). Direct imaging of human SWI/SNF-remodeled mono- and polynucleosomes by atomic force microscopy employing carbon nanotube tips. Mol Cell Biol *21*, 8504-8511.

Seelig, H. P., Moosbrugger, I., Ehrfeld, H., Fink, T., Renz, M., and Genth, E. (1995). The major dermatomyositis-specific Mi-2 autoantigen is a presumed helicase involved in transcriptional activation. Arthritis Rheum *38*, 1389-1399.

Sengupta, S. M., Persinger, J., Bartholomew, B., and Peterson, C. L. (1999). Use of DNA photoaffinity labeling to study nucleosome remodeling by SWI/SNF. Methods *19*, 434-446.

Sengupta, S. M., VanKanegan, M., Persinger, J., Logie, C., Cairns, B. R., Peterson, C. L., and Bartholomew, B. (2001). The interactions of yeast SWI/SNF and RSC with the nucleosome before and after chromatin remodeling. J Biol Chem *276*, 12636-12644.

Sentani, K., Oue, N., Kondo, H., Kuraoka, K., Motoshita, J., Ito, R., Yokozaki, H., and Yasui, W. (2001). Increased expression but not genetic alteration of BRG1, a component of the SWI/SNF complex, is associated with the advanced stage of human gastric carcinomas. Pathobiology *69*, 315-320.

Shen, X., Mizuguchi, G., Hamiche, A., and Wu, C. (2000). A chromatin remodelling complex involved in transcription and DNA processing. Nature *406*, 541-544.

Simpson, R. T. (1978). Structure of the chromatosome, a chromatin particle containing 160 base pairs of DNA and all the histones. Biochemistry *17*, 5524-5531.

Smith, C. L., Horowitz-Scherer, R., Flanagan, J. F., Woodcock, C. L., and Peterson, C. L. (2003). Structural analysis of the yeast SWI/SNF chromatin remodeling complex. Nat Struct Biol *10*, 141-145.

Smith, C. L., and Peterson, C. L. (2003). Coupling tandem affinity purification and quantitative tyrosine iodination to determine subunit stoichiometry of protein complexes. Methods *31*, 104-109.

Smith, M. M. (2002). Centromeres and variant histones: what, where, when and why? Curr Opin Cell Biol *14*, 279-285.

Soultanas, P., Dillingham, M. S., Wiley, P., Webb, M. R., and Wigley, D. B. (2000). Uncoupling DNA translocation and helicase activity in PcrA: direct evidence for an active mechanism. EMBO J *19*, 3799-3810.

Staehling-Hampton, K., Ciampa, P. J., Brook, A., and Dyson, N. (1999). A genetic screen for modifiers of E2F in Drosophila melanogaster. Genetics *153*, 275-287.

Stern, M., Jensen, R., and Herskowitz, I. (1984). Five SWI/SNF genes are required for expression of the HO gene in yeast. J Mol Biol *178*, 853-868.

Stopka, T., and Skoultchi, A. I. (2003). The ISWI ATPase Snf2h is required for early mouse development. Proc Natl Acad Sci U S A *100*, 14097-14102.

Sudarsanam, P., Iyer, V. R., Brown, P. O., and Winston, F. (2000). Whole-genome expression analysis of snf/swi mutants of Saccharomyces cerevisiae. Proc Natl Acad Sci USA *97*, 3364-3369.

Szerlong, H., Saha, A., and Cairns, B. R. (2003). The nuclear actin-related proteins Arp7 and Arp9: a dimeric module that cooperates with architectural proteins for chromatin remodeling. EMBO J *22*, 3175-3187.

Tasto, J. J., Carnahan, R. H., McDonald, W. H., and Gould, K. L. (2001). Vectors and gene targeting modules for tandem affinity purification in Schizosaccharomyces pombe. Yeast *18*, 657-662.

Thoma, F., and Koller, T. (1977). Influence of histone H1 on chromatin structure. Cell *12*, 101-107.

Thoma, F., Koller, T., and Klug, A. (1979). Involvement of histone H1 in the organization of the nucleosome and of the salt-dependent superstructures of chromatin. J Cell Biol *83*, 403-427.

Thomas, J. O., and Kornberg, R. D. (1975). An octamer of histones in chromatin and free in solution. Proc Natl Acad Sci U S A *72*, 2626-2630.

Tong, J. K., Hassig, C. A., Schnitzler, G. R., Kingston, R. E., and Schreiber, S. L. (1998). Chromatin deacetylation by an ATP-dependent nucleosome remodelling complex. Nature *395*, 917-921.

Truss, M., Bartsch, J., Schelbert, A., Hache, R. J., and Beato, M. (1995). Hormone induces binding of receptors and transcription factors to a rearranged nucleosome on the MMTV promoter in vivo. EMBO J *14*, 1737-1751.

Tsuchiya, E., Hosotani, T., and Miyakawa, T. (1998). A mutation in NPS1/STH1, an essential gene encoding a component of a novel chromatin-remodeling complex RSC, alters the chromatin structure of Saccharomyces cerevisiae centromeres. Nucleic Acids Res *26*, 3286-3292.

Tsukiyama, T., Becker, P. B., and Wu, C. (1994). ATP-dependent nucleosome disruption at a heat-shock promoter mediated by binding of GAGA transcription factor [see comments]. Nature *367*, 525-532.

Tsukiyama, T., Palmer, J., Landel, C. C., Shiloach, J., and Wu, C. (1999). Characterization of the imitation switch subfamily of ATP-dependent chromatin-remodeling factors in Saccharomyces cerevisiae. Genes Dev *13*, 686-697.

Unhavaithaya, Y., Shin, T. H., Miliaras, N., Lee, J., Oyama, T., and Mello, C. C. (2002). MEP-1 and a homolog of the NURD complex component Mi-2 act together to maintain germline-soma distinctions in C. elegans. Cell *111*, 991-1002.

van Holde, K., and Yager, T. (2003). Models for chromatin remodeling: a critical comparison. Biochem Cell Biol *81*, 169-172.

Varga-Weisz, P. D., Wilm, M., Bonte, E., Dumas, K., Mann, M., and Becker, P. B. (1997). Chromatin-remodelling factor CHRAC contains the ATPases ISWI and topoisomerase II [published erratum appears in Nature 1997 Oct 30;389(6654):1003]. Nature *388*, 598-602.

Vary, J. C., Jr., Gangaraju, V. K., Qin, J., Landel, C. C., Kooperberg, C., Bartholomew, B., and Tsukiyama, T. (2003). Yeast Isw1p forms two separable complexes in vivo. Mol Cell Biol *23*, 80-91.

Velankar, S. S., Soultanas, P., Dillingham, M. S., Subramanya, H. S., and Wigley, D. B. (1999). Crystal structures of complexes of PcrA DNA helicase with a DNA substrate indicate an inchworm mechanism. Cell *97*, 75-84.

Versteege, I., Sevenet, N., Lange, J., Rousseau-Merck, M. F., Ambros, P., Handgretinger, R., Aurias, A., and Delattre, O. (1998). Truncating mutations of hSNF5/Ini1 in aggressive paediatric cancer. Nature *394*, 203-206.

Vignali, M., Hassan, A. H., Neely, K. E., and Workman, J. L. (2000). ATP-dependent chromatin-remodeling complexes. Mol Cell Biol *20*, 1899-1910.

Wade, P. A., Gegonne, A., Jones, P. L., Ballestar, E., Aubry, F., and Wolffe, A. P. (1999). Mi-2 complex couples DNA methylation to chromatin remodelling and histone deacetylation. Nat Genet *23*, 62-66.

Wade, P. A., Jones, P. L., Vermaak, D., Veenstra, G. J., Imhof, A., Sera, T., Tse, C., Ge, H., Shi, Y. B., Hansen, J. C., and Wolffe, A. P. (1998). Histone deacetylase directs the dominant silencing of transcription in chromatin: association with MeCP2 and the Mi-2 chromodomain SWI/SNF ATPase. Cold Spring Harb Symp Quant Biol *63*, 435-445.

Wade, P. A., Jones, Peter L., Vermaak, Danielle, Wolffe, Alan P. (1998). A multiple subunit Mi-2 histone deacetylase from Xenopus laevis cofractionates with an associated Snf2 superfamily ATPase. Current Biology 8, 843-846.

Wall, J. S., and Hainfeld, J. F. (1986). Mass mapping with the scanning transmission electron microscope. Annu Rev Biophys Biophys Chem 15, 355-376.

Wall, J. S., Hainfeld, J. F., and Simon, M. N. (1998). Scanning transmission electron microscopy of nuclear structures. Methods Cell Biol 53, 139-164.

Wechser, M. A., Kladde, M. P., Alfieri, J. A., and Peterson, C. L. (1997). Effects of Sin-versions of histone H4 on yeast chromatin structure and function. EMBO J 16, 2086-2095.

Whitehouse, I., Flaus, A., Cairns, B. R., White, M. F., Workman, J. L., and Owen-Hughes, T. (1999). Nucleosome mobilization catalysed by the yeast SWI/SNF complex. Nature 400, 784-787.

Whitehouse, I., Stockdale, C., Flaus, A., Szczelkun, M. D., and Owen-Hughes, T. (2003). Evidence for DNA translocation by the ISWI chromatin-remodeling enzyme. Mol Cell Biol 23, 1935-1945.

Winston, F., and Carlson, M. (1992). Yeast SNF/SWI transcriptional activators and the SPT/SIN chromatin connection. Trends Genet 8, 387-391.

Wolffe, A. (1998). Chromatin : structure and function, 3rd edn (San Diego, Academic Press).

Wong, A. K., Shanahan, F., Chen, Y., Lian, L., Ha, P., Hendricks, K., Ghaffari, S., Iliev, D., Penn, B., Woodland, A. M., et al. (2000). BRG1, a component of the SWI-SNF complex, is mutated in multiple human tumor cell lines. Cancer Res 60, 6171-6177.

Woodcock, C. L., Frado, L. L., and Rattner, J. B. (1984). The higher-order structure of chromatin: evidence for a helical ribbon arrangement. J Cell Biol 99, 42-52.

Woodcock, C. L., Woodcock, H., and Horowitz, R. A. (1991). Ultrastructure of chromatin. I. Negative staining of isolated fibers. J Cell Sci 99 (Pt 1), 99-106.

Yager, T. D., McMurray, C. T., and van Holde, K. E. (1989). Salt-induced release of DNA from nucleosome core particles. Biochemistry 28, 2271-2281.

Yao, N., Hesson, T., Cable, M., Hong, Z., Kwong, A. D., Le, H. V., and Weber, P. C. (1997). Structure of the hepatitis C virus RNA helicase domain. Nat Struct Biol 4, 463-467.

Zlatanova, J., and Leuba, S. H. (2003). Chromatin fibers, one-at-a-time. J Mol Biol *331*, 1-19.

Appendix

Table A1: Yeast Strains used in Thesis research

Name	Relevant genotype
CY 120	*MATα swi2Δ::*HIS3 *HO-lacZ*
CY 296	*MATa gal4Δ::*leu2, leu2Δ1, his3Δ200, trp1Δ99, ura3Δ99, lys2Δ99, ade2⁻
CY 337	*MATa* GAL⁺ ura3-52 trp1-Δ63 leu2⁻ his3-Δ1 prbl-1122 pep4-3 prc1-407
CY 394	*MATα swi2Δ::*HIS3 *ura3::swi2*(R1196A)-HA-6HIS *HO-lacZ*
CY 396	*MATα swi2Δ::*HIS3 *ura3::*SWI2-HA-6HIS *HO-lacZ*
CY 397	*MATα swi2Δ::*HIS3 *ura3::swi2*(K798A)-HA-6HIS *HO-lacZ*
CY 452	*MATα swi2Δ::*HIS3 *ura3::swi2*(P824A)-HA-6HIS *HO-lacZ*
CY 453	*MATα swi2Δ::*HIS3 *ura3::swi2*(P932A)-HA-6HIS *HO-lacZ*
CY 454	*MATα swi2Δ::*HIS3 *ura3::swi2*(W935A)-HA-6HIS *HO-lacZ*
CY 455	*MATα swi2Δ::*HIS3 *ura3::swi2*(R994A)-HA-6HIS *HO-lacZ*
CY 456	*MATα swi2Δ::*HIS3 *ura3::swi2*(H1061A)-HA-6HIS *HO-lacZ*
CY 457	*MATα swi2Δ::*HIS3 *ura3::swi2*(K1088A)-HA-6HIS *HO-lacZ*
CY 458	*MATα swi2Δ::*HIS3 *ura3::swi2*(R1164A)-HA-6HIS *HO-lacZ*
CY 519	*MATα swi2Δ::*HIS3 *ura3::swi2*(ΔSTRAGGLG)-HA-6HIS *HO-lacZ*
CY 831	*MATa swi2Δ::*HIS3 *ura3::*SWI2-HA-6HIS created from CY337
CY 832	*MATα swi2Δ::*TRP1 *trp1::*SWI2-18myc
CY 889	*MATa/α swi2Δ::*TRP1 *trp1::* SWI2-18myc *swi2Δ::*HIS *ura3::*SWI2-HA-6HIS created from CY832
CY 943*	*MATa/α swi2 Δ::*HIS3 *ura3::swi2*(K798A)-TAP *HO-lacZ* diploid from CY397xCY296
CY 944*	*MATα swi2Δ::*HIS3 *ura3::swi2*-TAP *HO-lacZ* created from CY396
CY 1114*	*MATa/α swi2Δ::*HIS3 *ura3::swi2*(P824A)-TAP *HO-lacZ* diploid from CY452xCY296
CY 1115*	*MATa/α swi2Δ::*HIS3 *ura3::swi2*(P832A)-TAP *HO-lacZ* diploid from CY453xCY296
CY 1116*	*MATa/α swi2Δ::*HIS3 *ura3::swi2*(W935A)-TAP *HO-lacZ* diploid from CY454xCY296
CY 1117*	*MATa/α swi2Δ::*HIS3 *ura3::swi2*(K1088A)-TAP *HO-lacZ* diploid from CY457xCY296
CY 1118*	*MATa/α swi2Δ::*HIS3 *ura3::swi2*(R1164A)-TAP *HO-lacZ* diploid from CY458xCY296
CY 1119*	*MATa/α swi2Δ::*HIS3 *ura3::swi2*(R1196A)-TAP *HO-lacZ* diploid from CY394xCY296
CY 1120*	*MATa/α swi2Δ::*HIS3 *ura3::swi2*(ΔSTRAGGLG)-TAP *HO-lacZ* diploid from CY519xCY296
CY 1121*	*MATa/α swi2Δ::*HIS3 *ura3::swi2*(H1061A)-TAP *HO-lacZ* diploid from CY456xCY296

*Yeast strains created for this thesis project